STUDIES ON NANOCOMPOSITES OF POLYPROPYLENE AND POLYLACTIC ACID BLENDS REINFORCED WITH HALLOYSITE NANOTUBES

A
THESIS

submitted by

KRISHNA PRASAD RAJAN

(131PG31207)

for the award of the degree

of

DOCTOR OF PHILOSOPHY

VIGNAN'S
FOUNDATION FOR SCIENCE, TECHNOLOGY AND RESEARCH
(Deemed to-be University U/s 3 of the UGC Act, 1956)
Accredited by NAAC with 'A' Grade

DIVISION OF CHEMISTRY/NANOTECHNOLOGY

VFSTR UNIVERSITY, VADLAMUDI

GUNTUR – 522213, ANDHRA PRADESH, INDIA

SEPTEMBER 2016

Dedicated

to

my family members…

DECLARATION

I, Krishna Prasad Rajan, hereby declare that I have personally carried out the work presented in the thesis entitled **"Studies on nanocomposites of polypropylene and polylactic acid blends reinforced with halloysite nanotubes"** under the guidance and supervision of Prof. Murthy Chavali, Professor, Analytical Chemistry and Nanotechnology, Vignan's University, Vadlamudi, Guntur, Andhra Pradesh. The results embodied in this thesis have not been submitted to any other University or Institute for any other degree or diploma.

Krishna Prasad Rajan

CONTENTS

ACKNOWLEDGEMENTS

List of figures

List of Tables

Glossary

α	-	Fractional extent of the reaction
β	-	Heating or cooling rate
$\dot{\gamma}$	-	Apparent shear rate
ΔP_e		Inlet pressure in the capillary
ε	-	Extensional rate
ηa	-	Apparent shear viscosity
η_e	-	Extensional viscosity
ASTM	-	American society for testing and materials
CMPS	-	Chemically modified thermoplastic starch
CO	-	Castor oil
DCP	-	Dicumyl peroxide
DEA	-	Dielectric analysis
DIA	-	Diisodecyl adipate
DMA	-	Dynamic mechanical analysis
DMTA	-	Dynamic mechanical thermal analysis
DSC	-	Differential scanning calorimetry
DTPS	-	Thermoplastic dry starch
E*	-	Complex modulus
E'	-	Storage or elastic modulus
E''	-	Loss modulus
E_a	-	Apparent activation energy
EBA-GMA	-	Ethylene-butyl acrylate glycidyl methacrylate terpolymer
EPDM	-	Ethylene propylene diene monomer
EP-g-MA	-	Ethylene propylene-g-maleic anhydride
ESO	-	Epoxidized soybean oil
FTIR	-	Fourier transform infrared spectroscopy
GPOE	-	Glycidyl methacrylate grafted poly (ethylene octane)

HDI	-	Hexamethylene diisocyante
HDPE	-	High density polyethylene
HDT	-	Heat deflection temperature
HNT	-	Halloysite nanotube
IDEX	-	Interdigitated comb type electrode
J	-	Joule
KBF	-	Kenaf bast fibre
LDPE	-	Low density polyethylene
LLDPE	-	Linear low density polyethylene
LNR	-	Liquid natural rubber
MA	-	Maleic anhydride
MA-g-PP	-	Maleic anhydride grafted polypropylene
MA-g-ST	-	Maleic anhydride grafted starch
MDI	-	Methylene diphenyl diisocyanate
MFI	-	Melt flow index
MFR	-	Melt flow rate
MMT	-	Montmorillonite
MPa	-	Megapascal
n	-	Reaction order, Avrami exponent, Power law constant
NaOH	-	Sodium hydroxide
NR	-	Natural rubber
PALF	-	Pineapple leaf fibre
PCL	-	Poly (ε-caprolactone)
PDLLA	-	Poly (D, L-lactic acid)
PE	-	Polyethylene
PEG	-	Polyethylene glycol
PE-g-GMA	-	Polyethylene-grafted-glycidyl methacrylate
PE-g-MA	-	Polyethylene-grafted-maleic anhydride
PEGMMA	-	Ethylene−glycidyl methacrylate−methyl acrylate terpolymer

PG	-	Propylene glycol
PHB	-	Polyhydroxybutyrate
PHBV	-	Poly(hydroxybutyrate-co-hydroxyvalerate)
PIF	-	Pressure induced flow
PLA	-	Polylactic acid
PLA-g-GMA	-	Poly(lactide)-graft-glycidyl methacrylate
PLLA	-	Poly (L-lactic acid)
POM	-	Polarized optical microscope
PP	-	Polypropylene
PP-g-PMMA	-	Polypropylene-graft-poly(methyl methacrylate)
PVAc	-	Polyvinyl acetate
PVOH	-	Polyvinyl alcohol
R	-	Universal gas constant
SBR	-	Styrene butadiene rubber
SEBS-g-MA	-	Styrene-ethylene-butylene-styrene-g-maleic anhydride
SEM	-	Scanning electron microscope
$t_{1/2}$	-	Crystallization half time
tan δ	-	Dissipation factor
TEM	-	Transmission electron microscope
T_g	-	Glass transition temperature
TGA	-	Thermogravimetric analysis
T_m	-	Melting temperature
TPS	-	Thermoplastic starch
UTM	-	Universal testing machine
VST	-	Vicat softening temperature
WAXS	-	Wide angle X-ray scattering
Xc	-	Percentage crystallinity
XRD	-	X-ray diffraction

Abstract

The studies in the field of polymer blends and composites have paved the ways to develop novel classes of materials in an economical approach. Blends and composites of polypropylene (PP) and polylactic acid (PLA) were chosen as the subject for the present investigation. The immiscible blend of PP and PLA were compatibilized by reactive compatibilization strategy using maleic anhydride grafted PP (MA-g-PP). The obtained blends were characterized by various characterization tools and the optimum composition was identified. Halloysite nanotubes (HNT) were incorporated in the optimum blend to yield nanocomposites with superior properties. The characterization techniques used in the study provided mechanical, dynamic mechanical, thermal, rheological, structural, morphological and dielectric behaviors of the blends and nanocomposites.

CHAPTER-1

INTRODUCTION

1.1. Polymer blends and composites

Researchers have tried to develop polymer blends and composites as a cost effective and efficient technique to create new materials with tailor-made properties. These materials are intended for applications which can't be fulfilled alone by any one of the individual component polymers or reinforcements. Polymer blends consist of a mixture of two or more polymers leading to the formation of a miscible blend or an immiscible compatibilized blend (also termed as polymer alloy). History of development of polymer blends and their commercial applications are well reported in the literature (Folkes and Hope 1993; Utracki 1995). Polymer blends can be classified into three different groups (Koning, Van Duin et al. 1998). The first one is completely miscible blends. These blendsexhibit homogeneity in the molecular level and also they have specific interactions with each other. The second category is partially miscible blends. In these type of blends, a small part of one of the blend components is dispersed in the other leading to a partially compatible phase morphology. The majority of polymer blends belong to the third category, which is fully immiscible polymer blends. They have very sharp and finite interfaces due to lack of specific interactions between the blend components. Various strategies were adopted to compatibilize an immiscible polyblend system (Koning, Van Duin et al. 1998; Utracki 2002), out of which use of a block or graft copolymer, which can react to both the blend components in-situ, is a very popular method to produce technologically compatible polymer blends. The author had prepared a polyblend system containing thermoplastic polyurethane (TPU) and polydimethylsiloxane rubber (PDMS) compatibilized by a copolymer of ethylene and methyl acrylate (EMA) as a reactive compatibilizer and studied their performance properties including biocompatibility evaluation (Rajan, Al-Ghamdi et al. 2012; Rajan, Al-Ghamdi et al. 2013).

The strength and modulus of the polymer matrix are further improved by the introduction of a reinforcing filler (either in the form of fibres or particles) leading to the development of high-performance composite materials. The composites exhibit

the stress transfer mechanism, where, the applied stress to the matrix is transferred to the reinforcing medium by the viscoelastic displacement (Hollaway 2001).While the dimensions of the reinforcing filler are of the order of micrometres (10^{-6}m) in conventional composites, at least one of the dimensions of the reinforcing filler is in the nanometer (10^{-9}m) range in polymer nanocomposites. In conventional composites, the interface of fillers is almost close to the bulk polymer matrix, whereas in nanocomposites, due to the nanoscale dimensions of the reinforcing filler, there is an added benefit of very large interfacial area per volume, and due to this, the distance between the matrix and filler constituents are exceptionally small. The enhanced molecular interaction between the polymer and the nanoparticles provide the polymer nanocomposites with an extraordinary set of material properties that conventional polymers could not exhibit (Koo 2006). As a result of the unique filler-polymer interaction, the nanocomposites exhibit many major performance properties including improved mechanical properties, thermal resistance, fire resistance, moisture resistance, improved barrier properties, charge dissipation, and chemical resistance (Ray and Okamoto 2003). A comprehensive review on polymer nanocomposites was published by the author and co-workers

1.2 Polypropylene (PP)

Polypropylene (PP) is a thermoplastic polyolefin prepared by polymerization of propylene monomer units.PP is a saturated aliphatic hydrocarbon polyolefin with alinear structure. Among polyolefins, PP possesses some of the unique set of properties such as very low density, high strength, very good optical properties and film puncture resistance,high softening point and high maximum service temperature compared with other polyolefins. It has a moderate permeability to gases and a superior resistance to water vapour, which is not affected by changes in humidity (Allahvaisi 2012). Due to these excellent set of properties, PP is an ideal choice for various packaging applications. The typical properties of a commercial grade PP (PP 500 P, SABIC) suitable for injection moulding and extrusion applications are given in table 1.1. The presence of methyl group in alternate carbon atoms of PP leads to apolymer with different tacticity such as isotactic, syndiotactic and atactic. Out of

these three, theisotactic structure has all methyl groups arranged towards one side of the molecule and provide more regularity. Commercially available PP are almost 90 to 95% isotactic. Isotactic semi-crystalline PP contains both crystalline and amorphous phases. The amount of crystalline and amorphous phaseswithin the polymer depends on the structuraland stereo chemical characteristics of the polymer chains as well as the processing operations and the processing parameters (Karian 2003). The size and type of the crystal structure decide the final properties of the PP and these, in turn,depend on the nucleation and growth of the crystals within the polymer molecule during various processing operations. The rate of cooling and the presence of nucleating agents can alter the nucleation and growth of the crystals.

Table 1-1Typical properties of a commercial grade PP

Property	Value	Test standard
Melt Flow Rate @ 230°C & 2.16 kg load	3 g/10 min.	ASTM D 1238
Density @ 23°C	905 kg/m^3	ASTM D 792
Tensile Strength	35 MPa	ASTM D 638
Elongation at break	10%	ASTM D 638
Flexural Modulus	1500 MPa	ASTM D 790A
Notched Izod Impact Strength @ 23°C	25 J/m	ASTM D 256
Rockwell Hardness	102	ASTM D 785
Vicat Softening Point	152°C	ASTM D 1525B
Heat Deflection Temperature @ 455 KPa	100°C	ASTM D 648

(https://www.sabic.com/corporate/en/images/Datasheet%20for%20Grade%20500P_tcm12-1036.pdf, accessed on 26-08-2016)

1.3 Polylactic acid (PLA)

Poly (lactic acid) (PLA) is a biodegradable biopolymer produced from natural resources. It is considered as one of the most promising bio-based polymers and hence

attracted the interest of researchers over the last two decades.The majority of the lactic acid available in the market today is produced by bacterial fermentation of carbohydrates such as corn, sugarcane, or tapioca(Prescott and Dunn 1949). Other carbohydrate feedstock for the production of lactic acid includes cassava starch, lignocellulose/hemicellulose hydrolysates, cottonseed hulls, corn cobs, corn stalks, beet molasses, wheat bran, rye flour, sweet sorghum, sugarcane press mud, cassava, barley starch, cellulose, carrot processing waste, molasses spent wash, corn fiber hydrolysates, and potato starch(Reddy, Altaf et al. 2008). Abdel-Rahman et al reviewed the recent developments in fermentation processes for lactic acid production(Abdel-Rahman, Tashiro et al. 2013). PLA can be synthesised from lactic acid by polycondensation of lactic acid or ring-opening polymerization of lactide. The stereochemical structure, molecular weight and crystallinity of the resulting polymer can easily be controlled by polymerising a mixture of l and d isomers of lactic acid. Large number of literatures is available describing the synthesis of PLA from lactic acid (Drumright, Gruber et al. 2000; Garlotta 2001; Henton, Gruber et al. 2005; Mehta, Kumar et al. 2005; Auras, Lim et al. 2011; Lasprilla, Martinez et al. 2012; Lopes, Jardini et al. 2012; Park, Kim et al. 2012). Recently Costa et al. (Costa, Tancini et al. 2016)developed an efficient catalyst deactivator, which can improve the efficiency of devolatilization of the unreacted monomer during PLA synthesis process. The major producers of PLA include NatureWorks® LLC, Mitsui Chemicals, Dai Nippon Printing Co., Shimadzu, NEC, Toyobo, Toyota (Japan), PURAC Biomaterials, Hycail (The Netherlands), Galactic (Belgium), Cereplast (U.S.A.), FkuR, Stanelco, Biomer, Inventa-Fischer (Germany), and Snamprogetti (China)(Jamshidian, Tehrany et al. 2010). PLA can be processed by conventional plastic processing techniques such as injection moulding, extrusion, blow moulding, thermoforming, foaming and fiber spinning process into various articles. In addition to its biodegradability and biocompatibility, PLA exhibits good transparency and processability, which makes it a versatile polymer for several commercial as well as medical applications(Auras, Lim et al. 2011). PLA exhibits major functional properties such as, high gloss and clarity, crimp (ability to hold a crease or fold), low-temperature heat seal, low coefficient of friction and resistance to oils, which makes it a suitable candidate for packaging applications(Kawashima, Ogawa et al. 2002).

Other applications include automotive interiors, consumer electronics, sportswear, boots, coffee cups and lids, game consoles and personal protection equipment.

1.4 Halloysite nanotubes (HNT)

Halloysite nanotubes (HNTs) reinforced polymer nanocomposites are gaining extensive popularity both from academic and industrial sectors due to their improved mechanical, thermal, electrical and fire-retardant properties (Prashantha, Lecouvet et al. 2013). The unique features of HNTs such as nanoscale lumens, high length to diameter (L/D) ratio, low hydroxyl group density on the surface and high-temperature resistance are some of the reasons behind itswidespread usage in various application sectors(Du, Guo et al. 2010). Moreover, HNTs are abundantly available from nature,environmentally friendly material and biocompatible and hence find applications in the biomedical field, alone as well as with various polymer matrices(Rawtani and Agrawal 2012; Liu, Jia et al. 2014). Structurally HNTs are very similar to kaolin type of clay with an empirical chemical formula $Al_2Si_2O_5$ $(OH)_4.H_2O$ and possess a tubular structure. The length of individual HNT tubes ranges from 0.2 to 2 μm. The inner and outer diameters of individual tubes are of the order of 10 to 40 nm and 40 to 70 nm, respectively which give them a unique feature of thevery high aspect ratio of 10 to 50(Liu, Jia et al. 2014; Lvov, Aerov et al. 2014). HNTs were used as reinforcing filler for almost all commercial polymer matrices and resulted in improvements in their performance properties(Ismail, Pasbakhsh et al. 2008; Jia, Luo et al. 2009; Du, Guo et al. 2010; Handge, Hedicke-Höchstötter et al. 2010; Ismail, Salleh et al. 2013; Lecouvet, Sclavons et al. 2013; Lee and Chang 2013; Liu, Zhang et al. 2013; Rybiński and Janowska 2013; Liu, Luo et al. 2014; Shemesh, Krepker et al. 2015; Singh, Vimal et al. 2016).

1.5 Objectives and scope of the present work

The objectives of the present work are;

i. Preparation of blends of PP and PLA in various PP rich ratios (90:10, 80:20 and 70:30) and selection of the optimum blend ratio based on their mechanical properties.

ii.   Preparation of a compatibilized blend of PP and PLA in the ratio 80:20 using MA-G-PP as a reactive compatibilizer by adopting melt blending technique.

iii.   Determination of the static and dynamic mechanical properties of the blends to find out the optimum compatibilizer content required to effectively compatibilize the blend in the selected ratio.

iv.   Carry out the detailed characterization of the blends and thermal analysis studies to elucidate the crystallisation kinetics and thermal degradation kinetics of the prepared blends.

v.   Selection of the polyblend system containing the optimum compatibilizer content to act as the matrix for reinforcement with halloysite nanotubes.

vi.   Preparation of the nanocomposites with varying amount of nanotubes (0 to 10 wt%).

vii.   Carry out the detailed characterization studies of the nanocomposites to find its suitability for various applications.

In the present investigation, a compatibilized blend of PP and PLA in the ratio 80:20 using MA-G-PP as a reactive compatibilizer was prepared and evaluated the mechanical and dynamic mechanical properties. Also, the non-isothermal crystallisation kinetics and thermal degradation kinetics of the blends were investigated. The compatibilized blend was further reinforced with HNT's and the nanocomposites were thoroughly characterised.

1.6 Organization of the thesis

The thesis comprises of eleven chapters. The chapter-1 of the thesis gives a general introduction to the raw materials used in the studies and also the objectives and scope of the present work. The detailed literature review related to the state of the art in the similar investigations and the identification of the exact problem based on this reviewis presented in chapter-2. The properties and source of the materials and various processing and characterization techniques used in the present investigations

are summarised in chapter-3. The static and dynamic mechanical analyses provide valuable information about the compatibility of the blends and the optimum dosage of the compatibilizer or the nanofiller. Chapter-4 feature about the mechanical properties of the blends and the nanocomposites. A Proper understanding of the crystallisation and thermal degradation of the blends plays a crucial role in deciding the processing conditions and the maximum service temperature of the articles made out of these materials. The thermal degradation and crystallisation kinetics of the blends are elaborated in chapter-5. IR spectroscopy and X-ray diffraction studies are essential to expound the interactions between the polymers and the fillers. The details of these investigations are presented in chapter-6. Rheological parameters such as shear stress, shear rate and viscosity are very important in deciding the processing techniques and the suitable processing temperature. The high shear rheological studies of the blends and nanocomposites are elaborated in chapter-7. The changes in X-ray diffraction patterns and the associated structural features of prepared blends and nanocomposites are discussed in chapter-8. Thermal analysis techniques such as DSC provide information about the transitions such as glass transition, melting and crystallisationbehaviour of the blends and nanocomposites, whereas TGAprovides valuable insights about the thermal degradation behaviour of these materials. The details of thethermal analysis are presented in chapter-9. In the dielectric analysis, a material is subjected to an oscillating electrical field and information regarding capacitive and conductive properties is elucidated from the response of the material. The details about DEA of the nanocomposites are elaborated in chapter-10. Microscopic techniques are used to get information about the morphology as well as thedispersion of thefiller in the matrix. TEM studies and POM studies are presented in chapter-11. The conclusions from the present investigations and the scope for future studies based on these results are presented in chapter-12.

CHAPTER-2

LITERATURE REVIEW

2.1   Polylactic acid (PLA)

Poly (lactic acid) (PLA) is a biodegradable biopolymer produced from natural resources. It is considered as one of the most promising bio-based polymers and hence attracted the interest of researchers over the last two decades. Figure 2.1 shows the tremendous increase in publications reported on PLA since the year 1996 (accessed on 27th August 2016 based on Scopus search using keyword " Polylactic acid").
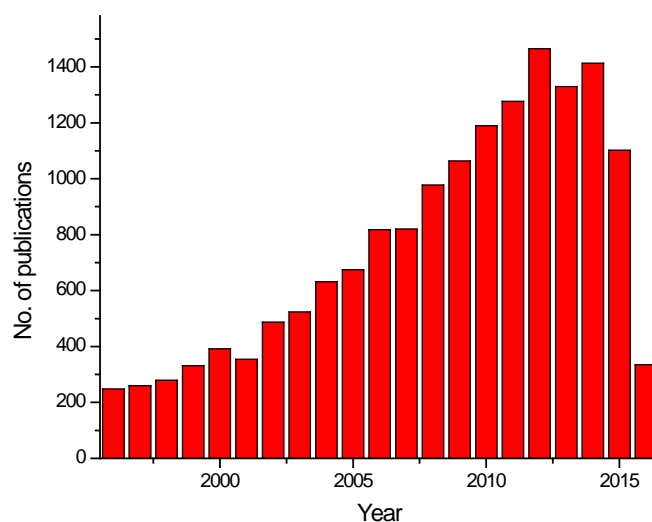
Figure 2.1 Polylactic acid based articles since 1996

The research on PLA is truly interdisciplinary in nature with the involvement of all branches of science and technology. Scarcely an area is untouched. Figure 2.2 shows the distribution of reported literature in figure 2.1 into various subject areas (source: Scopus, accessed on 27[th]August 2016)

.
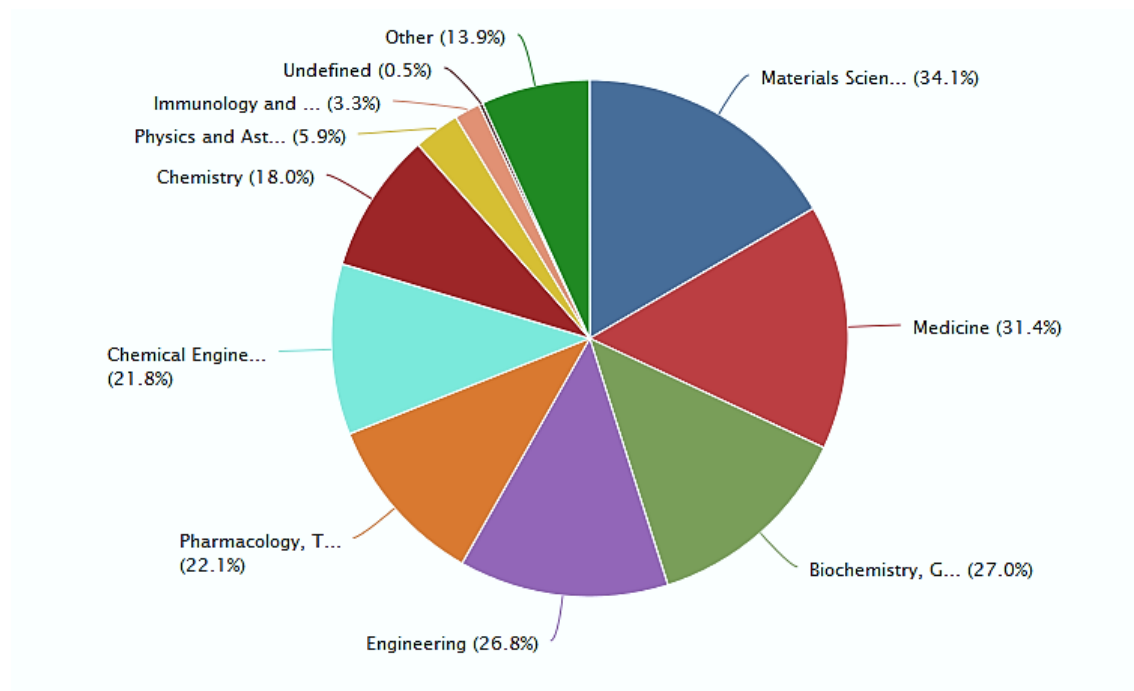
Figure 2.2Distribution of PLA publications

PLA belongs to the family of aliphatic polyesters, for which the starting materials are α-hydroxy acids. The main feedstock for PLA synthesis is lactic acid. The commercial production of lactic acid started in Japan during 1950(Benninga 1990). Chemically, lactic acid is 2-hydroxypropanoic acid. Due to the presence of a chiral carbon atom in its structure, it exists in two enantiomeric forms, widely known as L-lactic acid and D-lactic acid (figure 2.3).
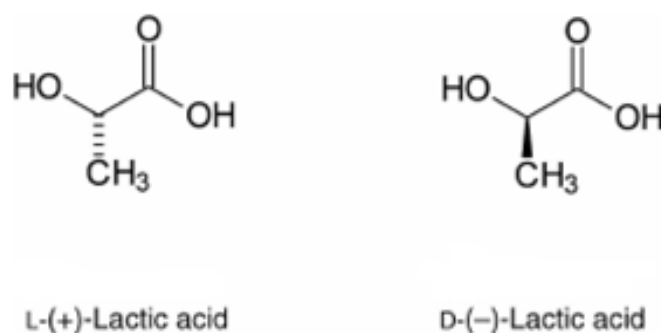
Figure 2.3Isomers of Lactic acid (L-lactic acid and D-Lactic acid)

The majority of the lactic acid available in the market today is produced by bacterial fermentation of carbohydrates such as corn, sugarcane, or tapioca(Prescott and Dunn

1949). Other carbohydrate feedstock for the production of lactic acid includes cassava starch, lignocellulose/hemicellulose hydrolysates,cottonseed hulls, corn cobs, corn stalks, beetmolasses, wheat bran, rye flour, sweet sorghum, sugarcane pressmud, cassava, barley starch, cellulose, carrot processing waste, molassespent wash, corn fiber hydrolysates, and potato starch(Reddy, Altaf et al. 2008). Abdel-Rahman et al reviewed the recent developments in fermentation processes for lactic acid production(Abdel-Rahman, Tashiro et al. 2013). PLA can be synthesised from lactic acid by polycondensation of lactic acid or ring-opening polymerization of lactide. The stereochemical structure, molecular weight and crystallinity of the resulting polymer can easily be controlled by polymerising a mixture of l and d isomers of lactic acid. Large number of literatures is available describing the synthesis of PLA from lactic acid (Drumright, Gruber et al. 2000; Garlotta 2001; Henton, Gruber et al. 2005; Mehta, Kumar et al. 2005; Auras, Lim et al. 2011; Lasprilla, Martinez et al. 2012; Lopes, Jardini et al. 2012; Park, Kim et al. 2012). The major producers of PLA include NatureWorks® LLC, Mitsui Chemicals, Dai Nippon Printing Co., Shimadzu,NEC, Toyobo, Toyota (Japan), PURAC Biomaterials, Hycail (The Netherlands),Galactic (Belgium), Cereplast (U.S.A.), FkuR, Stanelco,Biomer,Inventa-Fischer (Germany), and Snamprogetti (China)(Jamshidian, Tehrany et al. 2010). PLA can be processed by conventional plastic processing techniques such as injection moulding, extrusion, blow moulding, thermoforming, foaming and fibre spinning process into various articles. In addition to its biodegradability and biocompatibility, PLA exhibits good transparency and processability, which makes it a versatile polymer for several commercial as well as medical applications(Auras, Lim et al. 2011). PLA exhibits major functional properties such as, high gloss and clarity, crimp (ability to hold a crease or fold), low-temperature heat seal, low coefficient of friction and resistance to oils, which makes it a suitable candidate for packaging applications(Kawashima, Ogawa et al. 2002). Other applications include automotive interiors, consumer electronics, sportswear, boots, coffee cups and lids, game consoles and personal protection equipment.The properties of some of the commercial grades of Corbion PLA are summarised in table 2.1.

Table 2-1Properties of Corbion PLA grades (Source: http://www.corbion.com)

Properties /Grades	L 105 (Thin wall injection moulding grade)	L 130 (General purpose injection moulding, fibres)	L 175 (Thermoforming, fibres, extrusion)	LX 175 (Thermoforming, fibres, films, extrusion
Density, g/cm3	1.24	1.24	1.24	1.24
Optical purity, % L-isomer	>99	>99	>99	96
MFI (210°C, 2.16 kg), g/10 min	50	16	6	6
Melting temperature (Tm), ^{o}C	175	175	175	155
Glass transition temperature (Tm), ^{o}C	57	57	57	55
Tensile modulus, MPa	3500	3500	3500	3500
Tensile strength, MPa	50	50	50	45
Elongation at break, %	<5	<5	<5	<5
Charpy impact strength, kJ/m2	<5	<5	<5	<5
HDT B (amorphous) ^{o}C	55-60	55-60	55-60	55-60
HDT B (crystalline) ^{o}C	100-110	100-110	100-110	-

2.2   Modifications of PLA

Even though PLA exhibits several useful properties, its brittleness, susceptibility to hydrolysis, low impact resistance and low elongation at break are some of the limiting factors for widespread commercial application of this material. In order to overcome these deficiencies, several methods were developed by various researchers in this field and some of them are: i) blending with plasticisers, ii) copolymerization, iii) blending with other polymers, iv) preparing nanocomposites and v) surface modifications(Rasal, Janorkar et al. 2010). Preparation of blends and composites of PLA as a performance improvement technique for PLAis reviewed in detail in this article, with more emphasis on the recent developments.

2.2.1   Blends and composites of PLA with other biodegradable materials

The main attraction for the development of blends of PLA with other biodegradable materials is the improvement of properties of PLA without compromising the biodegradability of the resulting blend system. Blends of amorphous poly(D,L-lactic acid) (PDLLA) and crystalline poly(L-lactic acid) (PLLA) was prepared by Essawy and group(Essawy, Helaly et al. 2007).The preparation was carried out in one step by melt/solid polycondensation.

2.2.1.1   PLA with starch

Starch is blended with PLA by various research groups in order to improve the properties of PLA. Wang et al(Wang, Yu et al. 2007) prepared a blend of thermoplastic dry starch (DTPS) and PLAusing maleic anhydride (MA) as a compatibilizer in presence of di-cumyl peroxide using a twin screw extruder. The blend showed an improvement in tensile properties and thermal degradation behaviour compared with the individual components. Compatibility between starch and PLA is the major factor affecting the performance of the resulting blend. The various strategies adopted for compatibilizing starch/PLA blends were investigated by Schwach and co-workers(Schwach, Six et al. 2008). The different compatibilization

routes: (i) formation of urethane linkages in situ; (ii) peroxide coupling between starch and PLA, and (iii) the addition of PLA-grafted amylose (A-g-PLA). The compatibilization efficiency was analysed by measuring the mechanical and thermal properties of the blends. Based on the results, it was concluded that that peroxide reticulation and the addition of a copolymercompatibilizer (PLA-grafted amylose) gave the bestresults. But the best compatibilization effect, with a significant increase (up to 60%) of the tensile strengthwithout adecreasein the elongation at break, wasobtained with the copolymer (A-g-PLA). The crystallisation of PLA in a PLA/starch blend system was studied by Li et al (Li and Huneault 2008) and it was reported that crystallinity was more than 50% even at thecooling rate of 80^0C/minute. Thermal and physical degradation of PLA and its blends with starch and methylenediphenyl diisocyanate (MDI) was investigated by Acioli and co-workers(Acioli-Moura and Sun 2008). Nanocomposite foams containing tapioca starch, PLA and nanoclay (Cloisite 30B) were prepared by Lee et al(Lee and Hanna 2009) using melt intercalation technique. Nanocomposites of thermoplastic starch (TPS) and PLA with natural montmorillonite (MMT) were prepared by Arroyo and coworkers (Arroyo, Huneault et al. 2010) using a twin-screw extruder and the structure-property relationship of the nanocomposite was characterisedto examine the use of water to enhance clay exfoliation. It was observed that the TPS can intercalate the clay structure and the clay was preferentially located in the TPS phase or at the blend interface, leading to an improvement in tensile modulus and strength and to a reduction in fracture toughness.

In another study, TPS/PLA composites were prepared by melt blending with glycerol plasticizedstarch and the isothermal crystallisation kinetics of TPS/PLA composites was performed by differential scanning calorimetry (DSC) at different crystallisation temperatures(Cai, Liu et al. 2011). Avrami theory, which was applied to describe the process of isothermal crystallisation, indicated that TPS acted as a nucleating agent, improving the spherulite growth rate, overall crystallisation rate, and activation energy of TPS/PLA composites. Biodegradation of starch/polylactic acid/poly(hydroxyesterether) composite bars in soil was reported by Shogren and co-workers(Shogren, Doane et al. 2003), whereas, water absorption and enzymatic

degradation of poly(lactic acid)/rice starch composites were investigated by research group of Yew(Yew, Mohd Yusof et al. 2005). Recently, sea water degradation of starch/PLA composite was studied by Chen et al(Chen, Wang et al. 2011). Their one-year long observation showed that starch particles were lost from the composite material due to microbial action and the water was acting as a plasticiser. The observed degradation rate was very slow. Biodegradation of thermoplastic starch and its blends with PLA and polyethylene was investigated by Li et al(Li, Sarazin et al. 2011).

Mechanical, thermal and biodegradability properties of PLA/modified starch blends were investigated by Gao et al and observed that addition of 15 wt% of modified starch resulted in a decrease of melting temperature and vicat softening temperature (VST) of the blend(Gao, Hu et al. 2011). But similar blends of PLA with maleic anhydride grafted starch (MA-*g*-ST) exhibited slightly improved thermal stability. A blend of PLA with MA-*g*-ST showed improvementsin notched impact strength, elongation at break, and tensile strength and biodegradability compared with the unmodified blend system, which means MA-*g*-ST is suitable filler for improving the toughness of PLA. Blends of TPS and PLA with and without theaddition of glycidyl methacrylate grafted poly (ethylene octane) (GPOE) were prepared using Haake Mixer by Shi and co-workers(Shi, Chen et al. 2011). They have investigated mechanical properties, morphology, thermal properties, water absorption and degradation of these binary and ternary blends. The blends showed excellent biodegradability too. Shin et al blended PLA with chemically modified thermoplastic starch (CMPS) using a twin-screw extruder(Shin, Jang et al. 2011).Morphology, thermal, and mechanical properties and biodegradability of the resulting blend was investigated. Scanning electron microscopy (SEM) and Fourier transform infrared (FTIR) studies revealed the formation of PLA-g-starch copolymersthat were formed at the interface through a transesterification reaction between PLA and CMPS, which improved the interfacial adhesion between the blend components. It was also observed that the biodegradability of the blends increased with increasing CMPS content. Shogren et al studied the effect of fibre orientation on the morphology and mechanical properties of PLA/starch composite filaments (Shogren, Selling et al.

2011). It was reported that tensile strength and moduli increased with increasing draw ratio but decreased with increasing starch content. They have concluded that fibreorientation greatly increased the flexibility of PLA/starch composites.

Silva et al (Silva, Tarverdi et al. 2011) incorporated wheat starch and coupling agents into poly(lactic acid) in an attempt to develop biodegradable composites. They have studied the effects of incorporating different coupling agents on the physical properties and morphology of the composites. They have observed that with the addition of 10% wheat starch and 2% MDI, blends of wheat starch/PLA exhibit tensile strength, elongation at break and impact strength properties similar to that of raw PLA and in the presence of 2% MDI and 10% glycerol, blends of PLA and starch exhibits enhanced flexibility. The role of polylactide modified with reactive anhydride groups (PLA(m)) as a compatibilizer for PLA and TPS was investigated by Swierz et al (Swierz-Motysia, Jeziorska et al. 2011). It was reported that the blends with the compatibilizer showed improved tensile, flexural and impact properties as compared to the composites without compatibilizer. The authors report that the interphase interactions between the hydrogen atoms of the anhydride groups in the compatibilizer and the hydroxyl groups of the starch during the reactive extrusion process are the reason behind this property enhancement. As a result of this improved interaction between the blend components, the rate of biodegradation of the blends decreases with an increase in the content of compatibilizer.

There are various strategies to improve the compatibility of PLA with various other polymers. A detailed report on these strategies is available in the recent review article authored by Zeng et al.(Zeng, Li et al. 2015). In an attempt to increase the compatibility between PLA and starch, Wu et al(Wu 2011) added glycerin into the blend system and found that the higher the glycerin content, the better the compatibility between PLA and starch. They have also tried to crosslink the starch as a strategy to improve its compatibility with PLA and found that crosslinking greatly improved the compatibility. Yokesahachart et al(Yokesahachart and Yoksan 2011) modified the thermoplastic starch by adding three different types of amphiphilic molecules and prepared binary blends of modified starch with PLA. It was found that

the amphiphilesimproved the processability, flowability and extensibility of the blends.Chabrat and co-workers(Chabrat, Abdillahi et al. 2012) plasticized wheat flour with glycerol and blended with PLA using a twin screw extruder in presence of citric acid and water. Here, citric acid acted as a compatibilizer by promoting depolymerization of both starch and PLA. Hence its dosage has to be limited to a maximum of 2%, in order to avoid adecrease in mechanical properties. Here the role of water is tominimise PLA depolymerization and to favourstarch plasticization by citric acid and thus improve phase repartition.PLA was grafted onto starch nanoparticles by Garcia et al(Garcia, Lamanna et al. 2012). The reactions include three steps and the first step is theprotection of hydroxyl groups of PLA by benzoylation. This step is followed by activation of carboxyl groups using thionyl chloride and at last the modified PLA was grafted onto starch nanoparticles. The benzoylation step helped in decreasing the glass transition temperature (T_g). The nano grafted PLA exhibited a slightly lower degradation temperature than that of pure PLA.

Poly(lactide)-graft-glycidyl methacrylate (PLA-g-GMA) copolymer was prepared by Liu et al(Liu, Jiang et al. 2012) by grafting GMA onto PLA using benzoyl peroxide as an initiator.PLA-g-GMA copolymer was used as a compatibilizer for PLA/starch blends. The structure and properties of PLA/starch blends with and without PLA-g-GMA copolymer were characterised by SEM, DSC, tensile test and medium resistance test. The blending system with the compatibilizer exhibited an improvement in properties. Ouyang et al(Ouyang, Wang et al. 2012) did pre-treatment of PLA as a method to improve the compatibility between PLA and modified starch. DSC and SEM analysis were done to find the effectiveness of pretreatment and found that the pretreatment improved the compatibility of the composites. Phetwarotai and group(Phetwarotai, Potiyaraj et al. 2012)polylactide/gelatinized starch films by blending PLA with gelatinized starch in the presence of plasticisers and compatibilizer for improving interfacial bonding between two phases. Two types of starch (corn and tapioca) were used for blending with PLA. Polyethylene glycol (PEG400) and propylene glycol (PG) were used as plasticisers and methylenediphenyldiisocyanate was used as a compatibilizer. The role of

poly(ethylene glycol) (PEG) as a compatibilizer for PLA/TPS blend was studied by Favaro et al(Favaro Ferrarezi, Taipina et al. 2013). They havereported that incorporation of PEG resulted in the increase of PLA crystallisation, improved the interfacial interaction between TPS and PLA matrix, increased the impact strength of the ternary blend whereas the elastic modulus remained similar to the PLA/TPS blend. Xue et al(Xue, Wang et al. 2013) also studied the effect of adding PEG into TPS/PLA blends. The addition of PEG resulted in lower T_g and T_m as well as higher MFI for the blends. It was observed that the optimum mechanical properties can be obtained for the blend system with theaddition of 3 wt % PEG. Li et al(Li, Xiong et al. 2013) studied the non-isothermalcrystallisation kinetics of pure PLA and TPS/PLA composites by DSC. It was observed that TPS acted as a nucleating agent and improved the crystallinity of the PLA and restricted the mobility of the PLA chains. They have also usedtheoretical models to describe the process of non-isothermalcrystallisation.

The effect of nanoclay on the on the properties of thermoplastic Starch/PLAblends were investigated in detail by Paglicawan and group(Paglicawan, Basilia et al. 2013). Thermoplastic starch nanocomposites with different amounts of nanoclaywere prepared initially and these nanocomposites were blended with PLA in presence of maleic anhydride. The mechanical properties, thermal characteristics, microstructure and water resistance of the biodegradable nanocomposite blends were studied in detail. Biodegradable films from blends of TPS and PLA plasticized with different adipate or citrate esters were prepared by Shirai and group(Shirai, Grossmann et al. 2013). The films were prepared by blown film extrusion process and it was concluded that adipate esters were the most effective plasticisers based on the desired mechanical properties of the films. In another study, sheets were prepared from a blend of TPS/PLA (70:30 wt/wt) by them pressing(Soares, Yamashita et al. 2013). The sheets so prepared were coated with cross-linked chitosan by two different methods: spraying and immersion.The chitosan coating reduced the water solubility and water vapour permeability of the sheets due to the hydrophobic nature of chitosan. The coated sheets exhibited higher tensile strength than the uncoated sheets. It was concluded that coating by spraying was more effective at changing the sheet

properties than coating by immersion. Xiong et al used tung oil anhydride (TOA) as a plasticiser for PLA/starch blends (Xiong, Li et al. 2013). The addition of TOA improved the compatibility between starch and PLA and resulted in an enhancement of mechanical properties of the resulting blend. Epoxidizedsoybean oil (ESO) was used as a reactive compatibilizer for PLA and starch blend by Xiong et al (Xiong, Yang et al. 2013). In the beginning, starch granules were grafted with maleic anhydride to improve its reactivity with ESO. The same research group has studied the effect of castor oil (CO) on the properties of starch/PLA blend (Xiong, Zhang et al. 2013). They have tried to graft hexamethylenediisocyanate (HDI) with starch in order to accumulate the CO on thestarch surface. The accumulation of CO on starch greatly improved the toughness and impact strength of PLA/starch blends.Zhang et al(Zhang, Feng et al. 2013) investigated pressure-induced flow (PIF) processing as a method to produce a layer-like microstructure along the flow direction in PLA/starch blends. It was observed that impact and tensile strength can be improved by 200% and 40% respectively with the formation of thelayer-like microstructure. Composites of PLA with chitin nanowhiskers were prepared by Rizvi (Rizvi, Cochrane et al. 2011) and group adopting melt blending technique. The incorporation of chitin resulted in a decrease in viscosity and thermal stability of the composites. The stiffness of the composites increased with an increase in chitin content. They have also prepared a porous composite structure of these composite materials by two stage batch foaming technique. The production of micro-fibrillated cellulose-reinforced polylactide cellular biocomposites was described by Boissard et al (Boissard, Bourban et al. 2012). They have used a wet mixing technique combined with supercritical carbon dioxide foaming to achieve the cellular composites.

Blends of PLA and TPS in various proportions, plasticized by two types of adipate esters were prepared by Shirai et al. (Shirai, Olivato et al. 2016). Sheets were extruded and subjected to mechanical testing, water vapour permeability testing and morphological evaluation. With increase in starch content, the water vapour permeability increased and the mechanical properties decreased. Compared with diethyl adipate, inclusion of diisodecyl adipate (DIA) to the blend resulted in an improvement of the mechanical and barrier properties of the sheets.

2.2.1.2   PLA and natural fibres

The incorporation of natural fibre to a PLA matrix leads to the development of a completely bio-based composite material. The study conducted by Graupner et al(Graupner, Herrmann et al. 2009) showed that incorporation of kenaf and hempfibresinto PLA resulted in an improvement in tensile strength and Young's modulus values of the resulting composites. Cotton/PLA composites exhibited excellent impact properties, whereas, Lyocell/PLA composites possess improved tensile strength, Young's modulus and impact properties. Nettle fibres were used as a reinforcement for PLA by Fischer et al (Fischer, Werwein et al. 2012). They have also compiled the effect of other fibres such as hemp, flax, jute, bamboo, kenaf and ramie as reinforcements for PLA reported by other research groups. A detailed description of the developments in the field of natural fibre reinforced PLA is available in the review article of Faruk et al (Faruk, Bledzki et al. 2012). In addition to the above-mentionedfibres, they have also mentioned the use of natural and man-made cellulose fibres, coir fibres and recycled newspapers as reinforcements for PLA matrix.

The influence of various natural fibres on mechanical properties and biodegradation of PLA was reviewed by White and co-workers(Wahit, Akos et al. 2012). Hu et al(Hu and Lim 2007) prepared completely biodegradable composites of PLA with hemp fibres. Effect of fibre surface treatment with alkali on the properties of the composites was also investigated. It was observed that incorporation of 40 vol% of treated fibres into PLA resulted in optimum mechanical properties of the composites. Alkali treated kenafbastfibre (KBF) was used as a reinforcement for plasticized PLA by Nor Azowa Ibrahim(Nor Azowa Ibrahim, Yunus et al. 2011) and group. The effect of KBF surface treatment on the static and dynamic mechanical properties of the composites was studied in detail. It was observed that 4% of NaOH-treated KBF produced composites with optimum properties. Biocomposites of PLA with banana fibres were prepared by Jandas and group(Jandas, Mohanty et al. 2011). The surface treatment of banana fibre was carried out by NaOH and various silanes and the effect of these treatments on the properties of the composites was also investigated. Jute fibre reinforced PLA was prepared by Hongwei(Hongwei Ma and Chang Whan Joo 2011)

and co-workers. They have investigated the effect of jute fibre content, processing temperature and alkali treatment on the structure and mechanical properties of jute/PLA composites. The morphology of the composite was analysed using SEM. It was found that a fibre content of 15 wt% and a processing temperature of 210°C resulted in optimum tensile properties of the composites. Recently, Smitthipong et al. studied the role of pineapple leaf fibre (PALF) as reinforcement along with TPS and TPS/PLA blend as the matrices(Smitthipong, Tantatherdtam et al. 2013). They have reported that the optimum fibre volume fraction of PALF for tensile strength improvement for TPS based composites is 8%. They have also observed that the tensile strength of TPS withPALF/PLA composite was higher than that of the TPS/PLA blend until 60 wt% of TPS.Beyond this concentration, phase reversion was observed between TPS and PLA. TPS with PALF/PLA composite gavebetter mechanical properties and water resistance than the TPS/PLA blend. The effect of surface treatment of sisal fibres on the properties of PLA/sisal fibre composites was studied by Jiang et al(Jiang, Xi et al. 2012). It was found that the mechanical properties of the fibres, as well as the composites, were greatly influenced by the fibre surface treatment methods. Similar studies were carried out by Zou et al (Zou, Wang et al. 2012) for short sisal fibre reinforced PLA. Akos et al(Akos, Wahit et al. 2013; Akos, Wahit et al. 2013) prepared blends of poly(ε-caprolactone) (PCL) and PLA reinforced with Dura and Tenera palm press fibres. Dicumyl peroxide (DCP) was used as acompatibilizerfor the blend system and resulted in good interfacial adhesion between the matrix and the reinforcements and thereby increased the mechanical properties of the composites. Flax fibre was used as a reinforcement for PLA by Oksman et al (Oksman, Skrifvars et al. 2003). The composite was prepared by extrusion followed by compression moulding. The properties of the composites were compared with that of PP/fax composites, which are widely used in making automobile components. The PLA/flax fibre composites showed 50% better strength compared with the PP counterpart. The SEM micrographs of the fractured surface (figure 2.4) showed that the fibre–matrix adhesion needs to be improved in order to improve the performance properties of PLA/natural fibre composites.
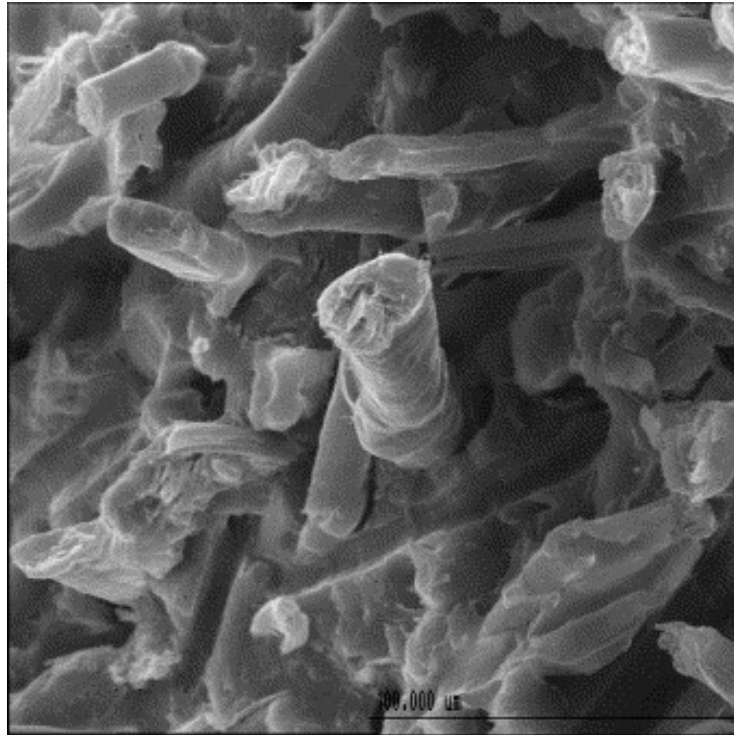
(a)
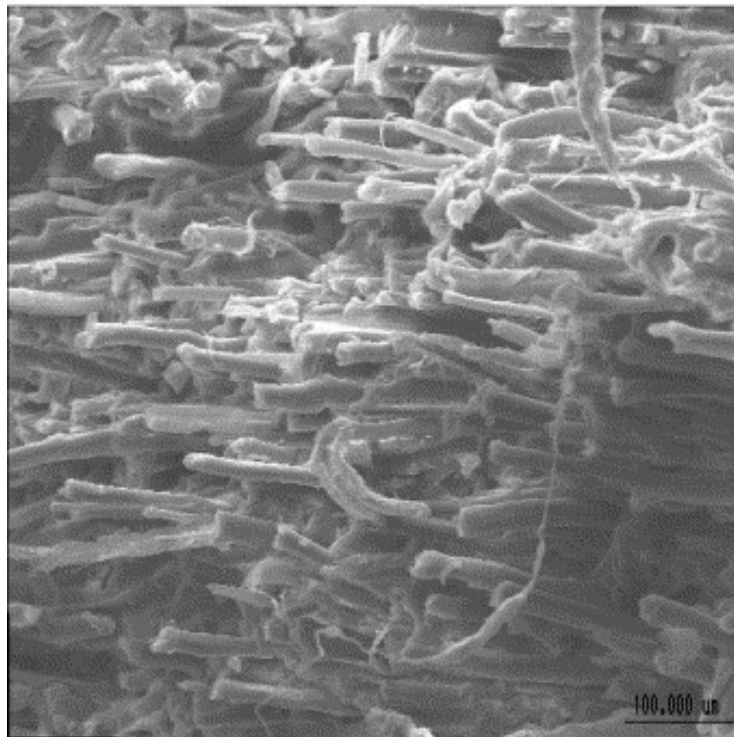
(b)

Figure 2.4SEM micrographs of thefractured surface of PLA/flax fibre composites
a) Detailed view and b) overview clearly showing alack of adhesion between fibres
and the matrix ((Reproduced with permission).

23

Flax fibre reinforced PLA composites were prepared by Alimuzzaman et al(Alimuzzaman, Gong et al. 2013). They have prepared fibre webs offlax and PLA fibresusing an air-laying process.Prepregs were prepared from thesefibre webs and subsequently, these prepregs were converted to composites by compression moulding. It was reported that mechanical properties of the composites were increased as the falxfibre content was increased. Also, the mechanical properties of the composites were decreased with an increase in the moulding time and moulding temperature. Siengchin et al (Siengchin, Pohl et al. 2013) prepared nanocomposites of PLA and woven flax fibre textiles containing nano alumina. TiO_2 grafted flax fibres were used as a reinforcement for PLA by Foruzanmehr et al(Foruzanmehr, Vuillaume et al. 2016). The modified fibres exhibited better adhesion and bonding towards PLA and thereby resulted in a three-fold improvement in the impact resistance of PLA. Also, the water absorption of PLA was reduced by 18% due to the incorporation of modified flax fibres. Wu et al(Wu, Kuo et al. 2013) prepared α-cellulose short-fiber reinforced PLA composites and investigated the isothermal crystallisationbehaviour of these composites. The crystallinity of the composites was greatly improved due to the presence of cellulose fibres. Sugarcane bagasse residues from bio-refinery processes were used as a reinforcement for the production of PLA based green composites by Wang et al(Wang, Tong et al. 2013). The results proved that PLA composite with pretreated residue, in the presence of 2 % coupling agent,exhibited the optimum strength properties. The effect of fibre surface treatments on the performance properties of PLA/jute fibre composites was studied by Goriparthi et al(Goriparthi, Suman et al. 2012). In this study, Jute fibres treated with NaOH solution, permanganate acetone, benzoyl peroxideacetone solution, 3-amino propyl tri-methoxysilane (silane 1) and tri-methoxy methylsilane (silane 2). The tensile and flexural properties of the treated composites showed improvements compared with the untreated composites. The thermal stability of the silane treated fibre composites were higher than the untreatedfibre composites whereas, all other treatments resulted in lower thermal stability for the composites. They have shown that the fiber-matrix adhesion was better in silane 2 treated fibre composites. The SEM images of the untreated composites and silane treated composites are shown in figure 2.5. From the figure, it is clear that the silane 2 treatment improves the fiber-matrix adhesion, and

thereby results in an improvement of the properties of the resulting composites. A recent study by Zafar et al(Zafar, Maiti et al. 2016)describe in detail about various surface treatments and their effects on the interfacial adhesion between jute fibre and PLA.
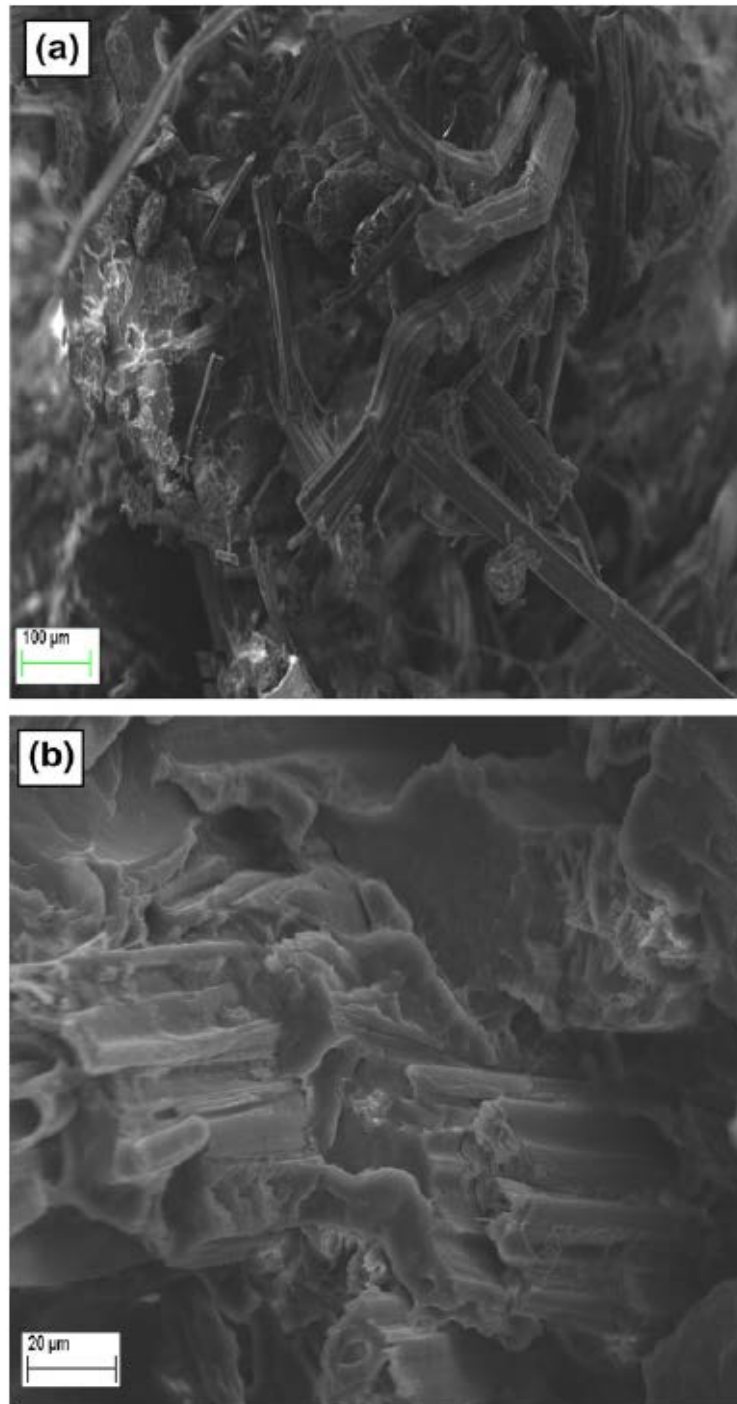
Figure 2.5SEM micrographs of thefractured surface of jute/PLA composites.

a) Before surface treatment, b) after surface treatment (Reproduced with permission)

2.2.1.3   PLA with Poly (ε-caprolactone) (PCL)

Poly (ε-caprolactone) (PCL) is a completely biodegradable polyester. Combining the properties of PCL with PLA attracted theinterest of researchers in recent years. Reasonably good number of publications is available in this area (Grijpma, Zondervan et al. 1991; Dunnen, Schakenraad et al. 1993; Hiljanen-Vainio, Varpomaa et al. 1996; de Groot, Zijlstra et al. 1997; Deng, Zhu et al. 1997; Wang, Ma et al. 1998; Huang, Li et al. 2004; Cohn and Hotovely Salomon 2005; López-Rodríguez, López-Arraiza et al. 2006; Semba, Kitagawa et al. 2006; Takayama, Todo et al. 2006; Harada, Iida et al. 2008; Ren, Yu et al. 2008; Sarazin, Li et al. 2008; Takayama, Todo et al. 2011; Wu, Lin et al. 2011). Composites of poly(ε-caprolactone) (PCL) with PLA fibres were prepared by theresearch group of Ju et al(Ju, Han et al. 2013). They have investigated the influence of PLA fibres on the crystallisation, mechanical properties and enzymatic degradation of its composites with PCL. Salehiyan et al. prepared nanocomposites of PLA/PCL/montmorillonite (MMT) toughened with metallocene-catalyzed linear low-density polyethene (mLLDPE)(Salehiyan, Yussuf et al. 2013). It was proved that 2 phrMMT resulted in improvement of properties owing to the intercalated structure of the clays. Jiao et al(Jiao, Yang et al. 2013) designed a series of PCL/PLA multiblock copolymers by a two-step process and characterised. A block copolymer of poly(ethylene glycol) and poly(propylene glycol) was used as a compatibilizer for PLA/PCL blends by Chavalitpanya et al(Chavalitpanya and Phattanarudee 2013). An 80:20 blend of PLA/PCL was prepared by melt blending and the block copolymer content was varied from 1-10 phr. The blending system was characterised in for morphology, mechanical and thermal properties. It was concluded that 7.5 phr of block copolymer provided a notableimprovement in tensile strain at break compared to that of the neat PLA/PCL blend. Gloria et al describe the use of PCL/PLA blends as scaffolds for bone tissue regeneration(Gloria, Bártolo et al. 2013). The effect of MMT on the non-linear viscoelastic properties of PLA/PCL blends was investigated by Salehiyan et al(Salehiyan and Hyun 2013). Ternary blends of PLA/starch/PCL containing triclosan-loaded polylactic acid (LATC30) nanoparticles was prepared by Davoodi et al. by adopting melt blending technique (Davoodi, Oliaei

et al. 2016). The included nanoparticles improved the compatibility between starch and PLA resulting in an improvement of mechanical properties and also imparted antibacterial properties to the resulting blend, which suggests that the material is an ideal choice for various biomedical applications.

2.2.1.4   PLA with Polyhydroxy butyrate (PHB)

Like PLA, PHB also belongs to the family of biodegradable polyesters and finds its application in various areas due to its biodegradability, biocompatibility and sustainability. It is reported that both PLA and PHB are brittle at room temperature and process poor processing properties(Park, Doi et al. 2004). As part of improving their mechanical properties and processing characteristics, several strategies have been tried by researchers, and blending PLA with PHB is one among them. Blending of PLA with PHB has been carried out by several research groups(Blümm and Owen 1995; Koyama and Doi 1995; Zhang, Xiong et al. 1996; Koyama and Doi 1997; Ohkoshi, Abe et al. 2000; Ferreira, Zavaglia et al. 2002; Focarete, Scandola et al. 2002; Park, Doi et al. 2004; Vogel, Wessel et al. 2007; Vogel and Siesler 2008; Vogel, Hoffmann et al. 2009). These studies proved that the miscibility between PLA and PHB depends on the molecular weight of the minor component in the blend system. In thecase of high molecular weight blend components, PLA is immiscible withPHB in all compositions. Also, it was concluded that the mechanical properties of the blends are intermediate between those ofthe individual blend components. The effect of processing conditions on the miscibility, crystallisation and melting behaviour and morphology of blends of PHB and PLA with and without poly(vinyl acetate) (PVAc) was studied by El-Hadi(El-Hadi 2011). The results showed that PVAc can be used as an effective compatibilizer for immiscible polymer blends of PHB and PLA. Morphology, thermal properties, mechanical properties, and biodegradation behaviour of PLA/PHB blends were investigated by Zhang et al (Zhang and Thomas 2011). The results showed that blending PHBwith PLA is a cost effectivemethod to improve the mechanical properties of PLA as the 75/25 blend of PLA/PHBshowed significantimprovement inmechanical properties compared with pure PLA. The authors correlate this to the observation that finely dispersed PHB

crystals acted as a filler and nucleating agent in PLA. A polyester plasticiser was used for PLA/PHB blend by Abdelwahab et al(Abdelwahab, Flynn et al. 2012) and the blend system was characterised by TGA, DSC, XRD, SEM, mechanical testing and biodegradation studies. The rheological properties and the morphology of PLA/poly(hydroxybutyrate-co-hydroxyvalerate) (PHBV) blends were studied by Gerard et al(Gerard and Budtova 2012). Zhao et al. also (Zhao, Cui et al. 2013)blended PHBV with PLA. They have also prepared PLA/PHBV/clay nanocomposites and applied conventional and microcellular injectionmoulding processes to produce solid and microcellular specimens. Bartczak et al(Bartczak, Galeski et al. 2013) prepared blends of Poly(lactide) and amorphous poly([R,S]-3-hydroxy butyrate) for packaging applications and characterised by DSC, TGA, SEM, WAXS, DMTA and tensile tests. The effects of PHB and talc on the non-isothermal cold crystallisation kinetics of PLA were investigated by Tri et al(Tri, Domenek et al. 2013). They have reported a synergistic nucleating effect of PHB and talc on isothermal crystallisation of PLA from the melt. The effect of gamma irradiation on the morphology and performance properties of PHBV/PLA blends were reported by Idris et al (Zembouai, Kaci et al. 2016). PHBV-*g*-MA was used as a compatibilizer and organomodified montmorillonite was used as a reinforcing filler with the blends. It was reported that the mechanical properties of the blends did not decrease noticeably even with a radiation dosage of 100kGy. The loss in thermal stability and fire retardancy of the irradiated blends were compensated by the compatibilizing effect of organomodified clay. They have further assessed the safe dosage of irradiation of the blends and found that at 10 kGy, the samples were completely safe. And moreover, the samples exhibited complete non-toxicity under ecotoxicity testing (Zembouai, Kaci et al.).

2.2.1.5   PLA with Polyvinyl alcohol (PVOH)

Polyvinyl alcohol (PVOH) is a water soluble and biodegradable synthetic polymer. Melt blending of PLA with PVOH can give rise to a partially miscible biodegradable blend system with improved flexibility than virgin PLA(Yeh, Yang et al. 2008). However, solution blending of PVOH with PLA leads to an immiscible blend when

the PLA content in the blend system is more than 60 wt%(Shuai, He et al. 2001; Tsuji and Muramatsu 2001). Molecular modelling simulations and thermodynamic approaches were utilised for predicting the compatibility of PLA/PVOH blend system by Jawalkar et al (Jawalkar and Aminabhavi 2006). Enzymatic and non-enzymatic hydrolysis of blends of PLA and PVOH were investigated by Tsuji et al(Tsuji and Muramatsu 2001). Use of PVOH as a compatibilizer for starch/PLA blend system was investigated byTianyi et al(Ke and Sun 2003). It was observed that above 30wt%, PVOH formed a continuous phase with starch. The optimum tensile strength of starch/PLA blends was obtained at a PVOH addition of 40 wt%. 70/30 blends of PVOH and PLA were melt spun into continuous nanofibrils of average diameter 60 nm by An Tran et al(An Tran, Brünig et al. 2013). The PVOH was subsequently removed from the fibre. This process produced 2D and 3D PLA textile structures suitable for scaffolds in tissue engineering. Hu et al(Hu, Wang et al. 2013) prepared composite films from starch-g-PLA/PVOH. In the first step, starch-g-PLA was prepared by in situ copolymerization of starch grafted with lactic acid catalysed with sodium hydroxide. This was then mixed with PVOH to get composite films. It was observed that the compatibility, mechanical properties and thermal stability of the composite film was improved compared with Starch/PVA film.

2.2.2 Blends and composites of PLA with polyolefins

The blending of PLA with polyolefins is carried out by several researchers as a method to improve the resistance to hydrolysis and biodegradation, and also to toughen PLA. But the main barrier in blending polyolefins with PLA is the formation of an immiscible blend due to the lack of chemical interactions between the blend components. Wang et al(Wang and Hillmyer 2001) prepared solution blend of LDPE and PLA using a diblock copolymer (PE-b-PLLA) as the compatibilizer. The particle size and distribution of the dispersed phase (LDPE) was observed to decrease sharply and the mechanical properties were significantly improved with the incorporation of the diblock copolymer. Anderson et al(Anderson, Lim et al. 2003) carried out melt blending of linear low-densitypolyethylene (LLDPE) with PLA. Polylactide-polyethylene (PLLA-PE) block copolymers were used as compatibilizers for the

blend. Young et al(Kim, Choi et al. 2004) used PE-g-GMA as a reactive compatibilizer for the immiscible blend system consisting of LLDPE and PLA. For PLA matrix blends, the reactive compatibilizer reduced the domain size of thedispersed phase (LLDPE) and enhanced the tensile properties of the blend. In an attempt to improve the dyeability and resistance to biodegradation and hydrolysis of PLA, Reddy et al(Reddy, Nama et al. 2008) prepared polyblend fibres of PP and PLA. Polypropylene-*graft*-poly(methyl methacrylate) (PP-*g*-PMMA) graft copolymers were synthesised as effective compatibilizers for PP/PLA blends by Kaneko et al(Kaneko, Saito et al. 2009). Tensile and flexural strength and modulus of the PP/PLA blends were significantly improved by adding PP-*g*-PMMA, whereas, the compatibilizer could not succeed in improving the izod impact strength and elongation at break of the blends. Choudhary et al.also used Maleic anhydride grafted PP(MAH-g-PP) and glycidyl methacrylate in PLA/PP blends as reactive compatibilizers(Choudhary, Mohanty et al. 2011). Recently, ZuzannaDonnelly patented the technology related to the blends of PLA with polyolefins(Donnelly 2010). Hong et al(Hong 2012) patented the process for thepreparation of eco-friendly PP/PLA composite composition containing a compatibilizer. Rheological and mechanical properties of PP/PLA blends werecharacterised by Hamad et al(Hamad, Kaseem et al. 2011). The rheological measurements showed that the true viscosity of the blends was in between the viscosity of neat PP and PLA, whereas, the mechanical properties clearly indicated the incompatibility between PP and PLA.

Polyblends of PP and PLA in the ratio 80:20 were prepared by Yoo et al (Yoo, Yoon et al. 2010). Polypropylene-g-maleic anhydride (PP-g-MAH) and styrene-ethylene-butylene-styrene-g-maleic anhydride (SEBS-g-MAH) were used as compatibilizers. It was reported that at 3 wt% of PP-g-MAH content, the tensile strength reached a maximum value and the tensile strength did not change appreciably even after hydrolysis. Ternary blends of PP, PLA and a toughening modifier in the ratio 60:30:10 were prepared by Lee et al (Lee and Kim 2012). PP-g-MAH and polyethylene-g- glycidyl methacrylate (PE-g-GMA) and a hybrid compatibilizer composed of these two were incorporated into the ternary blends in various ratios. It was reported that 3 wt% of the hybrid compatibilizer enhanced the mechanical

properties of the ternary blend before and after hydrolysis. Recently, the effectiveness of ethylene−glycidyl methacrylate−methyl acrylate terpolymer(PEGMMA) as a reactive compatibilizer for PLA and PP blends (in the ratio 90:10) was reported by Xu et al (Xu, Loi et al. 2015). This compatibilization strategy resulted in reduced interfacial tension, enhancement of tensile toughness and elongation at break of the resulting polyblend system. The isothermal crystallisation process of PLA and PP blends with and without MA-g-PP was studied by Bai et al (BAI and DOU 2015). It was shown that blending PLA with PP resulted in a reduction in the size of spherulites and the presence of MA-g-PP in blends of PLA with PP promoted the growth of spherulites during the crystallisation process. The effect of ethylene-butyl acrylateglycidyl methacrylate terpolymer (EBA-GMA) as a compatibilizer for 70:30 blend of PLA and PP was investigated by Kang et al (Kang, Lu et al. 2015). Based on the mechanical properties, it was shown that at 2.5 wt% of EBA-GMA, the tensile strength of the blend reached a maximum, whereas, the impact strength showed a steady increase with anincrease in compatibilizer content.

Kim et al (Kim and Kim 2013) prepared natural-flour-filled PP/PLA bio-composites. Bamboo flour and wood flour were used as the reinforcing filler. Modifications of these natural flours were carried out by treating them with maleic anhydride-grafted PP and acrylic acid-grafted PP. Tensile and flexural strengths of biocomposites were found to improve as a result of themodification. In a similar investigation, oat hull fibrewas used as reinforcement for PP/PLA based biocomposites by Reddy et al(Reddy, Misra et al. 2013). They have prepared a PP/PLA (90/10) blend reinforced with 30 wt% oat hull and investigated the effect of ethylene propylene-g-maleic anhydride (EP-g-Ma) as a compatibilizer for this biocomposite. Nunez et al(Nunez, Rosales et al. 2011) prepared PLA/PP blends compatibilized by four different grafted polymers and subsequently prepared their nanocomposites with Sepiolite. The blend containing grafted metallocene polyethylene as the compatibilizer exhibited the highest tensile toughness. The incorporation of Sepiolite into the compatibilized blend resulted in an improvement in mechanical properties, complex viscosity and storage modulus compared with similar nanocomposites containing only PLA as the matrix. Gallego et al synthesised three random copolymers of PLA and PE and studied their

effectiveness as compatibilizers for PLA-HDPE blends(Gallego, López-Quintana et al. 2013). The compatibilizers were prepared by three different methods: reactive extrusion, ring-opening polymerization and polycondensation of lactide with PE. The PLA-HDPE blends containing the compatibilizer prepared by ring opening polymerization of lactide with PE exhibited the highest tensile toughness.

Table 2-2 Recent literature related to the present investigations

S. No.	Description of the investigation	Result	Reference
1.	Preparation of polyblend fibres of PP and PLA.	The inclusion of PP to PLA resulted in an improvement in the dyeability and resistance to biodegradation and hydrolysis of PLA.	Reddy et al. (Reddy, Nama et al. 2008)
2.	Polypropylene-*graft*-poly (methyl methacrylate) (PP-*g*-PMMA) graft copolymers as effective compatibilizers for PP/PLA blends	Tensile and flexural strength and modulus of the PP/PLA blends were significantly improved by adding PP-g-PMMA, whereas, the compatibilizer could not succeed in improving the Izod impact strength and elongation at break of the blends.	Kaneko et al. (Kaneko, Saito et al. 2009).
3.	Maleic anhydride grafted PP (MAH-g-PP) and glycidyl methacrylate in PLA/PP blends as reactive compatibilizers	Improved the compatibility between PP and PLA	Choudhary et al. (Choudhary, Mohanty et al. 2011).
4.	The technology related to the blends of PLA with polyolefins	Patent	Zuzanna Donnelly (Donnelly 2010).
5.	The process for the preparation of eco-friendly PP/PLA composite composition containing a compatibilizer.	Patent	Hong et al (Hong 2012)
6.	Characterization of rheological and mechanical properties of PP/PLA blends.	The rheological measurements showed that the true viscosity of the blends was in between the viscosity of neat PP and PLA, whereas, the mechanical properties clearly indicated the incompatibility between PP and PLA.	Hamad et al (Hamad, Kaseem et al. 2011).
7.	Polyblends of PP and PLA in the ratio 80:20.Polypropylene-g-maleic anhydride (PP-g-MAH) and styrene-ethylene-butylene-styrene-g-maleic anhydride (SEBS-g-MAH) were used as compatibilizers.	At 3 wt% of PP-g-MAH content, the tensile strength reached a maximum value and the tensile strength did not change appreciably even after hydrolysis.	Yoo et al. (Yoo, Yoon et al. 2010).

8.	Ternary blends of PP, PLA and a toughening modifier in the ratio 60:30:10 PP-g-MAH and polyethylene-g- glycidyl methacrylate (PE-g-GMA) and a hybrid compatibilizer composed of these two were incorporated into the ternary blends in various ratios.	3 wt% of the hybrid compatibilizer enhanced the mechanical properties of the ternary blend before and after hydrolysis.	Lee et al. (Lee and Kim 2012).
9.	The effectiveness of ethylene−glycidyl methacrylate−methyl acrylate terpolymer (PEGMMA) as a reactive compatibilizer for PLA and PP blends (in the ratio 90:10)	This compatibilization strategy resulted in reduced interfacial tension, enhancement of tensile toughness and elongation at break of the resulting polyblend system	Xu et al. (Xu, Loi et al. 2015).
10.	Investigation of the isothermal crystallisation process of PLA and PP blends with and without MA-g-PP	Blending PLA with PP resulted in a reduction in the size of spherulites and the presence of MA-g-PP in blends of PLA with PP promoted the growth of spherulites during the crystallisation process.	Bai et al. (BAI and DOU 2015).
11.	The effect of ethylene-butyl acrylate glycidyl methacrylate terpolymer (EBA-GMA) as a compatibilizer for 70:30 blend of PLA and PP	Based on the mechanical properties, it was shown that at 2.5 wt% of EBA-GMA, the tensile strength of the blend reached a maximum, whereas, the impact strength showed a steady increase with an increase in compatibilizer content.	Kang et al. (Kang, Lu et al. 2015).
12.	Preparation of natural-flour-filled PP/PLA bio-composites. Bamboo flour and wood flour were used as the reinforcing filler. Modifications of these natural flours were carried out by treating them with maleic anhydride-grafted PP and acrylic acid-grafted PP.	Tensile and flexural strengths of biocomposites were found to improve as a result of the modification.	Kim et al. (Kim and Kim 2013)
13.	Oat hull fibre as a reinforcement for PP/PLA based biocomposites. PP/PLA	Investigated the effect of ethylene propylene-g-maleic anhydride (EP-g-Ma) as a compatibilizer for this biocomposite.	Reddy et al. (Reddy, Misra et al. 2013).

	(90/10) blend reinforced with 30 wt% oat hull.		
14.	PLA/PP blends compatibilized by four different grafted polymers and subsequently prepared their nanocomposites with Sepiolite.	The blend containing grafted metallocene polyethene as the compatibilizer exhibited the highest tensile toughness. Incorporation of Sepiolite into the compatibilized blend resulted in improvement in mechanical properties, complex viscosity and storage modulus compared with similar nanocomposites containing only PLA as a matrix.	Nunez et al. (Nunez, Rosales et al. 2011)
15.	PLA melt blended with PP using liquid natural rubber (LNR) as a compatibilizer in the ratio PLA/PP (90/10), PLA/PP/LNR (90/10/10)	Mechanical properties such as elongation at break, flexural strength and impact strength improved considerably with the incorporation of LNR as a compatibilizer to immiscible blend of PLA and PP.	Bijarimi et al. (Bijarimi, Piah et al. 2012)
16.	PP/PLA blends compatibilized with MA-g-PP prepared by melt blending technique.	6 wt% of MA-g-PP was found as the optimum compatibilizer content for the blend based on the evaluation of mechanical, chemical, morphological,and thermal properties. Bacterial degradation studies and subsequent thermal analysis showed that the blend is prone to biodegradation by microorganisms.	Jain et al. (Jain, Madhu et al. 2015)
17.	PP/PLA blends compatibilized with 16 phr of MA-g-PP	The nonisothermal crystallization kinetics of the blends were studied by applying Jeziorny's and Mo's models and the crystallization parameters were calculated by Lauritzen–Hoffman equation and Kissinger's equation. The blend exhibited fastest crystallization rate due to the nucleatingcapability of the dispersed PLA phase in the matrix of PP. The incorporation of MA-g-PP resulted in a reduction in the crystallization of PP.	Bai et al. (Bai and Dou)

2.3   Halloysite nanotubes (HNT) in polymer composites

As mentioned in chapter-1, HNT based polymer nanocomposites are attracting much attention in the recent years. The reasons behind their widespread application in polymer composites are their tubular structure and high aspect ratio. The typical properties of HNTsthat are very much relevant for their application in polymers can be summarised in table 2.3(Liu, Jia et al. 2014)

Table 2-3Typical properties of HNT

Sl. No.	Material aspects	Values
1	Chemical formula	$Al_2Si_2O_5(OH)_4 \cdot nH_2O$
2	Outer diameter	40–70 nm
3	Inner diameter	10–40 nm
4	Length	0.2–2 μm
5	Aspect ratio (L/D)	10–50
6	Elastic modulus	140 GPa
7	Particle size range in aqueous solution	50–400 nm
8	Density	2.14–2.59 g/cm^3
9	Average pore size	79.7–100.2 A$^{\circ}$
10	Pore space	14–46.8%

Due to their interesting set of properties and easy availability compared with other nanotubular reinforcing fillers, almost all commercially available polymer matrixes were reinforced with HNTs and the properties of these nanocomposites were reported in the literature. A summary of some of the interesting studies on HNT based nanocomposites is given in table 2.4. HNT reinforced nanocomposites of Polylactic acid (PLA) was prepared by various research groups. Prashantha et al (Prashantha, Lecouvet et al. 2013)prepared the nanocomposites of PLA with HNT using a masterbatch route with HNT various content (2, 4 and 6 wt%) . They have compared the effect of unmodified and quaternary ammonium salt modified HNT on various properties of the resulting nanocomposites. Mechanical properties of the nanocomposites exhibited significant improvement with the incorporation of HNT

and showed much better improvement with theincorporation of modified HNT. In another study, Murariu et al (Murariu, Dechief et al. 2012) prepared PLA/HNT composites containing 3 to 12 wt% HNT (both unmodified and silane modified HNTs). The nanocomposites exhibited higher mechanical properties compared to virgin PLA with no reduction in elongation at break and impact strength which is noticeable. The surface treatment of the HNT resulted in an improvement of filler dispersion in the matrix in all loadings. In this way, the impact properties were also improved.Nanocomposites of HNT and PLA were prepared by Liu et al (Liu, Zhang et al. 2013). They have prepared the nanocomposites with HNT content varying from 5 to 40 wt% with an increment of 5 wt%. The FTIR studies revealed hydrogen bonding interactions between PLA and HNT. Static and dynamic mechanical analysis revealed higher mechanical properties of the composites compared with virgin PLA. The softening temperature and thermal degradation characteristics significantly improved with the incorporation of HNTs. Yu Dong et al (Dong, Marshall et al. 2015) prepared composite mats of PLA with HNT (0, 1, 5 and 10 wt%) by adopting electrospinning technique. The effect of modification of HNT was also studied by them. From XRD results, it was observed that PLA resulted in an interaction of HNT tubes and the molecules of PLA were attached to the outer surface of HNT. The surface modification of HNT resulted in an improvement in the mechanical properties. The cold crystallisation temperature and thermal stability of PLA were improved with theincorporation of HNT. Recently, Cai, Ning et al (Cai, Dai et al. 2015) prepared nanofiber scaffolds of PLA with HNT and studied their mechanical properties. The results showed that at 4 wt% of HNT addition, the nanofibers exhibited the optimum mechanical property which is attributed to the excellent dispersion of HNT in the PLA matrix. The thermal stability and degree of crystallisation of the nanocomposites were also improved suggesting that the nanofibers are apotential candidate for tissue engineering applications.Chen et al (Chen, Geever et al. 2015) prepared HNT/PLA composites and thoroughly characterised the nanocomposites by atensile test, FTIR, DSC, TGA, contact angle studies and SEM. The overall mechanical properties showed significant improvement, whereas, the thermal stability of PLA was decreased with the addition of HNT and this was attributed to the presence of voids between the filler and the matrix.

Alkalized halloysite nanotube (HNTa)were incorporated into PLA by melt blending technique by Guo et al(Guo, Qiao et al. 2016). The nanocomposites exhibited higher mechanical and thermal properties compared with unmodified HNT/PLA composites. FTIR studies revealed hydrogen bonding interaction between PLA and HNT.

HNT based nanocomposites of PP is also a study of great interest in the recent years. Prashantha et al (Prashantha, Lacrampe et al. 2011) prepared PP/HNT nanocomposites by adopting a masterbatch route. Both unmodified and quaternary ammonium salttreated HNTs were incorporated into PP. Excellent distribution of nanotubes in PP matrix was observed. Mechanical properties of PP improved with the addition of HNT and it was reported that 6 wt% of HNT showed optimum properties. Modified HNT showed better properties compared with unmodified HNT. Du et al(Du, Guo et al. 2007) studied the kinetics of thermal decomposition and thermal ageing behaviour of HNT reinforced PP. The activation energy for thermal degradation increased with increase in HNT content. The silane modified HNT showed improvement in resistance to oxidative ageing. Thermal stability and flammability characteristics of PP/HNT composites were investigated by Du et al(Du, Guo et al. 2006). The incorporation of HNT resulted in a remarkable improvement of thermal stability and decrease in flammability of the resulting nanocomposites. The crystallisationbehaviour of PP/HNT nanocomposites were investigated by various research groups (Ning, Yin et al. 2007; Du, Guo et al. 2010;Wang and Huang 2013). HNT acted as a nucleating agent and thereby resulted in improvement of crystallisation rate and crystallisation temperature of PP.The nucleating effect of HNT for PP was also investigated by Liu et al (Liu, Guo et al. 2009). Tailoring of surface microstructure and thereby the wettability characteristics of PP by incorporation of HNT were reported by Liu et al (Liu, Jia et al. 2010). They have concluded that the size of the spherulites, surface roughness and the surface wetting characteristics of PP can be fine-tuned by proper incorporation of HNT. The effect of various surface modifiers of HNT on the properties of PP/HNT composites were investigated by Khunova et al (Khunova, Kristof et al. 2013). They have reported that urea-modified HNT containing 4,4'-diphenylmethylenedimaleinimide (DBMI) modifier showed thehighest improvement in mechanical properties.1, 3, 5 and 7 wt.% of HNT were

incorporated to PP by Agnieszka et al (Szczygielska and Kijeński 2011). The degree of crystallinity was reported to show a decrease with increase in HNT content. The surface modified HNT resulted in an improvement in mechanical and thermal properties of the composite.

Table 2-4Polymer nanocomposites containing HNT

Polymer	HNT content	Property investigated	Reference
HDPE	0 to 10 wt%	Morphology, rheology, mechanical and thermal properties	(Singh, Vimal et al. 2016)
LLDPE	0 to 8 wt%	Mechanical thermal and rheological properties and effect of surface treatment of HNT	(Pedrazzoli, Pegoretti et al. 2015)
LDPE		Diffusion of organic volatile molecules through nanocomposites	(Reyes-Alva, Gonzalez-Montiel et al. 2014)
PP	0 to 30 wt %	Morphology, rheology, mechanical and thermal properties	(Prashantha, Lacrampe et al. 2011, Du, Guo et al. 2007, (Du, Guo et al. 2006, Ning, Yin et al. 2007; Du, Guo et al. 2010; Wang and Huang 2013, Liu, Guo et al. 2009, Liu, Jia et al. 2010, Khunova, Kristof et al. 2013, Szczygielska and Kijeński 2011)
NR	0 to 40 phr	Mechanical and thermal properties	(Rooj, Das et al. 2010; Ismail, Salleh et al. 2013)
SBR	0 to 60 phr	Mechanical, structural,	(Rybinski,

		thermal and morphological characterizations	Janowska et al. 2012; Jia, Xu et al. 2016)
EPDM	0 to 100 wt%	Curing behaviour, thermal stability, flammability and mechanical properties	(Ismail, Pasbakhsh et al. 2008; Pasbakhsh, Ismail et al. 2010; Azarmgin, Kaffashi et al. 2015)
PLA	0 to 30 wt%	Thermal, mechanical and rheological properties	(Prashantha, Lecouvet et al. 2013, Murariu, Dechief et al. 2012, Liu, Zhang et al. 2013, Dong, Marshall et al. 2015, Cai, Dai et al. 2015, Chen, Geever et al. 2015, Guo, Qiao et al. 2016)
PCL	0 to 5 wt%	Thermal, mechanical, visoelastic and morphological properties	(Khunová, Kelnar et al. 2015; Kelnar, Kratochvíl et al. 2016; Lahcini, Elhakioui et al. 2016)

2.4   Problem identified from literature review

The literature shows that PP rich blend with a compatibilizer which can interact with both PLA and PP can produce a superior material with tailor-made properties. Hence, blends of PP and PLA with PP as a major component was selected for investigations. PP and PLA blends in the ratio 90:10. 80:20 and 70:30 were prepared. Based on their mechanical properties 80:20 blend was selected for further investigations. The blend was compatibilized by using Maleic anhydridegrafted PP (MA-G-PP) as a reactive compatibilizer. The present investigation is an advancement over the work carried out by Yoo et al (Yoo, Yoon et al. 2010). They have prepared a compatibilized blend of

PP and PLA in the ratio 80:20 using MA-G-PP as a reactive compatibilizer. They have evaluated the tensile strength of the blends before and after hydrolysis and found no change in the values. A comparison of the recent literature related to the present investigations is given in table 2.2.Also, HNT reinforced polymer composites are promising class of materials with anexcellent set of mechanical and thermal properties. The compatibilized blend of PP and PLA which contain optimum compatibilizer can be selected as the base matrix for reinforcement with HNTs. The composites preparation and thorough characterization of the blends and composites are described in detail in this thesis

CHAPTER-3

MATERIALS AND EXPERIMENTAL METHODS

3.1 Selection of the materials

Selection of the suitable materials plays a very important role in deciding the final properties of polymer blends and composites. The materials used in the present investigation are described below.

3.2 Materials

Polypropylene (PP) [500P, SABIC, MFR – 3g/10 min., 230ºC, 2.16 kg load] was supplied by SABIC, Yanbu, Kingdom of Saudi Arabia. Polylactic acid (PLA) [PURAPOL L100IXS, MFR – 50g/10 min., 210ºC, 2.16 kg load] used in the study, a homopolymer of L-Lactide, was supplied by Purac Biochem BV, Netherlands. Compatibilizer used in the study was maleic anhydride grafted PP (MA-g-PP, OPTIM P-408, MFR – 50g/10 min., 190ºC, 2.16 kg load), procured from Pluss Polymers Pvt. Ltd., Haryana, India. Halloysite nanotubes as a 30% master batch in PP (Pleximer) were obtained from NaturalNano, Inc, Rochester, NY. Table 3.1 describes the various materials used in the present investigation.

Table 3-1 Raw materials used

S. No.	Raw material	Source
1.	Polypropylene (PP) 500 P	SABIC, Saudi Arabia
2.	Polylactic acid (PLA), PURAPOL L100IXS	Purac Biochem bV, Netherlands
3.	Compatibilizer; Maleic anhydride grafted PP (MAGPP) (OPTIM P-408)	Pluss Polymers Pvt. Ltd., Haryana, India.
4.	HNT Powder and Pleximer PP1 (Halloysite nanotube-30% master batch in PP)	Natural Nano, Inc, NY, USA

3.3 Blend preparation

Polypropylene (PP), Polylactic acid (PLA) and Maleic anhydride grafted PP (MA-g-PP) were dried at 55°C for 6h prior to the blend preparation. After drying, the polymers were mixed together using a tumble mixer. Blends of PP and PLA in the ratio 80:20 was prepared using a single screw extruder (ME 20/2800 V3, OCS GmbH) with L/D ratio 25 and a screw speed of 200 rpm with a 5 zone temperature profile ranging from 190°C to 230°C. Compatibilizer was varied from 0 to 5 wt%. The strands from the extruder were passed through a water bath, dried and subsequently pelletized using an attached pelletizer.

3.4 Composite preparation

The nanocomposites were prepared by melt mixing technique using Haake Polylab Rheomix 600P equipped with roller rotors. The temperature for mixing was set as 190oC and rotor speed was 60 rpm. PP and PLA were introduced first to the chamber, melted and mixed well for 1 minute and then the compatibilizer (MA-g-PP) was added followed by HNT and mixed thoroughly. The total mixing time was 5 minutes for the blends and 7 minutes for the nanocomposites. HNT content was varied from 0 to 10 wt% and the resulting composites were designated as shown in Table 3.2.

Table 3-2Designation of nanocomposites

Sample	Designation
80:20:3 (PP:PLA:MA-g-PP) blend without HNT	HNT 0
80:20:3 (PP:PLA:MA-g-PP) blend with 1 wt% HNT	HNT 1
80:20:3 (PP:PLA:MA-g-PP) blend with 2wt% HNT	HNT 2
80:20:3 (PP:PLA:MA-g-PP) blend with 4 wt% HNT	HNT 4
80:20:3 (PP:PLA:MA-g-PP) blend with 6 wt% HNT	HNT 6
80:20:3 (PP:PLA:MA-g-PP) blend with 8 wt% HNT	HNT 8
80:20:3 (PP:PLA:MA-g-PP) blend with 10 wt% HNT	HNT 10

3.5 Test specimen preparation

The neat polymers and their blends were dried at 55ºC for 6 hours.Samples for static and dynamic mechanical property evaluation were injection moulded into type 5 test specimens as per ASTM D638 using a Thermo Haake MiniJet injection moulding machine.

3.6 Characterization of blends and composites

3.6.1   Static mechanical property testing

The mechanical properties were obtained using universal testing machine (ZwickProLine Z010TN) at 25 ± 2^{0}C according to ASTM D638.Five specimens were tested for each sample and the average values of tensile strength, tensile modulus and elongation at break were reported.

3.6.2   Dynamic mechanical analysis (DMA)

The dynamic mechanical properties (viscoelastic properties) of the blends and composites were measured using a TTDMA (Triton Technology Ltd, UK). Rectangular samples of dimension 15 x 10 x 4 (length x width x thickness) were tested in 3 points bending mode at a constant frequency of 1 Hz. The temperature was varied from -40ºC to +12ºC at a rate of 3ºC/minute. The viscoelastic properties such as storage modulus, loss modulus and loss tangent (tan δ) were obtained against the temperature.

3.6.3   Fourier transform infrared spectroscopy (FTIR)

FTIR spectra of the blends and composites were recorded with a Nicolet iS 5 FTIR spectrometer (Thermo Haake). The spectra in the range of 4000 to 400 cm^{-1} were recorded with a resolution of 4 cm^{-1}.

3.6.4 Wide angle X-ray scattering

Wide-angle X-ray scattering (WAXS) patterns of the virgin materials, the prepared blends and nanocomposites were collected using Cu Ka radiation (λ = 1.54 nm) generated by a benchtop X-ray diffractometer (Rigaku MiniFlex 600) operated at 30 kV and 10 mA.

3.6.5 Differential scanning calorimetry (DSC)

The melting and the crystallisation behaviour of the blends were analysed using a Differential scanning calorimeter (DSC) [TA instruments DSC-Q 1000]. Samples of approximately 5 to 8 mg were accurately weighed. The samples were heated from 25 to 240 °C, held at 240 °C for 2 minutes to erase the thermal history of the samples and then cooled to 25 °C at a constant rate of 5, 10, 15 and 20 °C per minute respectively. All the experiments were carried out under a nitrogen atmosphere (50 ml/min). For the nanocomposites, the experiments were performed from 25 to 200 °C, held at 200 °C for 2 minutes and then cooled to 25 °C and again heated to 200 °C. All these were performed at a constant heating/cooling rate of 10 °C per minute.

3.6.6 Thermogravimetric analysis (TGA)

Thermogravimetric analysis (TGA) of the blends and nanocomposites were carried out using TA instruments TA-SDT 2960. Samples of 10 ±5 mg were heated from ambient temperature to 600°C under an air atmosphere (50 ml/min) at a heating rate of 10°C /min and sample weight loss were continuously recorded against the sample temperature. Heating rates of 5, 10, 16 and 22°C /min were used to study the thermal degradation kinetics of the blends.

3.6.7 High shear rheology

Capillary rheometry was used to understand the high shear rheology of the prepared blends and composites. Rosand Advanced Rheometer System (RH 2200, Malvern Instruments, UK) with twin-bore capability was used for this purpose. Experiments were carried out using a 20 mm long die (L/D – 20 mm) in the left bore and orifice die (zero length die) of the same diameter (1 mm) in the right bore. The shear rates were varied from 10 to 5000 s^{-1} at 220ºC. Bagley and Rabinowitsch corrections (Cogswell 1981) were performed automatically in order to account for the pressure drop at the capillary entry and the shear rate at the wall of the barrel respectively.

In order to calculate the extensional viscosity (η_e) based on the shear viscosity data, Cogswell converging flow method (Cogswell 1972) was used. The assumption necessary for this model is that the apparent shear viscosity (η_a) depends on the apparent shear rate (γ) following a power-law model and $\eta_e$is independent of the extensional rate (ε). Then the following equations are applied (Cogswell 1972):

$$\varepsilon = \frac{4\,\eta_a\gamma^2}{3\,(n+1)\Delta P_e} \tag{3.1}$$

$$\eta_e = \frac{9\,(n+1)^2\Delta P_e{}^2}{32\eta\gamma\,2} \tag{3.2}$$

Where, n is the power law index and ΔP_e is the inlet pressure in the capillary in relation to the shear rate according to Bagley correction. All these data analyses were performed using Rosandrheometer control software (version 8.60)

3.6.8 Dielectric analysis

Dielectric analysis of the composite samples was performed using DEA 288 Epsilon (Netzsch-GMBH) dielectric analyser equipped with a DEA furnace. The sensor used was interdigitated comb type electrode sensor (IDEX). Rectangular sample of dimension 25mmX12.5mmX3mm was placed on the sensor surface and kept inside

the furnace. The sample was tightly kept on the sensor surface using Kapton adhesive tape. This step ensured excellent contact of the sample with the sensor surface. The test was carried out from 1 Hz to 1 kHz over a temperature range from 30 °C to 120 °C.

3.6.9   Polarised optical microscopy

The morphologies and growth of spherulites in the composites were observed and recorded using Zeiss AxioCam MRc 5 polarised optical microscope (POM) equipped with Linkam hot stage. Samples in the form of the thin film were placed between two glass slides, melted to 210 $^{\circ}$C and held for 2 minutes to erase the thermal history of the samples. The samples then cooled to their respective crystallisation peak temperature (obtained from DSC cooling curves) at a cooling rate of 1 $^{\circ}$C min^{-1} to record their final crystallite morphology.

3.6.10 Transmission electron microscopy (TEM)

The morphology of the nanocomposites and the dispersion of HNT in the matrix were observed using a transmission electron microscope (TEM, JEOL JEM-2100, 200 kV).

CHAPTER-4

MECHANICAL AND DYNAMIC MECHANICAL ANALYSIS OFTHE BLENDS AND NANOCOMPOSITES

4.1   Introduction

Understanding the mechanical properties of the materials is very much essential not only for the new material development but also for deciding the processing operations and the final applications. There are a set of required mechanical properties to be satisfied by polymer materials to enable them to be preferred for some specific applications. The mechanical properties can easily be correlated to the structure of the polymers and also to the presence and effect of other additives such as fillers or other modifiers incorporated into the polymer matrix.

In static mechanical tests, a static force is applied to a specimen and the resulting strain is monitored to get the required information from the tests. The applied force is commonly known as stress and denoted as σ and the deformation (strain) as γ. The slope of the stress-strain curvehelps us to get the relationship betweenstress tostrain and is considered as a measure of the material's stiffness, otherwise known as the modulus of the material. The modulus very much depends on the applied stressand the temperature at which the experiment was carried out. The modulus provides a rough indication of the suitability of the material forcertain specific applications in the real world (Menard 2008).

In dynamic mechanical tests, the force is applied in anoscillating manner and the material's response to this oscillating force is monitored and analysed. From thedynamic mechanical analysis, complex modulus(E^*), an elastic modulus (E'), and loss modulus (E'')are obtained from the material's response to the appliedoscillating force. The elastic modulus (E') shows the ability of the material to store the energy, loss modulus (E'') shows the energy lost and the ratio of E'' to E' provides tan delta (tan δ) or damping coefficient. In DMA, the experiments can be performed at various frequencies (frequency sweep) or at different temperatures (temperature sweep). The

temperature corresponding to tan δ peak is considered as the glass transition temperature (T_g). The T_g obtained from DMA is much more accurate than the T_g obtained from differential scanning calorimetry (DSC) (Sperling 2005).

4.2   Experimental procedure

4.2.1   Static mechanical test

The static mechanical properties were obtained using theuniversal testing machine (ZwickProLine Z010TN) at 27^0C. The neat polymers, their blends and the nanocomposites with HNT were dried at 55ºC for 6 hours and then injection moulded into type 5 test specimens as per ASTM D638 using a HaakeMiniJet injection moulding machine. Five specimens were tested for each sample and the average values were reported.

4.2.2   Dynamic mechanical analysis (DMA)

The dynamic mechanical properties (viscoelastic properties) of the blends and composites were measured using a TTDMA (Triton Technology Ltd, UK). Rectangular samples of dimension 15 x 10 x 4 (length x width x thickness) were tested in 3 points bending mode at a constant frequency of 1 Hz. The temperature was varied from -40ºC to +12ºC at a rate of 3ºC/minute. The viscoelastic properties such as storage modulus, loss modulus and loss tangent (tan δ) were obtained against the temperature of the test.

4.3   Results and discussion

4.3.1   Selection of the desired blend ratio

The mechanical properties of the virgin polymers and their PP rich blends (90:10, 80:20 and 70:30) are summarised in table 4.1. The virgin PP and PLA have tensile

strengths of 33 and 47 MPa respectively. Incorporation of 10 % of PLA to PP resulted in a marginal increase in the modulus of PP from 1265 to 1285 MPa, whereas tensile strength value of the blend was same as that of virgin PP (33 MPa). Elongation at break reduced from 30% to 24%. As the PLA content was increased to 20%, the tensile strength of the resulting blend (80:20, PP:PLA) increased to 34 MPa, modulus showed a drastic increase from 1285 to 1700 MPa, whereas, elongation at break reduced to 15%. The improvement in tensile strength and modulus and reduction in elongation at break can be co-related to the higher mechanical properties and low elongation at break values of virgin PLA. When the PLA content was further increased to 30 %, the tensile strength value of the resulting blend showed a decrease (33 MPa, similar to that of 90:10 blend), modulus slightly increased to 1828 MPa and the elongation at break reduced to 13 %. Moreover, the blend appeared as brittle and showed processing difficulty during extrusion and injection moulding operations. Considering the optimum set of mechanical properties and the associated processing easiness, the blend with 20 % PLA (80:20 blend of PP and PLA) was chosen as the desired blend ratio for the present investigation. Further studies on compatibilization and reinforcement with halloysite nanotubes (HNT) are all based on this blend ratio.

Table 4-1Mechanical properties of virgin polymers and PP rich blends

Sample	Tensile Strength (MPa)	Tensile Modulus (MPa)	Elongation at Break (%)
PP	33 (1.4)	1265 (30)	30 (2)
PLA	47 (3)	3375 (18)	6 (0.8)
90:10 (PP:PLA)	33 (0.4)	1285 (26)	24 (3)
80:20 (PP: PLA)	34 (0.7)	1700 (21)	15 (4)
70:30 (PP:PLA)	33 (0.3)	1828 (30)	13 4)

4.3.2   Mechanical properties of the blends

The mechanical properties of the virgin polymers and their 80:20 (PP:PLA) blends with various compatibilizer dosage are given in table 4.2. The incorporation of 20 wt% of PLA into the PP matrix resulted in a marginal increase of tensile strength to 34 MPa. But the modulus of the resulting blend increased to 1700 MPa, compared to 1265 MPa of virgin PP. The elongation at break of the blend showed a drastic decrease to 15% compared with 30% of virgin PP. These changes in modulus and elongation at break are due to the higher modulus and lower elongation at break of the brittle PLA. With the introduction of 1 wt% of acompatibilizer, the tensile strength increased to 36 MPa and it became 39 MPa with an increase in compatibilizer to 3 wt%. The decrease of tensile strength to 37 MPa with further increase in compatibilizer level (5 wt%) suggests that the optimum compatibilizer required to effectively compatibilize a blend of PP and PLA in the ratio 80:20 is 3 wt%. Tensile modulus, energy to break and elongation at break also followed the same trend.

Table 4-2Mechanical properties of virgin polymers and their blends

Sample	Tensile strength (MPa)	Tensile modulus (MPa)	Elongation at break (%)	Energy to break (J)
PP	33 (1.4)	1265 (30)	30 (2)	2.01 (0.4)
PLA	47 (3)	3375 (18)	6 (0.8)	0.21 (0.08)
80:20:0	34 (0.7)	1700 (21)	15 (4)	0.72 (0.2)
80:20:1	36 (1.2)	1750 (12)	22 (3.6)	1.19 (0.04)
80:20:3	39 (0.8)	1865 (26)	25 (2.1)	1.62 (0.08)
80:20:5	37 (0.5)	1700 (40)	21 (1.2)	1.53 (0.1)

*Values given in parenthesis correspond to the standard deviation

4.3.3   Mechanical properties of nanocomposites

Blends of PP and PLA in the ratio 80:20 compatibilized with 3 wt% of compatibilizer (MA-g-PP) was chosen as the matrix for reinforcement with HNT based on their optimum set of mechanical properties. The mechanical properties of the nanocomposites with varying amounts of HNT are given in table 4.3. The incorporation of HNT did not result in an improvement of tensile strength of the resulting nanocomposite up to an HNT wt % of 4, as evident from their tensile strength values. When the HNT content reached 6 wt%, the tensile strength showed an appreciable increase to 43 MPa from 39 MPa of the base matrix. Further increase in HNT addition (8 and 10 wt %) resulted in adecrease in the tensile strength values. Tensile modulus showed a slight decrease with 1 wt% of HNT addition to the base matrix but showed a steady improvement with afurther increase in HNT content up to 6 wt % of HNT. The value increased to 1992 MPa compared with 1865 MPa of the base matrix. Further increase in HNT addition (8 and 10 wt %) resulted in adecreasein the modulus values. Elongation at break values remains more or less same throughout the entire compositions, whereas at 6 wt% of HNT its value was same as that of base matrix. This indicates that the flexibility of the matrix is unchanged even with 6 wt% of nanofiller loading. From these results, it can be concluded that 6 wt% of HNT is sufficient to improve the mechanical properties and it can be considered as the optimum loading nanofiller to the base matrix.

Table 4-3Mechanical properties of nanocomposites

Sample	Tensile strength (MPa)	Tensile modulus (MPa)	Elongation at break (%)
HNT 0	39 (0.8)	1865 (26)	25 (2.1)
HNT 1	38 (0.7)	1820 (32)	24 (3.1)
HNT 2	40 (0.5)	1895 (38)	22 (2.6)
HNT 4	39 (0.8)	1905 (42)	22 (3.0)

HNT 6	43 (0.3)	1992 (36)	25 (2.5)
HNT 8	41 (0.5)	1900 (38)	23 (3.6)
HNT 10	40 (0.6)	1890 (29)	21 (2.9)

4.3.4   Dynamic mechanical analysis (DMA)

4.3.4.1   DMA of blends

The storage modulus (E') and tan δ traces against temperature for virgin PP are shown in figure 4.1. A sharp decrease in storage modulus with anincrease in temperature is clearly visible from the figure. The tan δ showed a peak at 13.5^{o}C corresponding to the glass transition temperature of PP. The storage modulus curves against temperature for the blends are shown in figure 4.2, whereas the tan δ curves is shown in figure 4.3. All the blends exhibited a two stage decrease for the storage modulus with anincrease in temperature and this is due the presence of two different phases (of PP and PLA) present in the blend. The storage modulus at 21°C and the tan δ peak (glass transition temperature) corresponding to PP and PLA in the blend are summarised in table 4.4
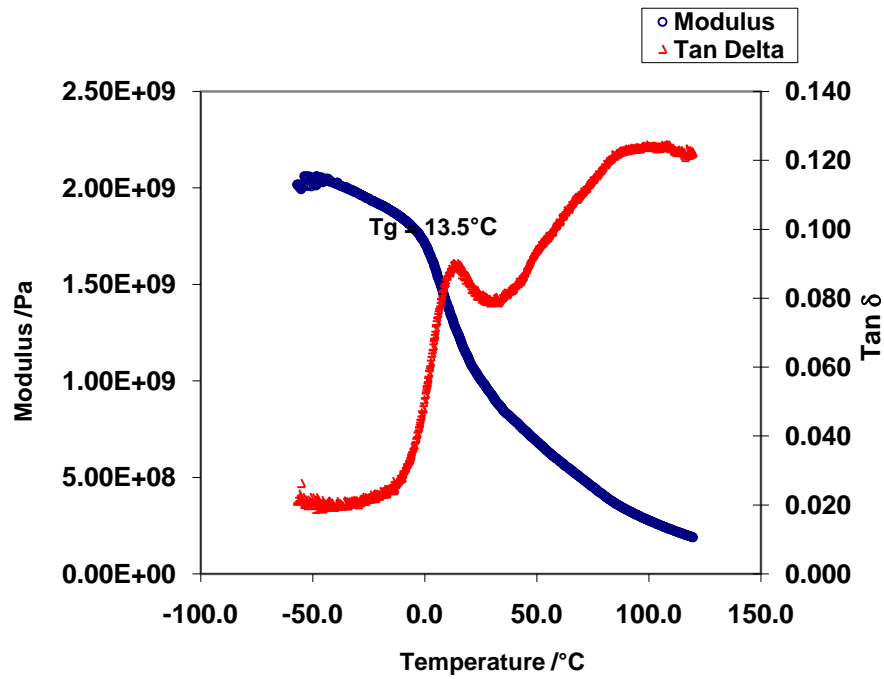
Figure 4.1Storage modulus and tan δ against temperature for PP
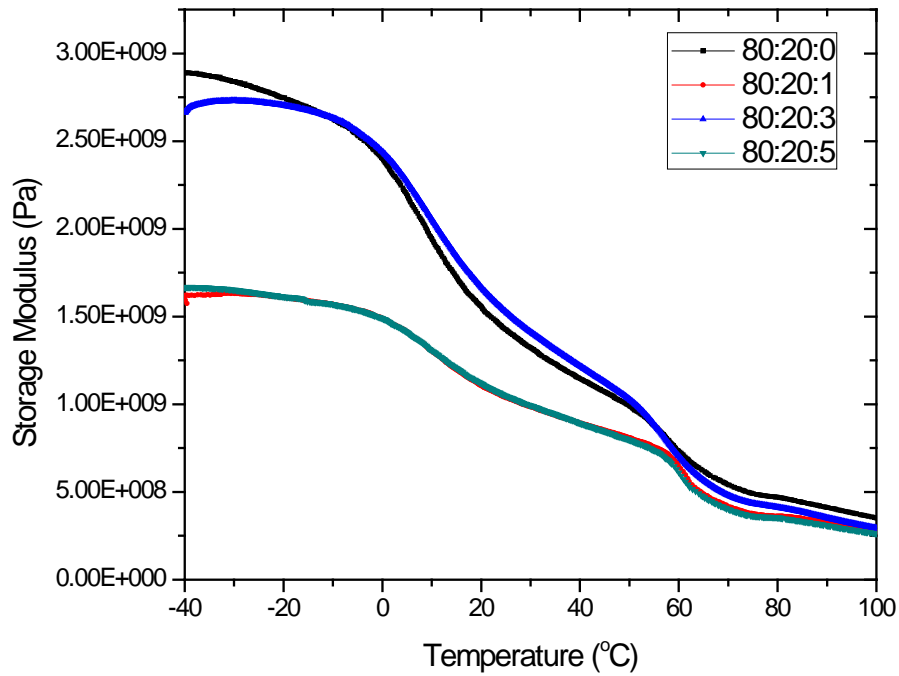
Figure 4.2Storage modulus curves for the blends
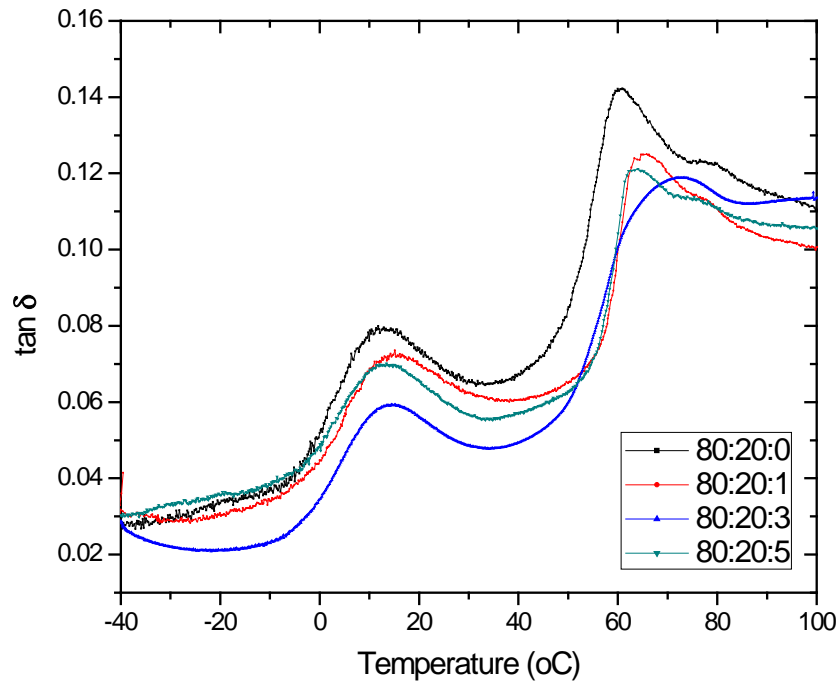
Figure 4.3tan δ curves for the blends

Table 4-4Storage modulus of the blends and T_g of blend components

Sample	T_g of PP (°C)	T_g of PLA (°C)	Modulus at 21°C (MPa)
PP	13.5	-	1078
80:20:0	13	61.5	1524
80:20:1	15.1	66.1	1092
80:20:3	14.7	72.1	1639
80:20:5	14	64.5	1103

The storage modulus value for virgin PP is 1078 MPa and it has a glass transition temperature (T_g) at 13.5°C. With the incorporation of 20% PLA to PP, the T_g of PP remained almost same and additionally, the tan δ showed another peak at 61.5°C

corresponding to the T_g of PLA. The modulus of this blend increased to 1524 MPa owing to the high modulus of PLA. When the compatibilizer is introduced at wt % to the blend, the T_g of both PP and PLA increased to 15.1^{o}C and 66.1^{o}C respectively. The shift in T_g of PP and PLA to higher value indicates that the compatibilizer is acting at the interphase between the two immiscible polymers. But interestingly, the modulus decreased compared with the un-compatibilized blend. When the compatibilizer is increased to 3 wt%, the T_g of PP slightly decreased to 14.7^{o}C, but that of PLA increased to 72.1^{o}C. This can be attributed to the interaction between the compatibilizer and PLA. Shifting of T_g of PLA to higher values was also reported by Choudhary et al. (Choudhary, Mohanty et al. 2011) in a 90:10 (PLA:PP) blend system compatibilized by MA-g-PP. The modulus value for 80:20:3blend was 1639 MPa which was highest among all the blend compositions investigated. As the compatibilizer was increased to 5 wt%, all the values showed a downward trend as evident from the table 4.4. Hence it can be concluded that 3 wt% of the compatibilizer effectively compatibilized the blends in the selected ratio.

4.3.4.2   DMA of nanocomposites

The storage modulus traces of the nanocomposites are shown in figure 4.4. From the curves, it is clear that the highest modulus is exhibited by HNT 6 (with 6 wt% of HNT).
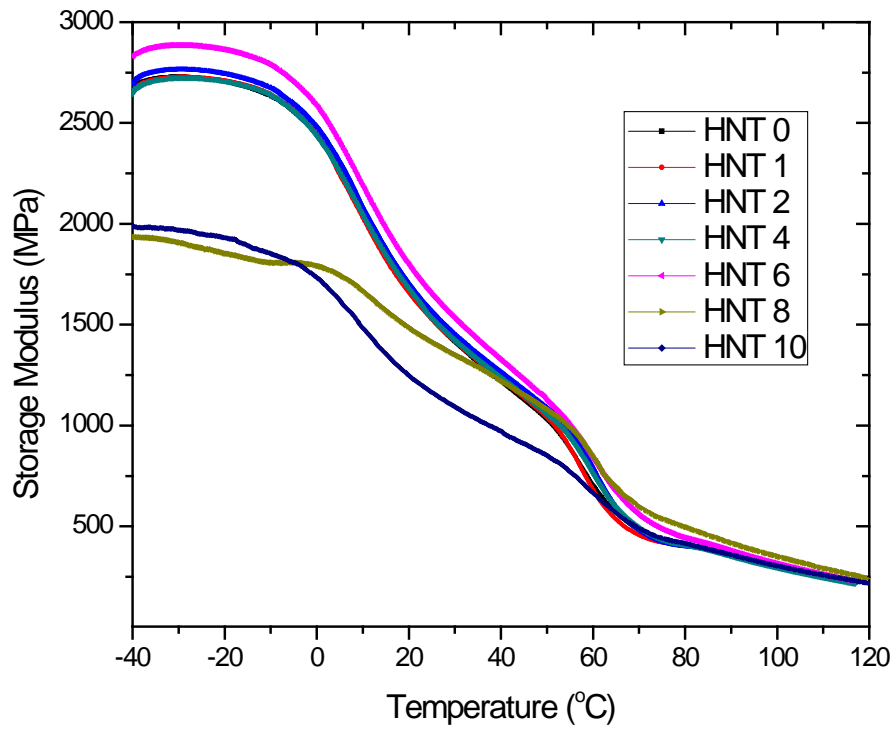
Figure 4.4Storage modulus traces of nanocomposites
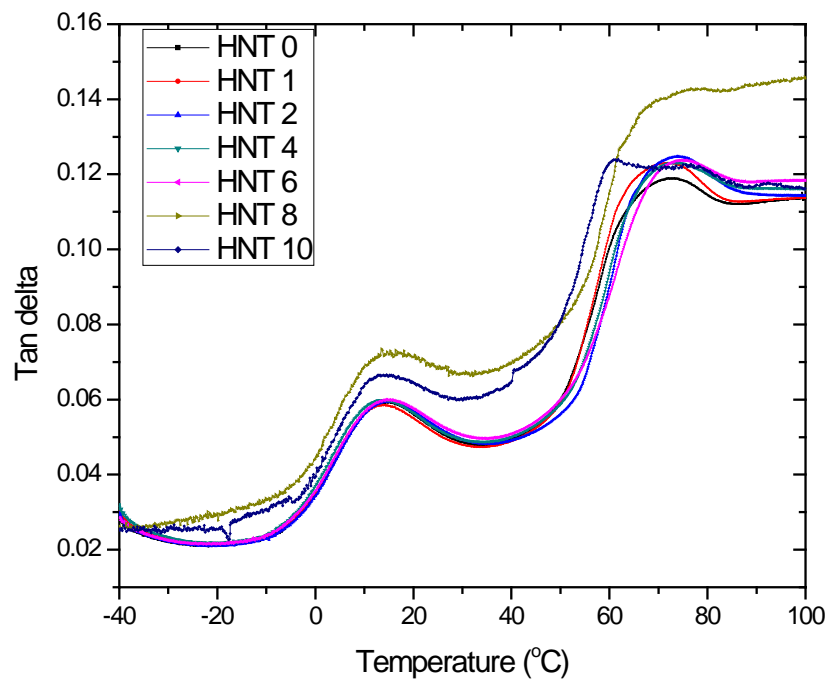
Figure 4.5tan δ curves for the nanocomposites

Table 4-5Storage modulus and $T_g$of the nanocomposites

Sample	T_g of PP (ºC)	T_g of PLA (ºC)	Modulus at 21ºC (MPa)
HNT 0	14.7	72.1	1639
HNT 1	13.8	71.28	1632
HNT 2	15.1	73.32	1678
HNT 4	14.3	73.32	1653
HNT 6	14.7	74.55	1773
HNT 8	16.4	70.6	1470
HNT 10	15	62.2	1230

The tan δ traces for the nanocomposites clearly showed two peaks corresponding to PP and PLA. The parameters obtained from figures 4.4 and 4.5 are summarised in table 4.5. From the table 4.5, it can be clearly seen that the T_g of PP remained almost same in the entire composition range, whereas, the T_g of PLA showed a step-wise increment with anincrease in the wt% of HNT. It reached a maximum value of 74.55ºC for HNT 6 (6 wt% of HNT). The increase in T_g of PLA with the addition of HNT was reported by Liu et al. (Liu, Zhang et al. 2013) and it was attributed to the hydrogen bonding interactions between HNT and PLA. The modulus value for HNT 6 was 1773 MPa, which is also the highest among all the nanocomposites investigated. Hence the optimum loading of HNT for improving the mechanical properties of the blend matrix is 6 wt%.

4.4   Conclusion

The mechanical and dynamic mechanical analysis of the blends and nanocomposites were performed and as indicated by the results, 3 wt% of the compatibilizer was the

optimum for effectively compatibilizing the blend of PP and PLA in the ratio 80:20. The HNT loading of 6 wt%, resulted in a marginal improvement of the mechanical properties of the blend matrix.

CHAPTER-5

THERMALDEGRADATIONANDCRYSTALLIZATIONKINETICS OF THE BLENDS

5.1 Introduction

The thermal stability and thermal degradation play a crucial role in determining the processing and recycling conditions of polymers and their blends. Thermogravimetric analysis (TGA) is the widely used technique to assess the thermal stability of polymer blends and composites(Gabbott 2008). It is also an effective tool to monitor the solid-state thermal degradation kinetics of polymers. In TGA, weight loss of a definite weight of thesample is continuously monitored under specified conditions of temperature rise.Overallthermal degradation kinetics can easily be obtained by measuring the change in mass of a sample with time and by analysing the degradation profile in both isothermal and non-isothermal conditions.

Thermal degradation mechanism of PLA in ablend with other polymers is reported recently. Blends of PLA with linear low-densitypolyethylene (LLDPE) and the degradation mechanism was reported by Omura et al.(Omura, Tsukegi et al. 2006). Similar works for PLA with PS, PBS and PBSA are also reported by the same research group (Omura, Tsukegi et al. 2007; Omura, Tsukegi et al. 2007). The TGA curves for these blends showed two-step weight loss profiles, corresponding to PLA and the other blend component.

The proper understanding of the crystallisation process of polymers and their blends gives us valuable information that is very useful to determine the processing parameters in most of the conventional plastics processing operations. Study of the mechanism of nucleation and crystal growth during the processing operations is critical in deciding the final product properties like thermal stability, crystal structure, physical, chemical, optical, electrical and mechanical properties (Dhanvijay and Shertukde 2011). The blending of PLA with PP alters the crystallisationbehaviour of the resulting blend and also the addition of the compatibilizer further affects this

process. The main aim of the present investigation is to understand the non-isothermalcrystallisation kinetics of PP and PLA blends in the selected ratio and to study the effect of theaddition of compatibilizer on the crystallisationbehaviour of PP in the blend. This chapter deals with the thermal degradation and crystallisation kinetics of PP/PLA blends compatibilized by MA-g-PP

5.2 Experimental procedure

5.2.1 Thermogravimetric analysis (TGA)

Thermogravimetric analysis (TGA) was carried out using TA instruments TA-SDT 2960. Samples of 10 ± 5 mg were heated from ambient temperature to 600°C under anair atmosphere (50 ml/min). Heating rates of 5, 10, 16 and 22°C /min were used and sample weight loss was continuously recorded against the sample temperature.

5.2.2 Mathematical modeling

Thermogravimetric analysis in the non-isothermal mode consists of heating a known weight of thesample at a constant heating rate and the weight loss curve is recorded. All the kinetic studies assume that the isothermal rate conversion $\frac{d\alpha}{dt}$ is a linear function of $k(T)$,which is a temperature dependent rate constant and $f(\alpha),$ a temperature independent function of the conversion. That is:

$$\frac{d\alpha}{dt} = k\,(T)f\,(\alpha) \tag{5.1}$$

Where α is the fractional extent of the reaction.$f(\alpha)$depends on particulardecomposition mechanism.

Arrhenius equation:

$$k\,(T) = A\exp\left(-\frac{E_a}{RT}\right) \tag{5.2}$$

Where, A is a pre-exponential factor, which is assumed as independent of temperature, E_a is the apparent activation energy, T is the temperature in the absolute scale and R is the universal gas constant.

Combining (5.1) and (5.2);

$$\frac{d\alpha}{dt} = A \exp\left(-\frac{E_a}{RT}\right) f(\alpha) \tag{5.3}$$

For non-isothermal measurements at constant heating rate, $\beta = \frac{dT}{dt}$, equation (5.3) transforms to;

$$\beta\left(\frac{d\alpha}{dT}\right) = A \exp\left(-\frac{E_a}{RT}\right) f(\alpha) \tag{5.4}$$

Apparent activation energy E_a can be calculated byvarious methods.

i) *Kissinger's method*

The most widely used method based on the parameters at maximum reaction rate was proposed by Kissinger in 1957(Kissinger 1957). In this method, the activation energy can be determined from the plots of logarithm of the heating rate versus the inverse of the temperature at the maximum reaction rate in constant heating rate experiments. Activation energy can be determined by Kissinger's method using the equation:

$$\ln\left(\frac{\beta}{T_m{}^2}\right) = -\left(\frac{E_a}{RT_m}\right) + \text{Constant} \tag{5.5}$$

Where, β is the heating rate, T_m is the temperature corresponding to maximum degradation obtained from the thermal degradation curves and R is the universal gas constant.

ii) **Horowitz and Metzger Method**(Horowitz and Metzger 1963)

The integral method proposed by Horowitz and Metzger helps to find the activation energy for decomposition by using the following equation:

$$\ln\left[\ln\frac{1}{(1-\alpha)}\right] = \frac{E_a\theta}{RT_{max}^2}$$

(5.6)

where, α is the decomposed fraction, T is the temperature, θ is $T - Tmax$ and R is the gas constant. By plotting, $\ln\left[ln\frac{1}{(1-\alpha)}\right]$ againstθ, E_a can be determined from the slope of the curves.

iii) Kissinger–Akahira–Sunose equation

An improved method that offers a significant improvement in the accuracy of activation energy values is proposed by Akahira et al.(Akahira and Sunose 1971) and is given by:

$$\ln\left(\frac{\beta}{T^2_{\alpha,i}}\right) = const. - \left(\frac{E_a}{RT_\alpha}\right)$$

(5.7)

To apply this equation, it is necessary to obtain at least three heating rates (β), the respective conversion curves being evaluated from the measured TG curves. For each conversionα, the plot of $\ln\left(\frac{\beta}{T^2}\right)$ against $\left(\frac{1}{T}\right)$ should provide a straight line with slope directly proportional to E_a and thus the activation energy is obtained as a function of conversion.

iv) Friedman model

The method proposed by Friedman in 1964(Friedman 1964)is a differential procedure which calculates kinetic parametersat a given α. Based on (5.1) and (5.2), Friedman

proposed to apply the logarithm of the conversion rate $\left(\frac{d\alpha}{dt}\right)$ as a function of the reciprocal of temperature in the form of:

$$\ln\left(\frac{d\alpha}{dt}\right) = \ln\left(\frac{A}{B}\right) + \ln[f(\alpha)] - \left(\frac{E_a}{RT}\right) \tag{5.8}$$

From (5.8), it is obvious that if the function $f(\alpha)$ is constant for a particular value of α, then the sum $\ln\left(\frac{A}{B}\right) + \ln[f(\alpha)]$ is also constant. By plotting $\ln\left(\frac{d\alpha}{dt}\right)$ against$\left(\frac{1}{T}\right)$, the value of $-\left(\frac{E}{R}\right)$ for a given value of α can be obtained directly. Also, it is possible to obtain values for E over a wide range of conversions.

v) ***Ozawa – Flynn and Wall (OFW) Method***(Flynn and Wall 1966; Ozawa 1970)

This is a "model-free" method, which assumes that the conversion function $f(\alpha)$ does not change with the changes in the heating rate for all values of α. In this method, the temperatures corresponding to fixed values of α are measured from experiments at different heating rates β.

$$\ln(\beta) = \ln\left[A\frac{f\alpha}{\left(\frac{d\alpha}{dt}\right)}\right] - \left[\frac{E_a}{RT}\right] \tag{5.9}$$

and by adopting the corrected Doyle's linear approximation proposed by Flynn (Flynn 1983) takes the form of:

$$\ln(\beta) = \left\{\ln\frac{AE}{g(\alpha)R} - 2.315\right\} - \frac{(0.457\,E_a)}{RT} \tag{5.10}$$

Therefore, plotting $\ln(\beta)$ against $\left(\frac{1}{T}\right)$ for different conversion α should give straight lines and the slopes of these straight lines are directly proportional to the activation energy $(-0.457E_a/R)$.

vi) ***Coats and Redfern Method****(Coats and Redfern 1964)*

This method is considered as the most versatile model for calculation of the kinetic parameters of thethermal degradation process. Rearrangement and integration of Equation (5.10) by this method leads to the following relation:

$$\ln\left[\frac{g(\alpha)}{T^2}\right] = \ln\left(\frac{AR}{\beta E}\right) - \frac{E_a}{RT} \tag{5.11}$$

Where, $g(\alpha) = \int_0^\alpha \frac{d\alpha}{f(\alpha)}$

A plot of $\ln\left[\frac{g(\alpha)}{T^2}\right]$ versus $1/T$ for a heating rate β and a selected degradation function $f(\alpha)$ give rise to the apparent activation energy E_a and the Arrhenius pre-exponential factor A. Most frequently cited reaction mechanism for solid-state processes and the corresponding algebraic expressions for $g(\alpha)$ are given in Table 5.1(Dai, Wang et al. 2014).

Table 5-1Reaction mechanisms of solid-state processes

Symbol	$g(\alpha)$	Model
R2	$2[1-\ln(1-\alpha)^{1/2}]$	Phase boundary controlled reaction (contracting area)
R3	$3[1-\ln(1-\alpha)^{1/3}]$	Phase boundary controlled reaction (contracting volume)
F1	$-\ln(1-\alpha)$	Random nucleation unimolecular decay law (Avrami-Erofeev eqn. n=1)
F2	$1/(1-\alpha)$	Random nucleation with two nuclei on the individual particle.
A2	$[-\ln(1-\alpha)]^2$	Two dimensional growth of nuclei (Avrami equation)
A3	$[-\ln(1-\alpha)]^3$	Three-dimensional growth of nuclei (Avrami equation)
A4	$[-\ln(1-\alpha)]^4$	Nuleation and growth

		(Avrami equation-3)
D1	α^2	One-dimensional diffusion
D2	$(1- \alpha)\ln(1- \alpha) + \alpha$	Two-dimensional diffusion
D3	$[1-\ln(1- \alpha)^{1/3}]^2$	Three-dimensional diffusion (Jander equation)
D4	$[1-(2/3) \alpha]-(1-\alpha)^{2/3}$	Three-dimensional diffusion (Ginstling-Brounshtein equation)

5.2.3   Differential scanning calorimetry (DSC)

The non-isothermal crystallisation experiments were performed using a differential scanning calorimeter (DSC) [TA instruments DSC-Q 1000]. Samples of approximately 5 to 8 mg were accurately weighed. The samples were heated from 298 to 513K , held at 513K for 2 minutes to erase the thermal history of the samples and then cooled to 298K at constant rate of 5, 10, 15 and 20 K per minute respectively. All the experiments were carried out under nitrogen atmosphere (50 ml/min).

The advanced thermokinetic software package AKTS-Thermokinetics,Ver. 4.15, was used for all kinetics analysis in this study.Notably, the baseline can significantly influence the values of thekinetic parameters determined for the reaction. However, in this study,the tangential baseline was used to analyse the DSC thermograph since it is more accurate than the linear baseline.

5.2.4   Mathematical models

From the DSC cooling curves obtained at a specific cooling rate, many useful parameters can be obtained which are used to describe the non-isothermal crystallisation of polymers. These parameters areT_i the temperature at which the crystallisation starts, crystallisation peak temperature, T_P , which is the temperature at

which the value of the heat flow is maximum and T_f, the end temperature of crystallisation. For the understanding of the crystallisation kinetics in a non-isothermal way, number experiments should be performed at various heating/cooling rates.

To elucidate the kinetic parameters of the crystallisation process, several mathematical models are available. Relative crystallinity (reaction progress) or commonly known as conversion fraction, $\alpha(t)$, can be expressed as a function of crystallisation time, t, as:

$$\alpha = 1 - \exp\left[-(kt)^n\right],$$ (5.12)

This equation is generally known as Johnson-Mehl-Avrami (JMA) method (Avrami 1939; Johnson and Mehl 1939; Avrami 1940;Avrami 1941), which is usually written in a double logarithmic form, as follows:

$$\ln\left[-\ln(1-\alpha_t)\right] = n\ln k + n\ln t,$$ (5.13)

Where,n is the Avrami exponent and k is the overall kinetic rate constant. Both k and n depend on the mechanism of nucleation as well as the growth geometry.

Plotting $\ln\left[-\ln(1-\alpha_t)\right]$ against $\ln t$ at a certain temperature yields straight lines, the intercept and slope of these lines give $n\ln k$ and the Avrami exponent n, respectively.

There are alarge variety of theoretical models and mathematical treatments to explain the estimation of crystallisation kinetics. We selected two of the most popular methods to calculate the activation energy for non-isothermal crystallisation,E.

By using Doyle approximation (Doyle 1962; Doyle 1965)Ozawa and Flynn and Wall (FWO) each independently developed a method for thedetermination of the activation energy, which is given as (Ozawa 1965; Flynn and Wall 1966):

$$\ln\beta_i = \text{costant} - 1.052\left(\frac{E_\alpha}{RT_{\alpha,i}}\right),$$ (5.14)

The subscript i denotes different cooling rates, β_i and R is the universal gas constant.

For a specific α value and several cooling ratesβ_i, pairs of$(\ln\beta_i)$ and $T_{\alpha,i}$ are determined experimentally from the DSCthermogram. The activation energyE_α, at

this specific valueof α, is then estimated from a plot of $\left(\ln\beta_i\right)$ versus $1/T_{\alpha,i}$ across at least three different cooling rates. The procedureis repeated for many values of α yielding continuousfunctions of α for E_α.

More accurate temperature integral approximations were developed by Murray and White(Murray and White 1955). This approximation was used by Kissinger-Akahira-Sunose (KAS)(Kissinger 1956; Kissinger 1957; Akahira and Sunose 1971) and they developed another integral non-isothermal equation to calculate the activation energy. This equation is known as KAS equation (or the generalisedKissinger method as it is sometimes called) and given as:

$$\ln\left(\frac{\beta_i}{T_{\alpha,i}^2}\right) = \text{constant} - \frac{E_\alpha}{RT_{\alpha,i}} \,, \tag{5.15}$$

The experimental determination of E_α is similar tothat of the FWO method. The activation energy E_α can be determined from the slope of the plot of $\ln\left(\beta_i/T_{\alpha,i}^2\right)$ against $1/T_{\alpha,i}$.

5.3   Results and discussion

5.3.1   Thermogravimetric analysis

The thermogravimetric analysis yields TG curves and DTG curves. The TG and DTG curves for the raw materials used in the present investigation at a heating rate of 10°C/min are shown in figure 5.1 (a-c).
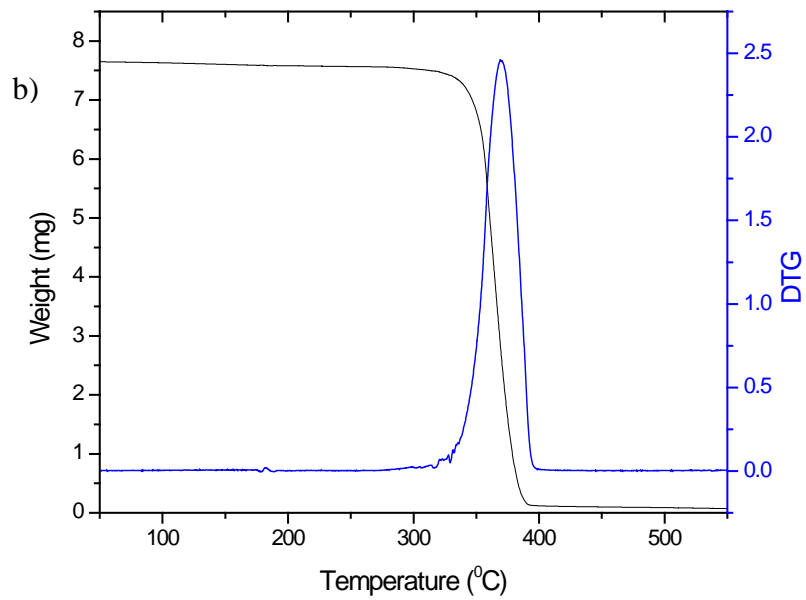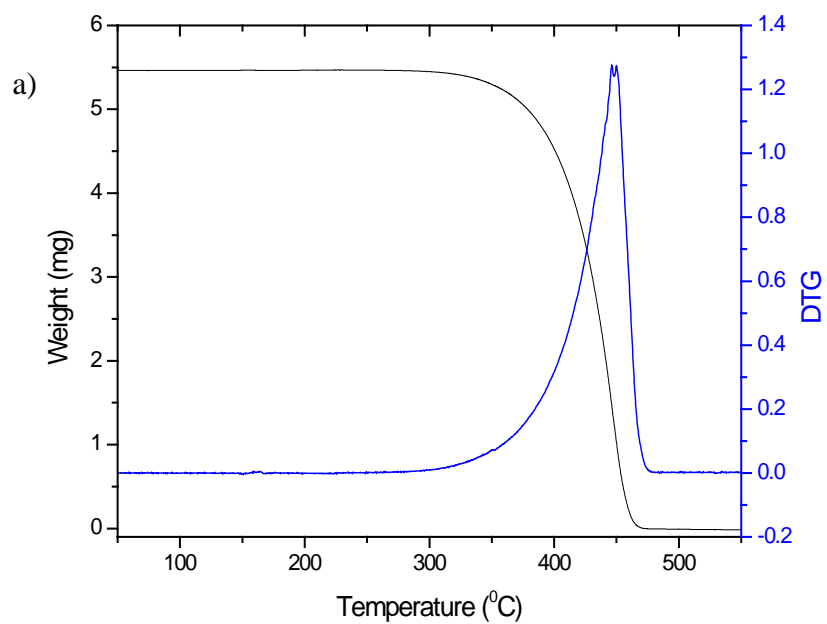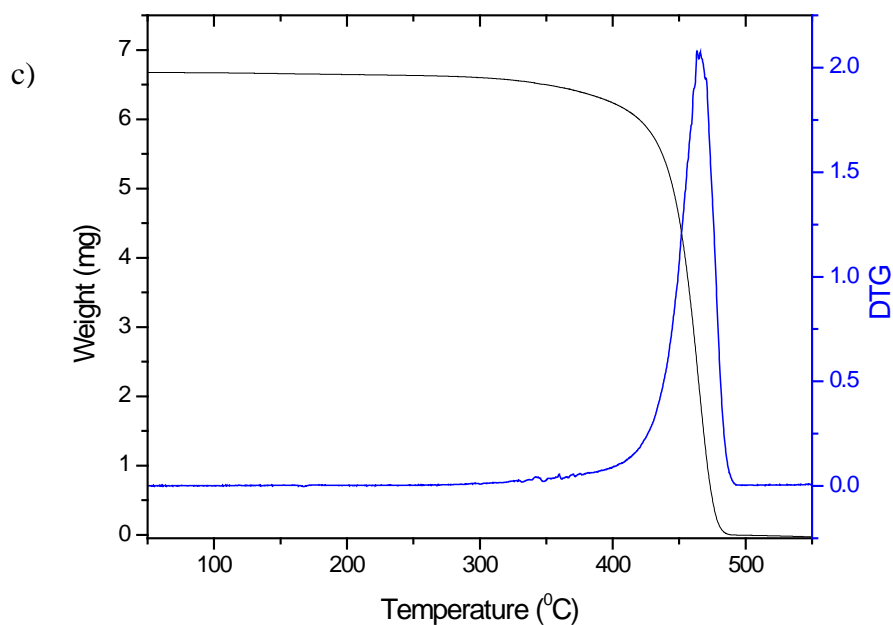
Figure 5.1TG and DTG curves for (a) PP (b) PLA and (c) MAGPP

PP shows one decomposition peak with maximum temperature at 448°C. PLA has maximum decomposition peak at 369°C whereas; the compatibilizer has maximum decomposition at a peak temperature of 465°C. In order to investigate the decomposition kinetics of 80:20 blends of PP and PLA and to study the influence of the addition of compatibilizer on the decomposition kinetics, TG curves for four heating rates (5, 10, 16 and 22°C/min) were measured. These curves are shown in figure 5.2.

(a)

(b)

(c)

(d)
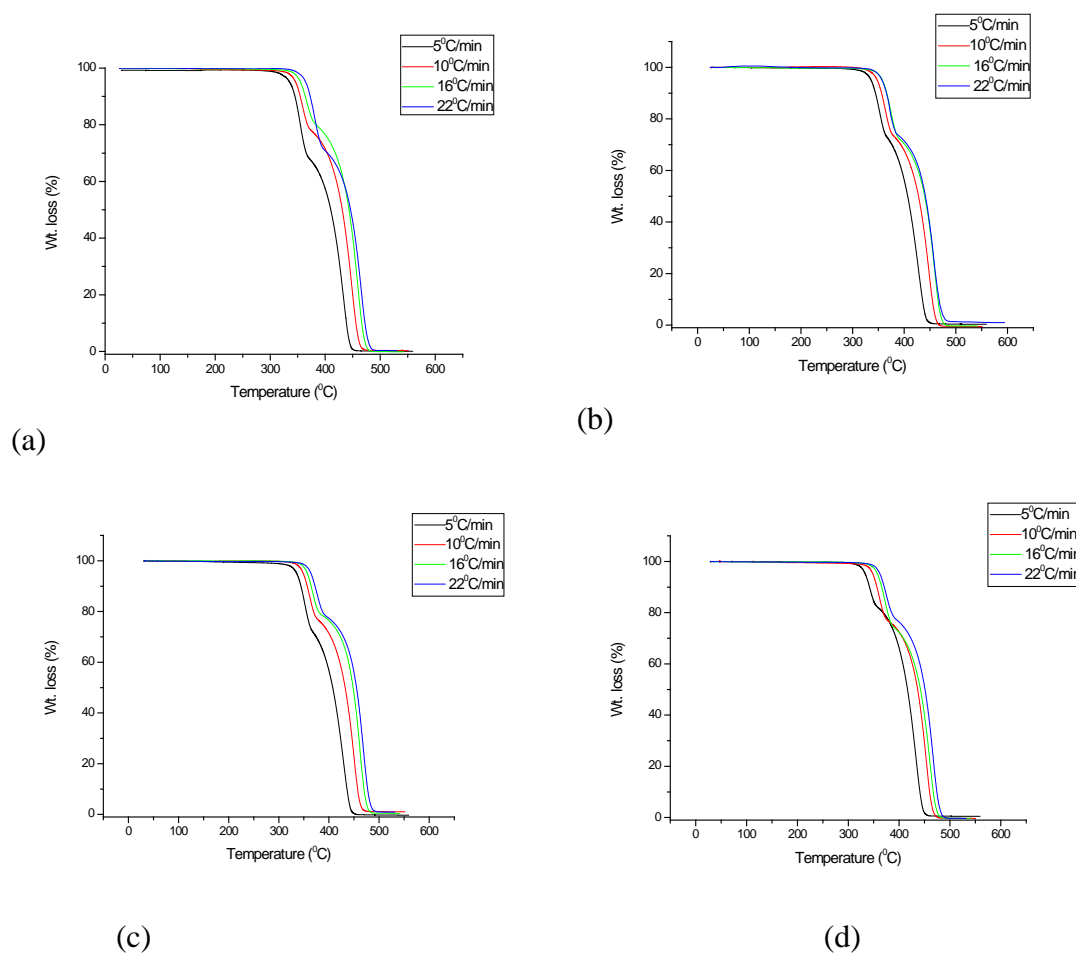
Figure 5.2TG curves at various heating rates for 80:20 blends of PP and PLA
(a) Without compatibilizer, (b) with 1 wt% compatibilizer, (c) with 3 wt%
compatibilizer and (d) with 5 wt% compatibilizer

Table 5-2Maximum degradation temperatures at different heating rates

Heating Rate (K/min)	PLA	First Peak (K)				PP	Second Peak (K)			
		80:20:0	80:20:1	80:20:3	80:20:5		80:20:0	80:20:1	80:20:3	80:20:5
5		628	625	626	617		708	701	702	706
10	642	633	638	636	635	721	723	722	724	730
16		642	648	642	647		733	733	736	735
22		657	656	651	650		741	741	743	742

All the TG curves have two stages, one corresponding to the PP component (second stage) and the other corresponding to the PLA (first stage) in the blend. The corresponding DTG peak values for the maximum decomposition temperature are given in table 5.2. From table 5.2, it can be understood that as the rate of heating increases, the maximum degradation temperatures for the individual blend components slightly shifted to higher values. This shift can be attributed to the shorter time requirement to reach a given temperature at higher heating rates.

Kissinger method

Kissinger method was used for the determination of activation energy of thermal degradation of blend components by plotting thelogarithm of the heating rate versus the inverse of the temperature at the maximum reaction rate. This method assumesthat the reaction order is close to 1. One of the major advantages of this method is that the activation energy can be calculated without a precise knowledge of the reaction mechanism (Kissinger 1956). The activation energy values obtained by applying this method are given in table 5.3.

Table 5-3Calculated E_a values by Kissinger method

Sample	Activation energy, E_a (kJ/mol)	
	First Peak (corresponding to PLA)	Second Peak (corresponding to PP)
80:20:0	161	197
80:20:1	164	196
80:20:3	177	183
80:20:5	167	186

The activation energy for thermal degradation ofPLA component in the blend is 161 kJ/mol, whereas the activation energy for the second peak corresponding to PP in the blend is 197 kJ/mol. By the incorporation of 1 wt% compatibilizer (MA-G-PP), the activation energy for PLA increased to 164 kJ/mol and afurther increase in the compatibilizer (3 wt%) resulted in an increase in the activation energy to 177 kJ/mol. As the compatibilizer content increased further to 5 wt%, the activation energy decreased slightly (167 kJ/mol), but still higher than that for ablend with 1 wt% ofcompatibilizer. This indicates that the compatibilizer is capable of imparting some sort of interactions between the blend components and improved the thermal stability of PLA in the blend. In the case of activation energyfor PP in the blend, the values decreased gradually from 197 to 183 kJ/mol as the compatibilizer increased from 0 to 3 wt%. Further increase in the addition of compatibilizer (5 wt%) resulted in slight increase in the $E_a$value to 186 kJ/mol.It can be concluded that the thermal stability of PLA in the blend is increased by the addition of the compatibilizer and it reached a maximum value of 177 kJ/mol, at a compatibilizer level of 3 wt%. The PP component in the blend exhibited a decrease in thermal stability by the addition of compatibilizer to the blend.

Marquesz et al (Márquez, Franco et al. 2012) reported the activation energy by Kissinger method in binary blends of PLA with other polymers. The value obtained in their study was 153 kJ/mol, which is very close to our results. Kissinger method, even though an approximation, gives well-defined values for the activation energy as it uses only the peak temperatures. Therefore, the activation energy from Kissinger method might be on the higher side compared to the other methods.

Horowitz and Metzger method

The E_a values obtained from Kissinger method are compared with those from Horowitz and Metzger method (Table 5.4). According to this model equation, calculated $E_a$values of PLA fraction in the blend are slightly higher than that of PP fraction. But the trend in E_a values is same as that for Kissinger method for PLA in the blend, i.e., the values increased with the increase in compatibilizer addition up to 3

wt% and then decreased. The same trend was observed for PP fraction in the blend with the E_a values increased from 163 to 187 kJ/mol as the compatibilizer level was increased from 0 to 3 wt% and afurther increase in compatibilizer resulted in a decrease in the E_a value.

Table 5-4Calculated E_a values by Horowitz and Metzger method

Sample	Activation energy, E_a(kJ/mol)	
	First Peak (corresponding to PLA)	Second Peak (corresponding to PP)
80:20:0	207	163
80:20:1	210	170
80:20:3	218	187
80:20:5	198	172

Kissinger–Akahira–Sunose (KAS) equation

One major limitation of Kissinger method is that it generates a single value for the activation energy for a process regardless of its actual kinetic complexity(Vyazovkin, Burnham et al. 2011).

In order to represent the multistep kinetics of the present investigation completely, determination of more than a single value of the activation energy for each composition is required. Therefore, it is necessary to use an iso-conversional method to check the reliability of the Kissinger method.Kissinger–Akahira–Sunose (KAS) equation was applied for 4 conversions (α), namely, 0.2, 0.4, 0.6 and 0.8. The E_a values corresponding to these four conversionsfrom the degradation curves for PLA and PP in the blend are given in table 5.5. From table 4.5, it can be seen that the E_a values for the PLA fraction in the 80:20 blend of PP and PLA is around 160 kJ/mol for various α values, whereas the E_a values for PP component in the blend increased from 153 kJ/mol for α=0.2 to 183 kJ/mole for α=0.8.

Table 5-5Calculated E_a values by Kissinger–Akahira–Sunose equation

Sample	E_a values for first peak (corresponding to PLA) [kJ/mol]				E_a values for second peak (corresponding to PP) [kJ/mol]			
	$\alpha = 0.2$	$\alpha = 0.4$	$\alpha = 0.6$	$\alpha = 0.8$	$\alpha = 0.2$	$\alpha = 0.4$	$\alpha = 0.6$	$\alpha = 0.8$
80:20:0	161	162	161	159	153	166	177	183
80:20:1	152	158	161	162	133	150	154	166
80:20:3	192	195	196	199	124	131	139	146
80:20:5	127	130	129	129	148	159	168	177

The activation energy of PLA is comparable to the earlier reports such as the one reported by Marquesz et al (Márquez, Franco et al. 2012). Because of the integration of the constant extent of the conversion rate, in order to find out the activation energy of degradation, the numerical value is always less than the Kissinger method. However, the method provides accurate results of activation energy for the kinetic analyses.

With the addition of 1 wt% compatibilizer to the blend, the E_a values for the PLA fraction slightly decreased in the lower conversions ($\alpha=0.2$ and 0.4), but almost remained same for $\alpha=0.6$ and 0.8, whereas E_a values for PP component in the blend decreased compared with the blend without compatibilizer. With further increase in the compatibilizer content to 3 wt%, the E_a values for the PLA fraction showed a drastic increase (192 kJ/mol for $\alpha=0.2$ and 199 kJ/mol for $\alpha=0.8$). The E_a values for PP component in the blend decreased further (124 kJ/mole for $\alpha=0.2$ and 146 kJ/mol for $\alpha=0.8$). This indicates that the thermal stability of PLA fraction increases with increase in compatibilizer ratio from 1 to 3 wt%, but PP fraction became less

thermally stable. When the compatibilizer content was further increased to 5 wt%, The E_a values for PLA component decreased drastically to 129 kJ/mol on an average, but the E_a values for PP component showed slight increase compared with the previous set of values, which indicates that 5 wt% of compatibilizer favors thermal stability of PP in the blend. In all cases, the E_a values for PP showed a large variation with increasing degree of conversion (α), which is an indication of a complex decomposition mechanism as reported in other systems(Chrissafis, Paraskevopoulos et al. 2005; Vyazovkin and Sbirrazzuoli 2006).

Friedman model

In order to compare the trend in E_a values for the blend components, Friedman model was used. The E_a values based on Friedman model are summarised in table 5.6. The trend in E_a values was same as those with KAS equation.

Table 5-6Calculated E_a values by Friedman model

Sample	E_a values for first peak (corresponding to PLA) [kJ/mol]				E_a values for second peak (corresponding to PP) [kJ/mol]			
	α = 0.2	α = 0.4	α = 0.6	α = 0.8	α = 0.2	α = 0.4	α = 0.6	α = 0.8
80:20:0	167	160	162	163	186	193	207	207
80:20:1	216	218	187	171	157	185	179	175
80:20:3	207	203	206	209	143	156	172	173
80:20:5	149	127	133	133	162	185	183	209

Friedman equation also follows the iso-conversional method to find out the activation energy. As it is a differential method depending on the conversion rate and temperature, the numerical value is similar to KAS method.The E_a values for PLA fraction in the blend increased with the compatibilizer addition to 3 wt% and

decreased when compatibilizer was increased to 5 wt%. For the PP fraction in the blend, the E_a values decreased with the incorporation of compatibilizerupto 3 wt% but slightly improved when compatibilizer was increased to 5 wt%. However, it is noteworthy to mention that the $E_a$valuesvaried with achange in conversion (α) for every particular composition.

Ozawa – Flynn and Wall (OFW) method

Ozawa – Flynn and Wall (OFW) method showed aslight variation in the trend of E_a values. The E_a values based on OFW method are shown in table 5.7.The numerical value of activation energy for PLA is equivalent to many other reports(Kopinke, Remmler et al. 1996; Fan, Nishida et al. 2003; Li, Zheng et al. 2009). The value shows an increase with respect to the conversion rate also.

Table 5-7 Calculated E_a values by Ozawa–Flynn and Wall (OFW) method

Sample	$E_a$values for first peak (corresponding to PLA) [kJ/mol]				E_a values for second peak (corresponding to PP) [kJ/mol]			
	α = 0.2	α = 0.4	α = 0.6	α = 0.8	α = 0.2	α = 0.4	α = 0.6	α = 0.8
80:20:0	159	164	178	178	157	169	179	185
80:20:1	154	160	163	164	125	133	142	150
80:20:3	192	195	196	199	128	136	143	150
80:20:5	131	134	133	132	152	162	171	180

The E_a values, corresponding to PLA in the blend decreased slightly with the compatibilizer addition of 1 wt% but showed a drastic increase when the compatibilizer content was increased to 3 wt%. The values showed a decreasing trend with afurther increase in the addition of compatibilizer (5 wt %). The trend of E_a values for PP fraction in the blend was same as that for previous two models. Here also the $E_a$valuesvaried with achange in conversion (α), which is a clear indication of complex decomposition mechanism as mentioned before.

The variation of E_a with α for PLA and PP components in the blend without compatibilizer and the blend with 3 wt% of compatibilizer according to Friedman, KAS and OFW methods are depicted graphically in figure 5.3. From the figure, it can be seen that OFW method and KAS equation follow the same trend in most of the cases.

(a)   (b)

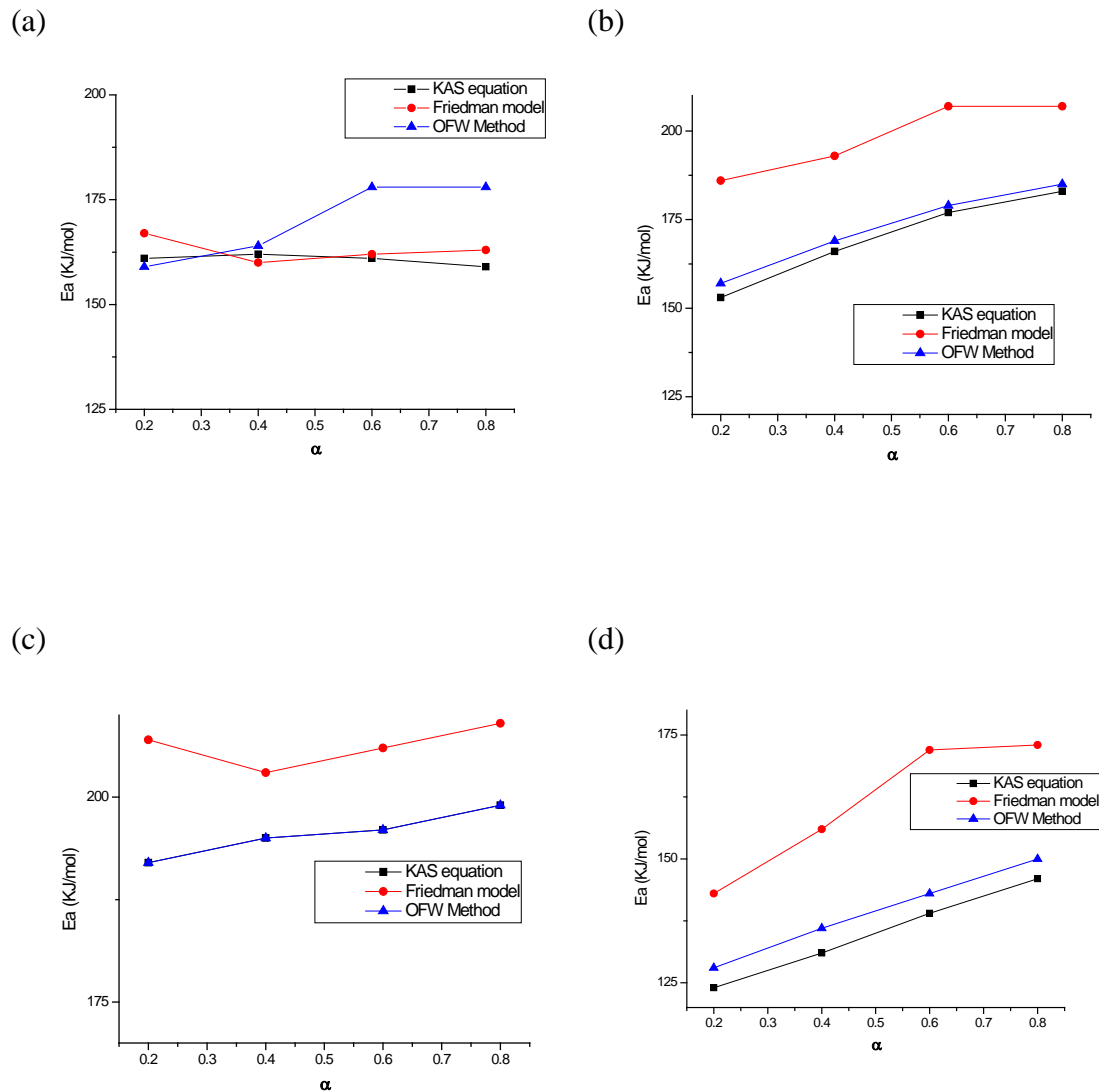(c)   (d)

Figure 5.3Comparison of E_a as a function of decomposition conversion rate (α) (a) PLA fraction of 80:20 blend, (b) PP fraction of 80:20 blend, (c) PLA fraction of 80:20:3 blend, (d) PP fraction of 80:20:3 blend

Coats and Redfern method

One of the main advantages of Coats-Redfern model equation is that in addition to the kinetic parameters of thermal degradation process, the mechanism for degradation process can also be elucidated by the proper selection and substitution of algebraic expression for $g(\alpha)$(Table 5.1) in equation (5.11). In order to enunciate the exact mechanism of thermal degradation of the chosen blend system, all the eleven algebraic expressions for $g(\alpha)$ given in Table 5.1 were substituted in equation (5.11). From the plots of $\ln\left[\frac{g(\alpha)}{T^2}\right]$ versus $1/T$ for different heating rates, the correlation coefficients were calculated and the expression for $g(\alpha)$ for which the correlation coefficient has a maximum value was selected as the mechanism for thermal degradation. Also, the expressions which lead to a big difference in values to the kinetic parameters obtained from other model equations were also excluded. For the present blend system, the best value for correlation was obtained by using the algebraic function F_1, $(g(\alpha) = -\ln(1 - \alpha))$. From the plots of $\ln\left[\frac{g(\alpha)}{T^2}\right]$ versus $1/T$, the apparent activation energy E_a and the Arrhenius pre-exponential factor A were calculated and are given in table 5.8. The E_a values are in very good agreement with the values obtained from other model equations. The present algebraic expression for $g(\alpha)$describes that the thermal degradation in the PP PLA blendsfollow first order mechanism with the solid state process of nucleation with one nucleus on the individual particle. In order to verify the reaction order, the following equation described by Park *et al.*(Woo Park, Cheon Oh et al. 2000) was also followed;

$$n(1 - \alpha_{max})^{n-1} = n - (n - 1)\left(1 + \frac{RT_{max}}{2E_a}\right) \qquad (5.16)$$

where, R is the universal gas constant, $\alpha_{max}$is the weight loss fraction corresponding to the maximum degradation temperature $T_{max}$and the values for the reaction order n are shown in table 5.9.The reaction order for both fractions is more or less close to 1 indicating a first-order degradation kinetics for the blends. The numerical values for peak one are almost constant for different compatibilizer loading and the same for peak two are gradually increasing to 1. The mechanism proposed for these processes are random nucleation with one nucleus on the individual particle and we believe that the compatibilizer molecules could be associated with the same.

The thermal degradation of PLA seems to follow a complex mechanism. The mechanism was investigated by various research groups(Babanalbandi, Hill et al. 1999; Lee, Hyun Kim et al. 2001;Aoyagi, Yamashita et al. 2002). Aoyagi et al. (Aoyagi, Yamashita et al. 2002) reported that the Ea values of PLA changed in the range of80–160 kJ/mol and Zou et al.(Zou, Yi et al. 2009) reported that theE_a values in the range 177-181 kJ/mol. Recently,Aboulkas et al. (Aboulkas, El harfi et al. 2010) reported the E_a values for PP by Friedman model, KAS equation and OFW method. The reported mean values for E_a as 188±6 kJ/mol, 179±8 kJ/mol and 183±8kJ/mol respectively. These values are in good agreement with the E_a values for the PP fraction in the PP/PLA blend in the present investigation. Moreover, the activation energy values deduced from different models are in agreement with the reported values for the different models in earlier studies.

Table 5-8Kinetic parameters from Coats-Redfern model

Sample	Heating Rate: 5 K/min			Heating Rate: 10 K/min			Heating Rate: 16 K/min			Heating Rate: 22 K/min		
	E_a(kJ/mol)	A (s^{-1})	R^2	E_a(kJ/mol)	A (s^{-1})	R^2	E_a(kJ/mol)	A (s^{-1})	R^2	E_a(kJ/mol)	A (s^{-1})	R^2
80:20:0 (Peak-1)	181	1.48 x 10^{23}	0.999	229	1.62 x 10^{32}	0.994	217	6.72 x 10^{29}	0.997	205	5.04 x 10^{26}	0.996
80:20:0 (Peak-2)	125	8.38 x 10^{9}	0.999	124	5.20 x 10^{9}	0.999	149	3.18 x 10^{13}	0.999	156	3.31 x 10^{14}	1
80:20:1 (Peak-1)	197	2.54 x 10^{26}	0.998	214	1.58 x 10^{29}	0.997	220	5.52 x 10^{29}	0.994	222	2.12 x 10^{27}	0.993
80:20:1 (Peak-2)	124	1.01 x 10^{10}	0.999	144	9.79 x 10^{12}	0.999	162	5.17 x 10^{15}	0.999	168	5.21 x 10^{16}	0.996
80:20:3 (Peak-1)	209	5 x 10^{28}	0.996	226	2.79 x 10^{31}	0.995	227	2.94 x 10^{31}	0.995	224	2.9 x 10^{30}	0.995
80:20:3 (Peak-2)	135	5.62 x 10^{11}	0.999	145	1.22 x 10^{13}	0.999	167	2.4 x 10^{16}	0.999	184	7.55 x 10^{18}	0.999
80:20:5 (Peak-1)	201	5.82 x 10^{27}	0.998	199	2.96 x 10^{26}	0.996	200	1.21 x 10^{26}	0.993	212	2.03 x 10^{28}	0.991
80:20:5 (Peak-2)	124	6.39 x 10^{9}	0.999	120	1.29 x 10^{11}	0.933	123	2.11 x 10^{9}	0.989	155	2.46 x 10^{14}	0.999

Table 5-9 Reaction order n

Sample	Reaction orders n	
	Peak - 1	Peak – 2
80:20:0	0.98	0.51
80:20:1	0.98	0.63
80:20:3	0.98	0.73
80:20:5	0.91	0.73

The thermal degradation kinetics followed first order mechanism and we were able to confirm it using two different methods. To the best of our knowledge, this is the first time the thermal degradation kinetics of compatibilized blends of PP/PLA blends are reported.

5.3.2   Crystallization kinetics

The non-isothermal crystallisation of PP, PP-PLA blends with compatibilizer varying from 0 to 5 wt% was carried out by differential scanning calorimetry (DSC) at different cooling rates, viz, 5, 10, 15 and 20 K min^{-1}. The representative thermogramfor the pure PP with PLA blend without compatibilizer is shown in figure5.4. From the figure, it is clear that there are two distinct peaks, the first is a small one and corresponds to PLA and the other corresponds to PP in the blend. As PP is the major component in the blend (80% by weight), the analysis in the present investigation is limited to the crystallisation behaviour of PP in the blend.
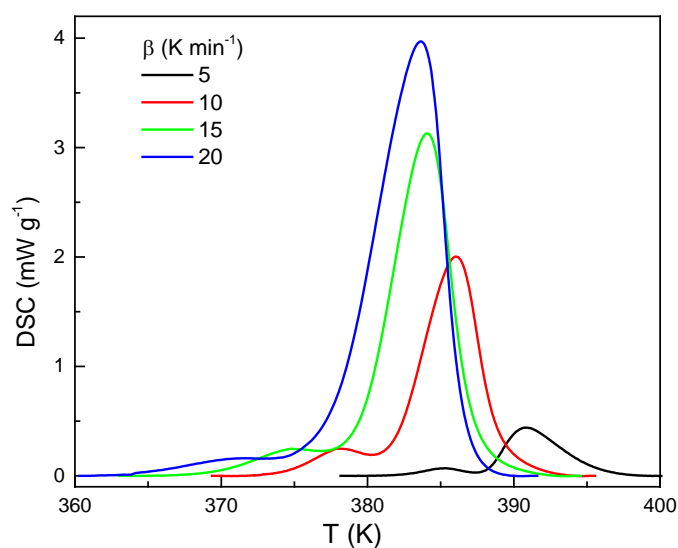
Figure 5.4. DSC thermogram of PP/PLA blends without compatibilizer

The crystallisation exothermic peaks traces of virgin PP and the PP/PLA blends with and without compatibilizer at different cooling rates are presented in figure. 5.5.
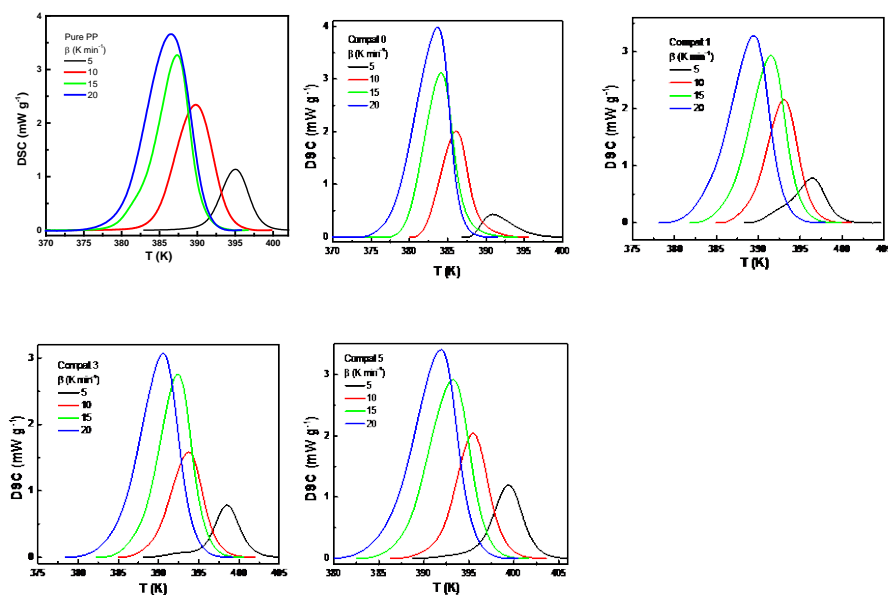
Figure 5.5 DSC thermographs of PP and blends
a) virgin PP, b) PP/PLA (80:20) blend without compatibilizer, c) PP/PLA/MA-g-PP (80:20:1), d) PP/PLA/MA-g-PP (80:20:3) and e) PP/PLA/MA-g-PP (80:20:5)

The common observation for all the samples is that as the cooling rate increases, the peak temperature of crystallisation, T_P moves to lower values. When a molten

polymer is cooled at a very low rate (5 K min^{-1} in the present study), the polymer chains get enough time to cross the nucleation energy barrier and due to this, the crystallization and spherulite growth takes place at a higher temperature, increasing the value of T_P (Sahoo, Mohanty et al. 2015). As the cooling rate is gradually increased (10, 15 and 20 Kmin^{-1}), time availability for crossing the nucleation energy barrier becomes lesser and lesser and as a result, T_P shifts to lower values (Zhang, Zhang et al. 2008). Moreover, the movement of PP chains are not able to follow the fast cooling temperature when the specimens are cooled fast. This is illustrated in figure5.6, where it is easily seen that the peak temperatureT_P decreased with increasing cooling rate β_i. Further, T_p shows a regular trend with respect to the blend components.
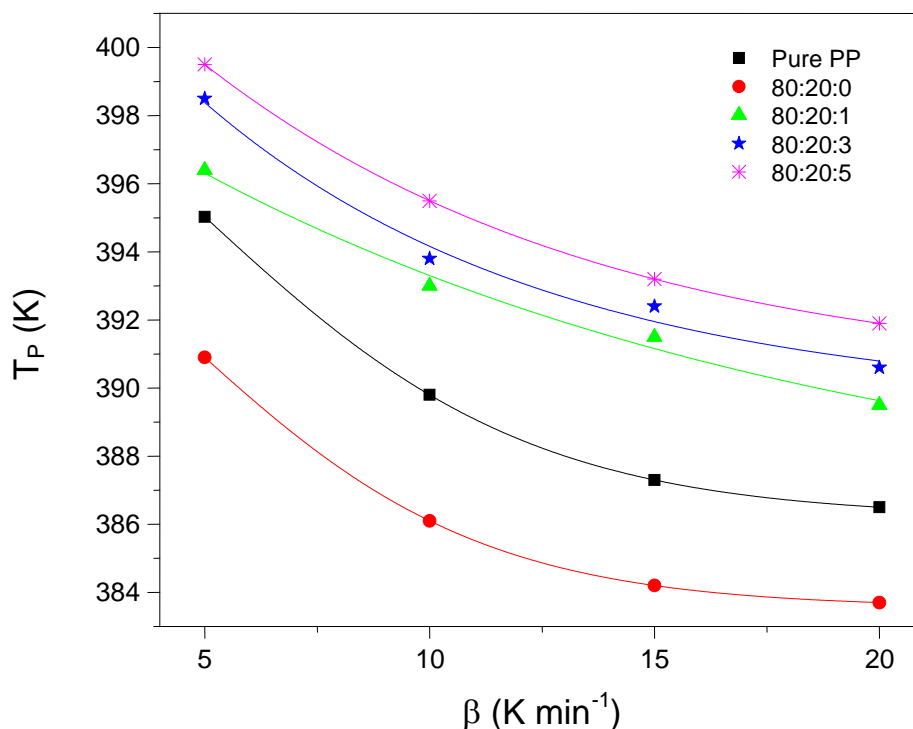
Figure 5.6Variation of crystallisation peak temperature (T_p) with cooling rate

If we compare a particular cooling rate, say 5 Kmin^{-1}, PP alone shows T_p as 395 K, when it is blended with 20 parts PLA the corresponding T_p is lowered to 391 K. This may be due to the incompatibility of the blend components and the PLA fraction acts as a heterogeneous nucleating agent thereby reducing the number of crystals formed.

When the compatibilizer is added the T_p of PP is increased to 397, 399 and 400 K for 1, 3 and 5 wt% respectively. It is believed that the compatibilizer is linked more with the PLA fraction and the chains restricts the segmental motion of PP thus increasing the crystallization peaktemperature thereby restricting easy crystallization in the blends. The carboxyl group of the PP-g-MAH and PLA fraction have heterogeneous nucleation effects on PP macromolecule segments.
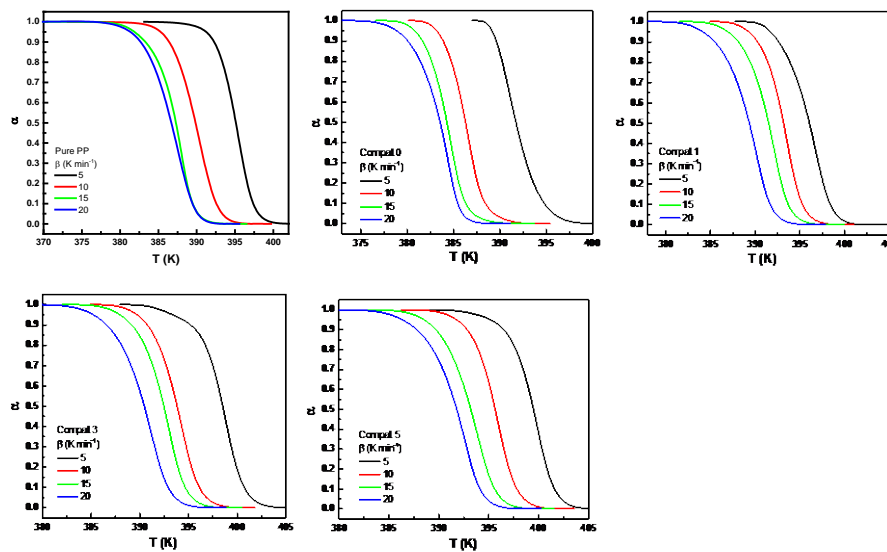
Figure 5.7The relative crystallinity α against temperature for different cooling rates
a) virgin PP, b) PP/PLA (80:20) blend without compatibilizer, c) PP/PLA/MA-g-PP (80:20:1), d) PP/PLA/MA-g-PP (80:20:3) and e) PP/PLA/MA-g-PP (80:20:5)

In order to calculate the activation energy *E* for the crystallizationof PP, PP-PLA blends, the two equations (FWO and KAS equations (5.14 and 5.15) were used over aconversion range of $\alpha = 0.5$ at different cooling rates β_i. The plots of $\left(\ln \beta_i\right)$ and $\ln\left(\beta_i / T_{\alpha,i}^2\right)$ against $10^3 / T_{\alpha,i}$ are shown in figures5.8 and 5.9.
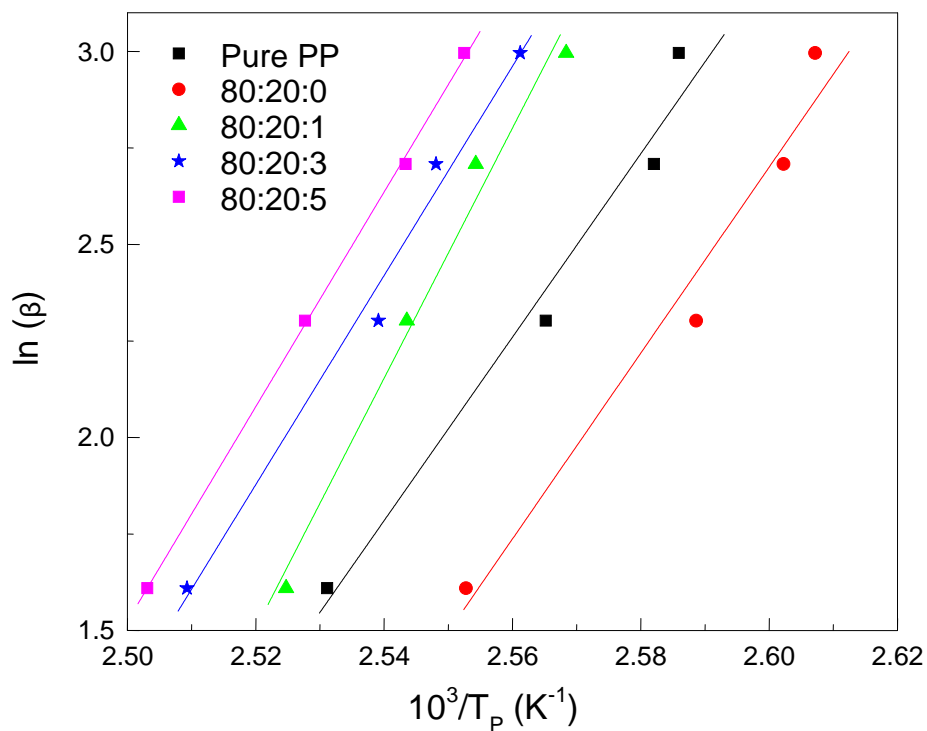
Figure 5.8Plots of $\left(\ln\beta_i\right)$ Vs $10^3\big/T_{\alpha,i}$
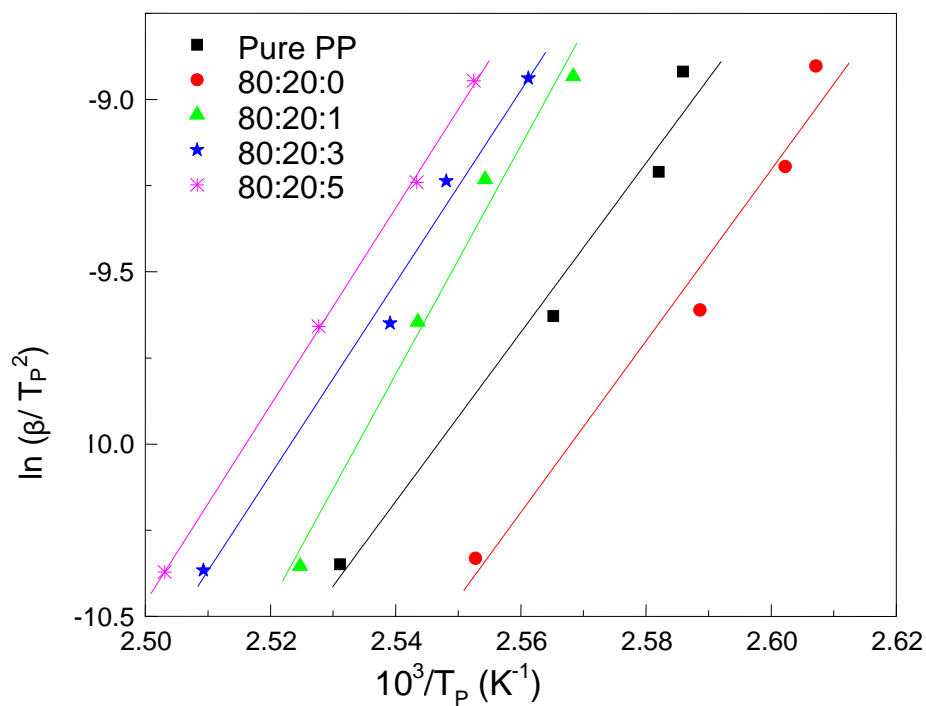
Figure 5.9Plots of $\ln\left(\beta_i\big/T_{\alpha,i}^2\right)$ Vs $10^3\big/T_{\alpha,i}$

The data in these two figures canbe fitted to a straight line leading to an activation energy for crystallisation in virgin PP is -187.8 kJ mol^{-1}by using FWO model and -204.1 kJmol^{-1} by using KAS model, which is very much similar to the values reported in other similar studies(Fan, Duan et al. 2015; Zhu, Liang et al. 2015). The ΔE value, for crystallisation of PP, decreased by the incorporation of 20 wt% of PLA as shown in figure5.10. This indicates that the PLA acted as a restriction for the PP chains during crystallisation process (confinement effect as reported in previous investigations involving PP(Zhu, Liang et al. 2015). Similar results can also be seen in other systems(Du, Guo et al. 2010).Interestingly, the activation energy values obtained for 1 wt% of compatibilizer from the two models are distinctly lower than the other blends. The compatibilizer is believed to react with the PLA fraction in the blend and forms heterogeneous nuclei which form a large number of crystals but the growth is restricted. Therefore, the chains are entangled and the activation energy becomes lower than the other blends. However, the increase in the compatibilizerwt% reverses the condition and shows similar values as that of 80/20 blend even though the numerical values are lesser than it.
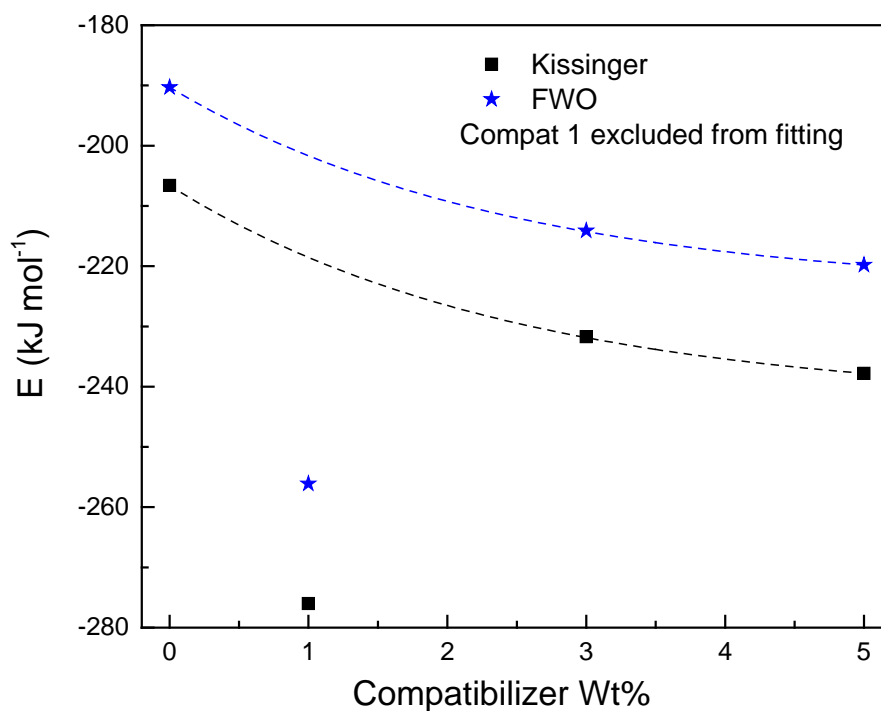
Figure 5.10Variation of activation energy with addition of compatibilizer

The dependence of E_α on the volume fractioncrystallised, α, is shown in figure 5.11, which was obtained by applying isoconversional method on the two models KAS and FWO mentioned above. The results obtained shows that by adding compatibilizer to PP-PLA blends, the activation energy, E_α, become particularlyindependent of the value of α in the $\alpha > 0.7$ range. The activation energy values for virgin PP and 80/20 blend up to 0.7 range of α are in close proximity in terms of numerical values. The values steadily increase for virgin PP, however for 80/20 blend it shows a decrease up to α equals to 0.5 and thereafter it increases. In the case of compatibilized blends the 1 wt% showed a drastic decrease in the activation energy, however exhibited the similar trend as PP. Increase in compatibilizerwt% increased the activation energy in the whole region compared to 1 wt%, however, all the three combinations have less activation energy than the virgin PP and the 80/20 blend. In short, the heteregoneous nucleation effect of the compatibilizer at low concentration is exhibited here also.

Thedependence of the activation energy for crystallisation E_α, on the temperatures, is shown in figure5.12. Activation energy shows a decrease for virgin PP as the temperature increases. In the case of 80/20 blend the activation energy decreases from 383 to 386 K and thereafter it increases until 390 K. The compatibilized blends show different trends, however, all of them have lower activation energies than the virgin PP or the 80/20 blend. The 1 wt% compatibilized system shows similar trend as that of virgin PP and other blends show a different trend with higher numerical values. It is believed that the 1 wt% of the compatibilizer reacts with the PLA fraction and the heterogeneous nature of the nucleation of both the components shift the activation energy to lower values and to higher temperatures than the virgin PP and the blend. However, increase in compatibilizer concentration does not affect the region of crystallization for the blends but with a higher numerical value.
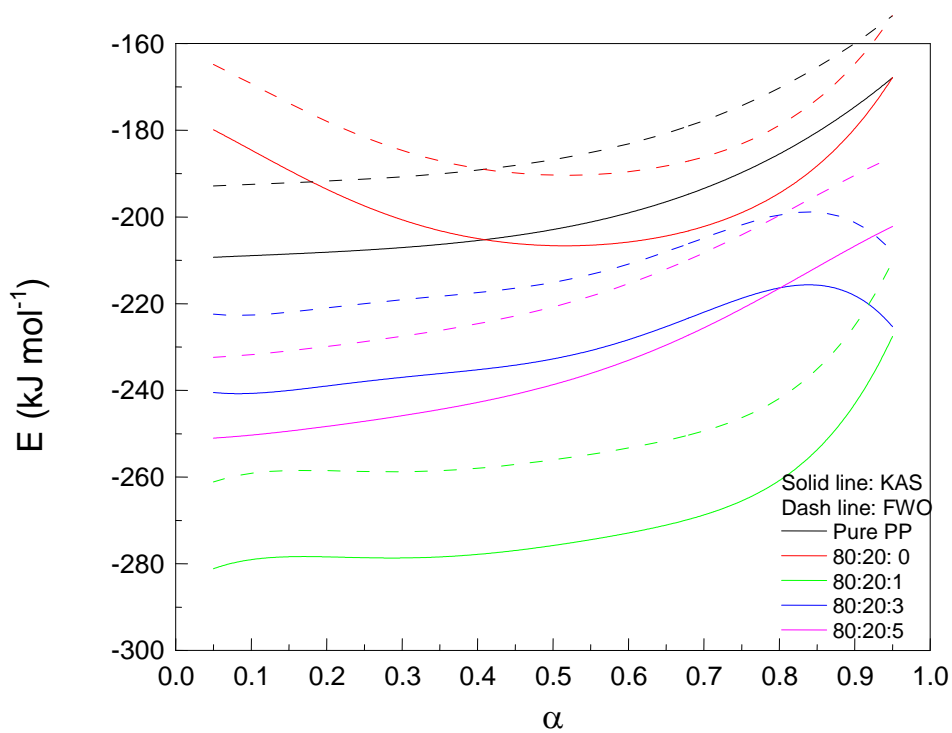
Figure 5.11Variation of activation energy with the volume fraction crystallized
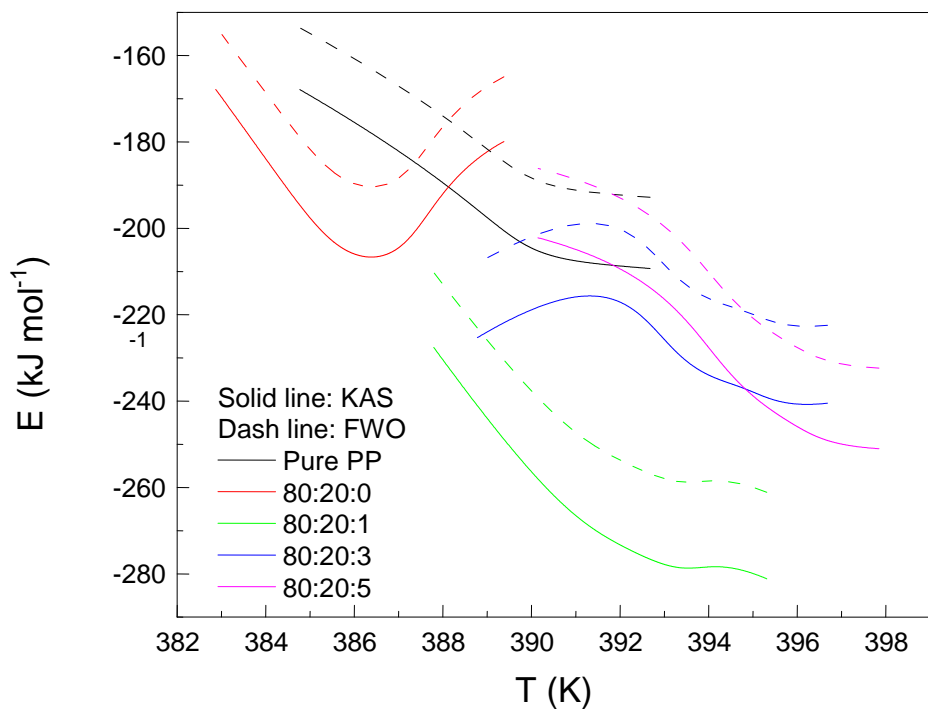
Figure 5.12Variation of activation energy with temperature

By using the AKTS-Thermokinetics software package, the extent of the reaction progress α could bedetermined under any temperature mode, including the isothermal mode(Burnham and Dinh 2007; Roduit, Xia et al. 2008; Joraid and Alhosuini 2014; JORAID, EL-OYOUN et al. 2016). Based on the calculated kinetic parameters obtained from the non-isothermal experiments, AKTS package allows us to predict the crystallized volume in the isothermal mode. Figure 5.13 presents the predicted reaction progress as s function of time under the isothermal mode for the virginPP and the samples mixed with different ratios ofcompatibilizer. The prediction of the isothermal reaction progress was obtained at different temperatures as reflected in the plots. This temperaturewas selected to be within initial and end of the crystallisation process observed experimentallythat are presented in figure 5.5.
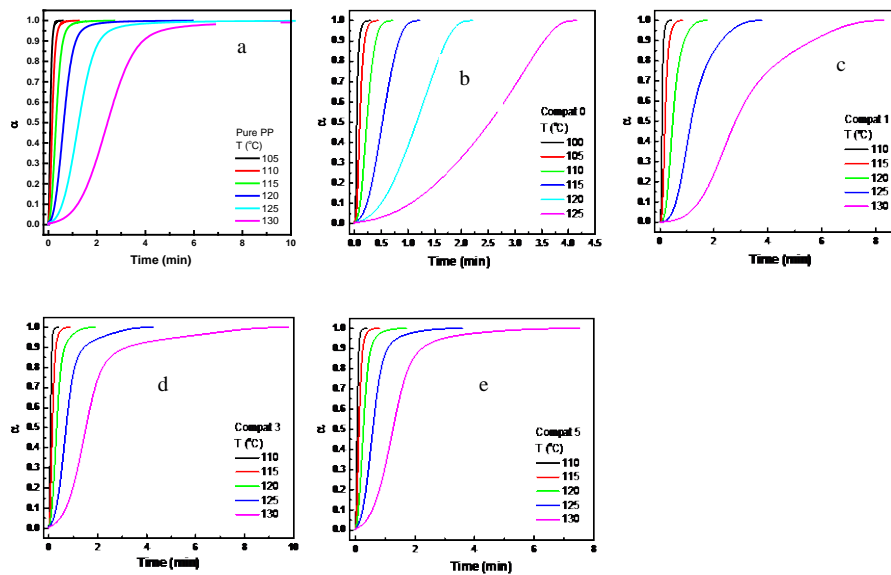
Figure 5.13 Predictionsfor the isothermal conversion fraction α
a) virgin PP, b) PP/PLA (80:20) blend without compatibilizer, c) PP/PLA/MA-g-PP (80:20:1), d) PP/PLA/MA-g-PP (80:20:3) and e) PP/PLA/MA-g-PP (80:20:5)

The isothermal crystallisation kinetics of PP and PP-PLA blends were analysed on the basis of the well-known JMA equation (5.13). The double natural logarithmic plots for the JMA analysis are shown in figure5.14. It is clear from the figure that, all plots of $\ln\left[-\ln\left(1-\alpha_t\right)\right]$ vs. $\ln t$ at different temperatures were linear. The Avrami

exponent *n*and the overall kinetic rate constant *k*were obtained from the slope and intercept of these lines. Fig. 4.15 shows that the values of *n*somewhat vary with temperature. The Avrami exponents indicate that the mechanism of crystallisation is mainly that of two-dimensional growth. When a molten polymer is set to crystalline at a high temperature, the polymer chains get enough time to cross the nucleation energy barrier and due to this, the crystallisation growth takes place at higher dimension, i.e. high *n*value. This is very clear from figure5.15.But there are two different scenarios with respect to the blends. The 80/20 blend and 1 wt% compatibilized system differs from the other three, virgin PP and 3 and 5 wt% compatibilized systems. The virgin PP shows a two dimensional crystal growth in the region 1.8-2.5 in the temperature scale of 380-405 K. Similar behaviour is shown by the compatibilized blends of 3 and 5 wt%. The blending of PP with 20 parts PLA changes the crystallization mechanism given by Avrami constant as 2.5 and higher. A similar trend is shown by 1 wt% of compatibilized blends but with a lower Avrami constant of 1.75 and so on in the temperature region we studied. The PLA fraction and the compatibilizer are behaving like heterogeneous nucleating agents and thereby affect the nucleation process. The recation between compatibilizer and PLA contribute to change the nucleation mechanism close to 2 and it remains the same for the designated temperature region. It is understandable that the mechanism of crystallization for 1 wt% is entirely different than 3 and 5 wt% and other studies are necessary to corroborate this phenomenon explicitly.
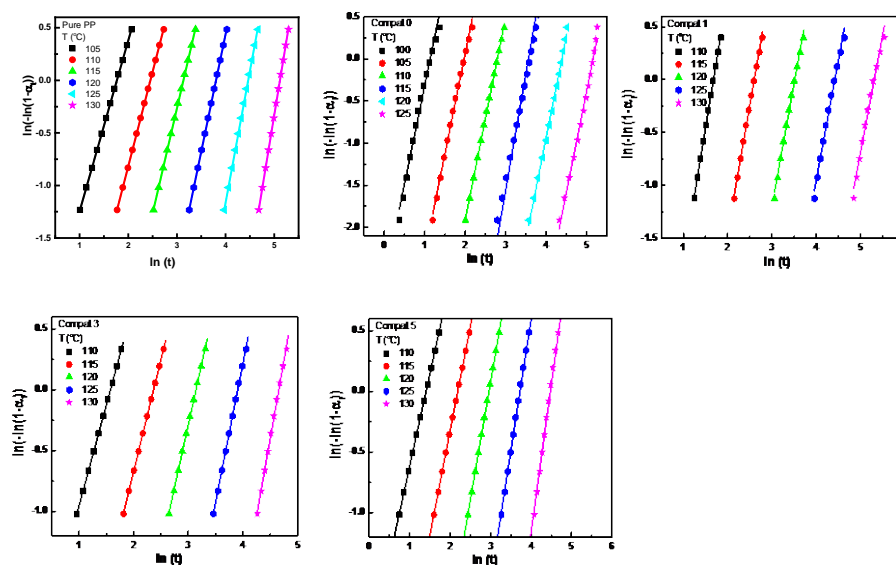
Figure 5.14Plots of $[-\ln(1 - \alpha_t)]$ Vs $\ln_t$
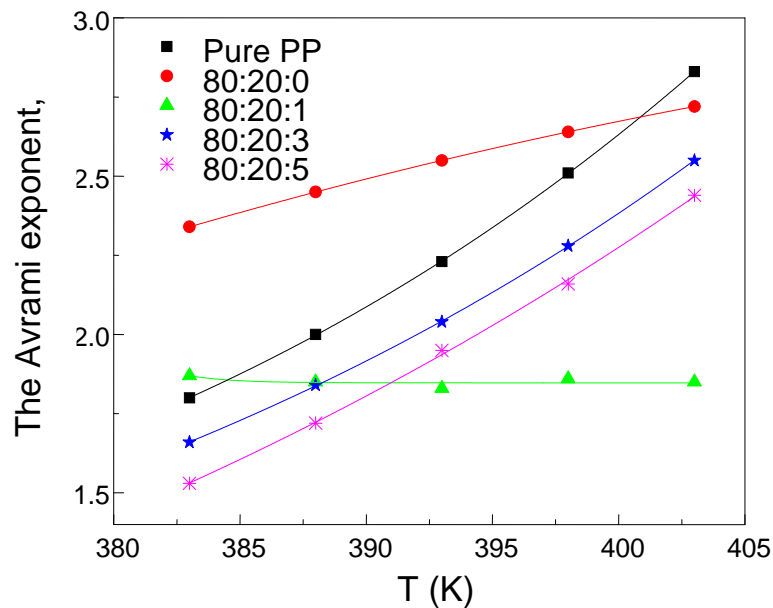
Figure 5.15Variation of Avrami exponent n with temperature

Another important parameter is the crystallisation half time, $t_{1/2}$, which is the time to achieve 50 % of relative crystallinity starting from the onset of crystallisation. The crystallisation half-time$t_{1/2}$, can be determined from the measured kinetic parameters using the following equation(Sencadas, Costa et al. 2010; Joraid and Alhosuini 2014;Xu, Wang et al. 2014):

$$t_{1/2} = \left(\frac{\ln 2}{k} \right)^{\frac{1}{n}},$$ (5.17)

The crystallisation half-time over the whole temperature range for the PP and PP-PLA blends was evaluated. The values of the overall kinetic rate constant$k$and the crystallisation half-time $t_{1/2}$ are shown in figures5.16 and 5.17, respectively. Figure 5.16 indicated that the blending of PP with PLA lowered the reaction rate constant and the compatibilization of the blends increased it to a significant level at 383 K. Thus compatibilization resulted in modifying the compatibility between the blend components and thereby the crystallization rate constant. It iswell recognized from

figure 5.17 that the crystallization half-time increases gradually with increasing the crystallization onset temperatures.The 80/20 blend and 1 wt% compatibilized system shows similar trend as shown in the previous calculations owing to the heterogeneous nature of the nucleating ability (Xu, Liang et al. 2003). The crystallization half time for virgin PP and the blends with compatibilizers 3 and 5 wt% are closing to the same value at around 400 K. Also, for a particular onset crystallization temperature, the $t_{1/2}$ of all the blends are lower than that of virgin PP, indicating that the blending of PLA and subsequent addition of compatibilizer in to the blend resulted in accelerating the non-isothermal crystallization process.
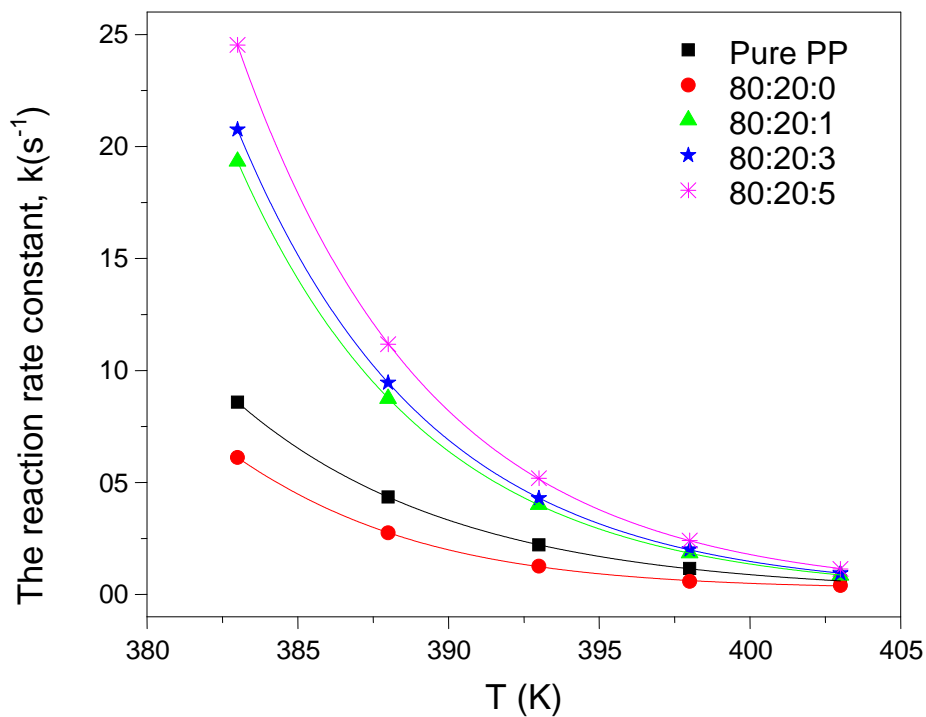
Figure 5.16Variation of reaction rate constant k with temperature
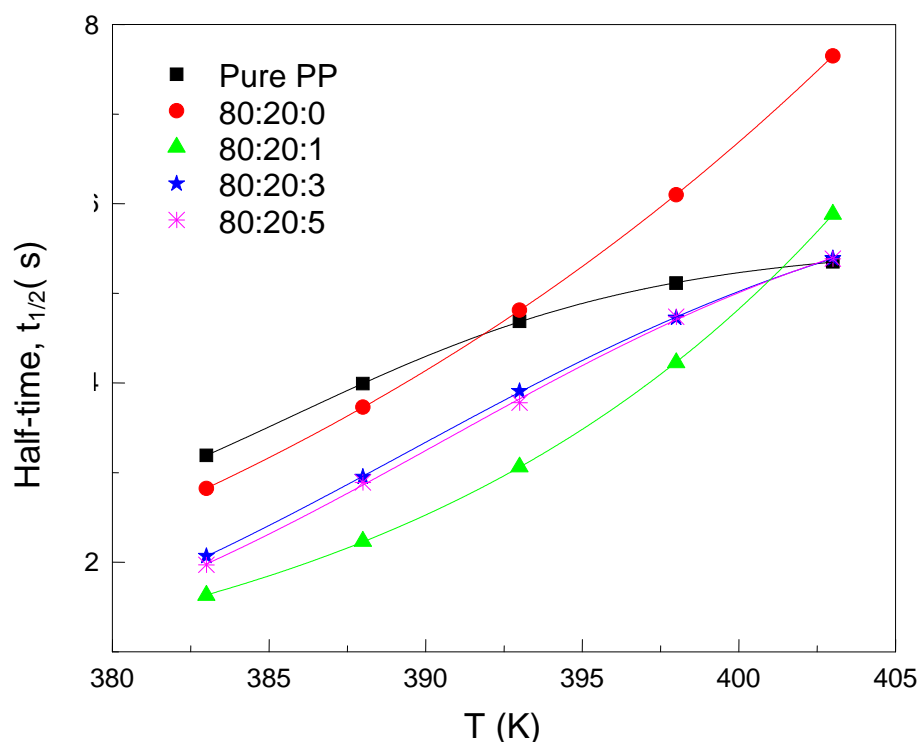
Figure 5.17Variation of crystallisation half time $t_{1/2}$ with temperature

5.4 Conclusion

The non-isothermal degradation kinetics of blends werestudied using a choice of mathematical models.The equations such as Kissinger, Friedman, Kissinger–Akahira–Sunose,Osawa Flynn Wall and Coates Redfern were used to study the kinetics of degradation in 80:20 blends of PP and PLA and their compatibilized ones. The obtained E_a values were in good agreement with those reported for the individual blend components. The E_a values corresponding to PLA in the blend increased with the increase in compatibilizer content up to 3 wt%, whereas, PP showed a decreasing trend in the E_a values.The thermal degradation mechanism for the blend system was found to follow a first order kinetics with random nucleation model.

The crystallisation kinetics of PP and PP/PLA (80/20) blends with varying amounts of compatibilizer weight percentage were done based on DSC studies for different heating rates. The activation energy for the crystallisation process was calculated

using different mathematical models which showed a decrease with respect to the concentration of the compatibilizer. From the isothermal crystallisation analysis, the Avrami exponents were calculated and indicated that the mechanism of crystallisation is mainly that of two-dimensional growth. The crystallisation half time calculated concluded the compatibilizer addition assisted the acceleration of the non-isothermal crystallisation process of the blends.

CHAPTER-6

INFRARED SPECTROSCOPY OF THE BLENDS AND NANOCOMPOSITES

6.1   Introduction

Infrared (IR) spectroscopy is a cost effective and powerful technique for the analysis of polymer systems. IR spectroscopy is a highly sensitive and molecularly specific tool for the structural analysis of molecules. It is based on the absorption of electromagnetic radiation by the material and the resulting specific motion of chemical bonds within the molecules of the subject material (Koenig 2001). The % transmittance peak at a characteristic frequency is considered as a measure of the concentration of the chemical species being explored in the sample.

6.2   Experimental procedure

FTIR spectra of the raw materials, blends and composites were recorded with a Nicolet iS 5 FTIR spectrometer (ThermoHaake). The spectra in the range of 4000 to 400 cm^{-1} were recorded in the attenuated total reflectance mode using diamond ATR accessory. A total of 32 scans were recorded with a resolution of 4 cm^{-1}. The spectral analysis was carried out using Omnic software of Thermo Fisher Scientific Inc.

6.3   Results and discussion

The FTIR spectra of the raw material used for the preparation of the blends are shown in figure 6.1. PP is characterized by the following peaks; at 809cm^{-1} corresponding to CH$_2$ rocking and C-C chain stretching, at 841 cm^{-1} corresponding to CH$_2$ rocking and C-CH$_3$ stretching, at 897 cm^{-1} corresponding to CH$_3$ rocking and CH bending, at 940 cm^{-1} corresponding to CH$_3$ rocking and C-C chain stretching (crystalline phase), at 971 cm^{-1} corresponding to CH$_3$ rocking and C-C chain stretching (amorphous phase), at 997 cm^{-1} corresponding to CH$_3$ rocking, CH$_2$ wagging and CH bending, at 1045 cm^{-1} corresponding to C-CH$_3$ stretching, C-C chain stretching and CH bending, at

1102 cm^{-1} corresponding to C-C chain stretching, CH$_3$rocking and CH$_2$ wagging, at 1167 cm^{-1} corresponding to C-C chain stretching, CH$_3$ rocking and CH bending, at 1255 cm^{-1} corresponding to CH bending, CH$_2$ twisting and CH$_3$ rocking, at 1377cm^{-1} corresponding to CH$_3$ symmetric bending and CH$_2$ wagging, at 3000-2800 cm^{-1} corresponding to Aliphatic CH stretching (Socrates 2004).
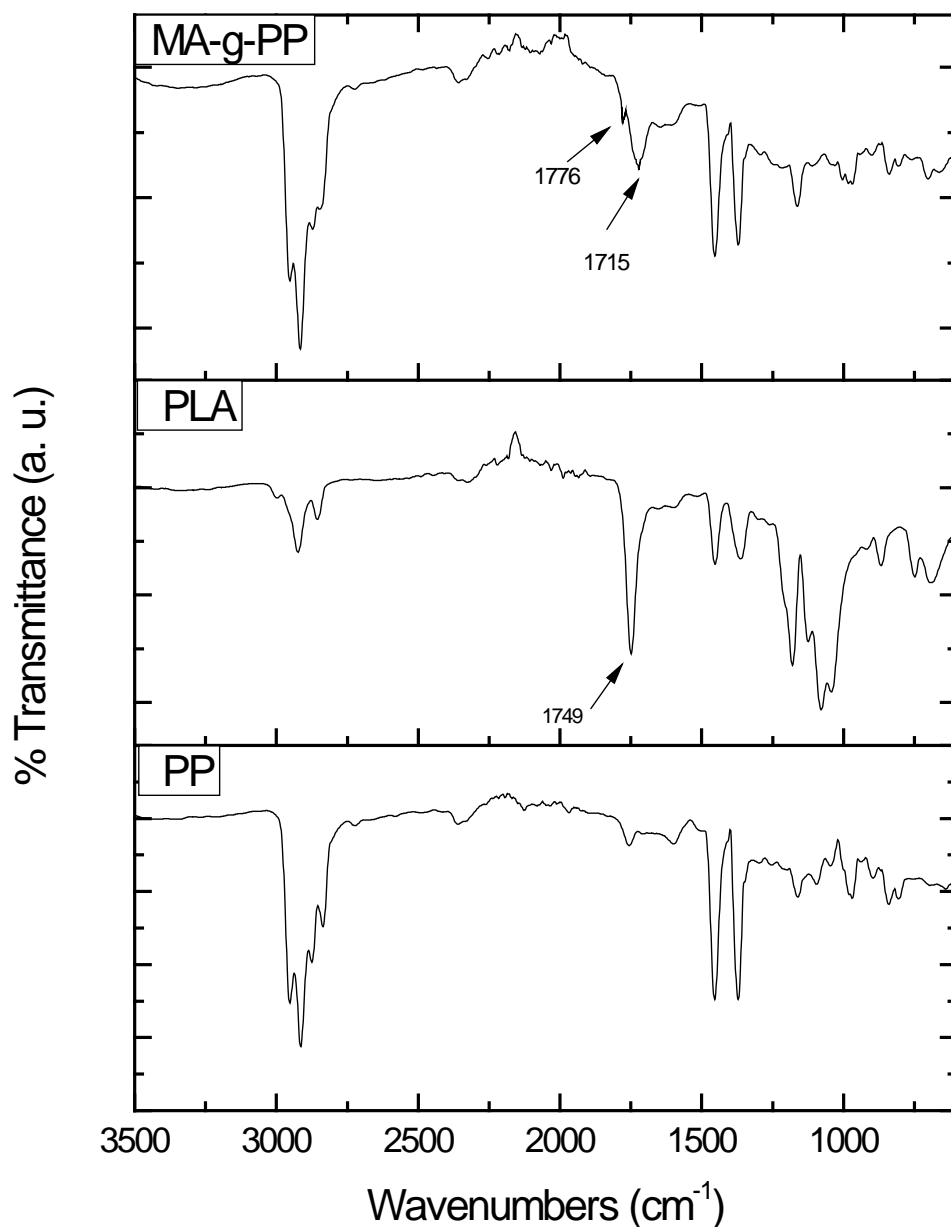
Figure 6.1FTIR spectra of PP, PLA and MA-g-PP

The PLA used in the studies is characterized by the following peaks; at 756 cm^{-1} corresponding to -C=O group, at 867 cm^{-1} corresponding to –C–C– stretch, at 956 cm^{-}

[1]corresponding to –CH$_3$ rocking modes, at 1041 cm^{-1} corresponding to –OH bend, at 1081 and 1180 cm^{-1} corresponding to COC, at 1129 cm^{-1} corresponding to –C–O– stretch, at 1268 cm^{-1} corresponding to CH and COC, at 1358 and 1382cm$^-$ [1]corresponding to -CH- deformations, at 1452 cm^{-1} corresponding to -CH$_3$ bending and at 1750cm^{-1} corresponding to -C=O carbonyl stretching. MA-g-PP, which is the compatibilizer used in the present investigation is characterised by peaks corresponding to that of PP along with the C=O stretching bands at 1776 corresponding to anhydride groups grafted on to PP.

6.3.1 Blends of PP and PLA
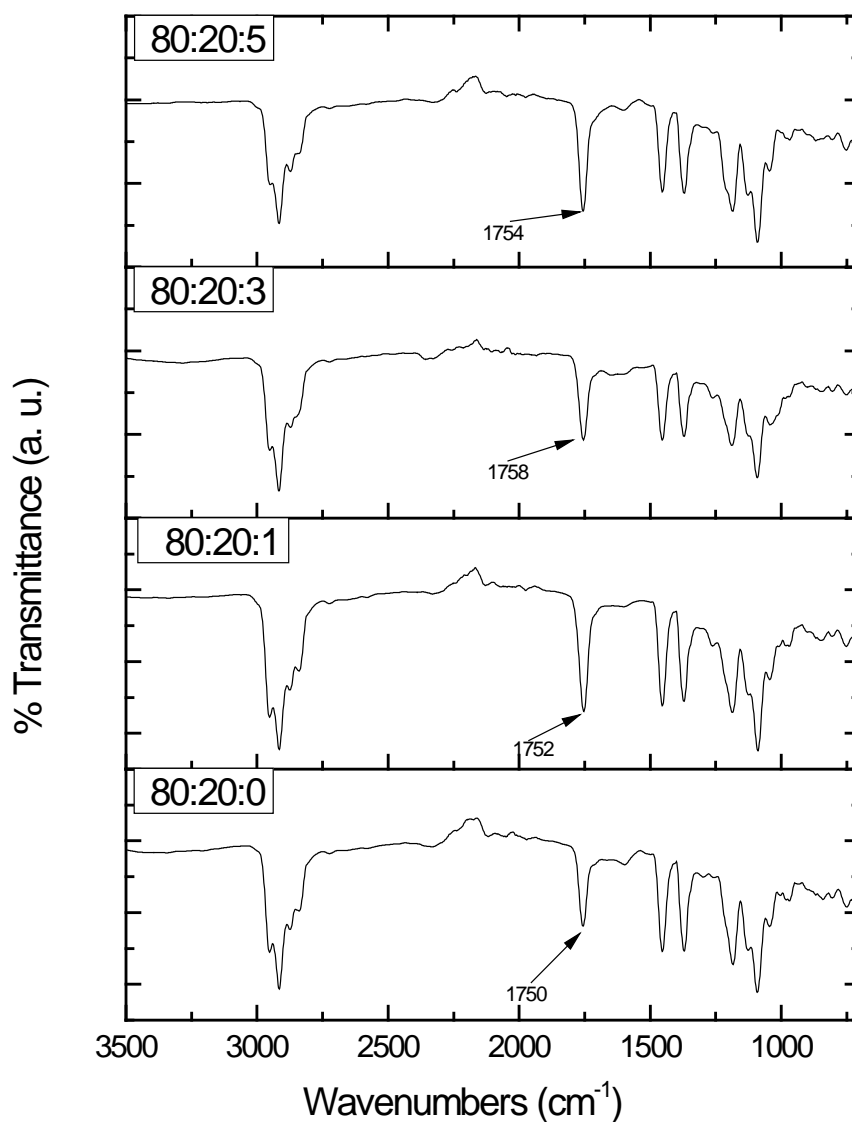
Figure 6.2FTIR spectra of the blends

The characteristic peaks corresponding to PP and PLA are present in the 80:20 blend of PP and PLA without compatibilizer (80:20:0). The peak at 1750 cm^{-1} corresponds to the C=O carbonyl stretching of the ester group in PLA. When 1 wt% of the compatibilizer is introduced to the blend, the spectra of the resulting blend (80:20:1) showed a shifting of the C=O carbonyl stretching peak to 1752 cm^{-1}, which indicates interaction of the PLA with the compatibilizer through the carbonyl group. As the compatibilizer is increased to 3 wt% (80:20:3), the shift in the carbonyl stretching peak became more prominent with a shift to 1758cm^{-1}, which shows the interaction between PLA and MA-g-PP is improved at this compatibilizer level. With further increase in compatibilizer content to 5 wt% (80:20:5), the shift in the carbonyl peak became less prominent with a shift to 1754 cm^{-1}.this indicates that the interaction between PLA in the blend and compatibilizer is maximum at a compatibilizer content of 3 wt%.
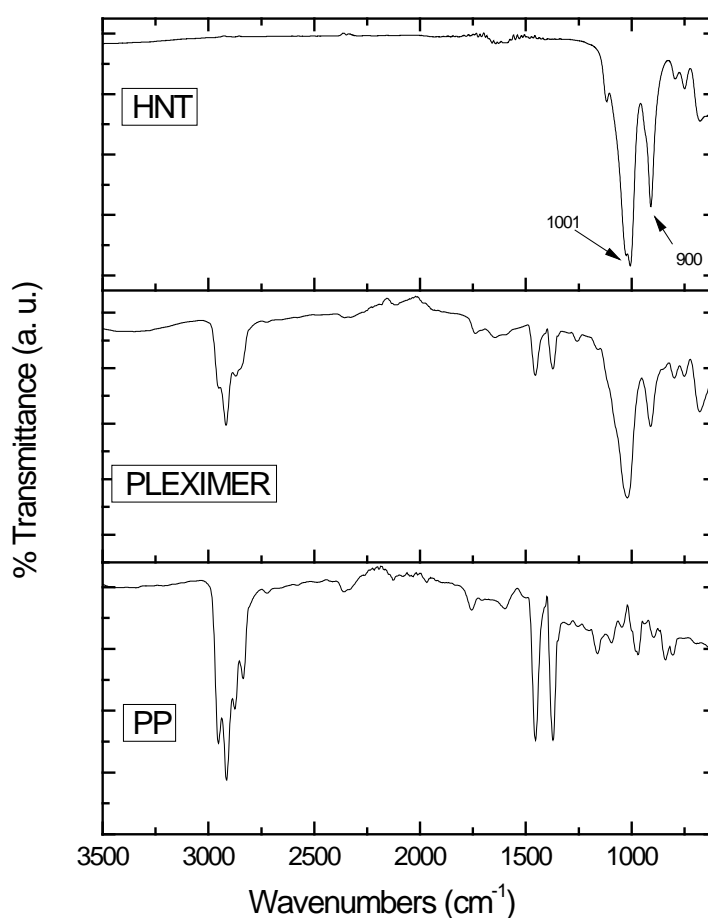
Figure 6.3FTIR spectra of PP, Pleximer and HNT

6.3.2   FTIR spectra of nanocomposites

The nanofiller used in the present investigation isPleximer, which is 30% masterbatch of halloysite nanotubes (HNT) in PP. The FTIR spectra of PP, HNT and the masterbatch (Pleximer) are shown in figure 6.3. In addition to the characteristic peaks of PP, Pleximer contains two typical peaks at 900 and 1001 cm^{-1}, which indicates the presence of silica and alumina on the surface of the nanotubes. The spectra of the base matrix (HNT 0) and the nanocomposites with HNT content up to 4 wt% (HNT 1, HNT 2 and HNT 4) are shown in figure 6.4.
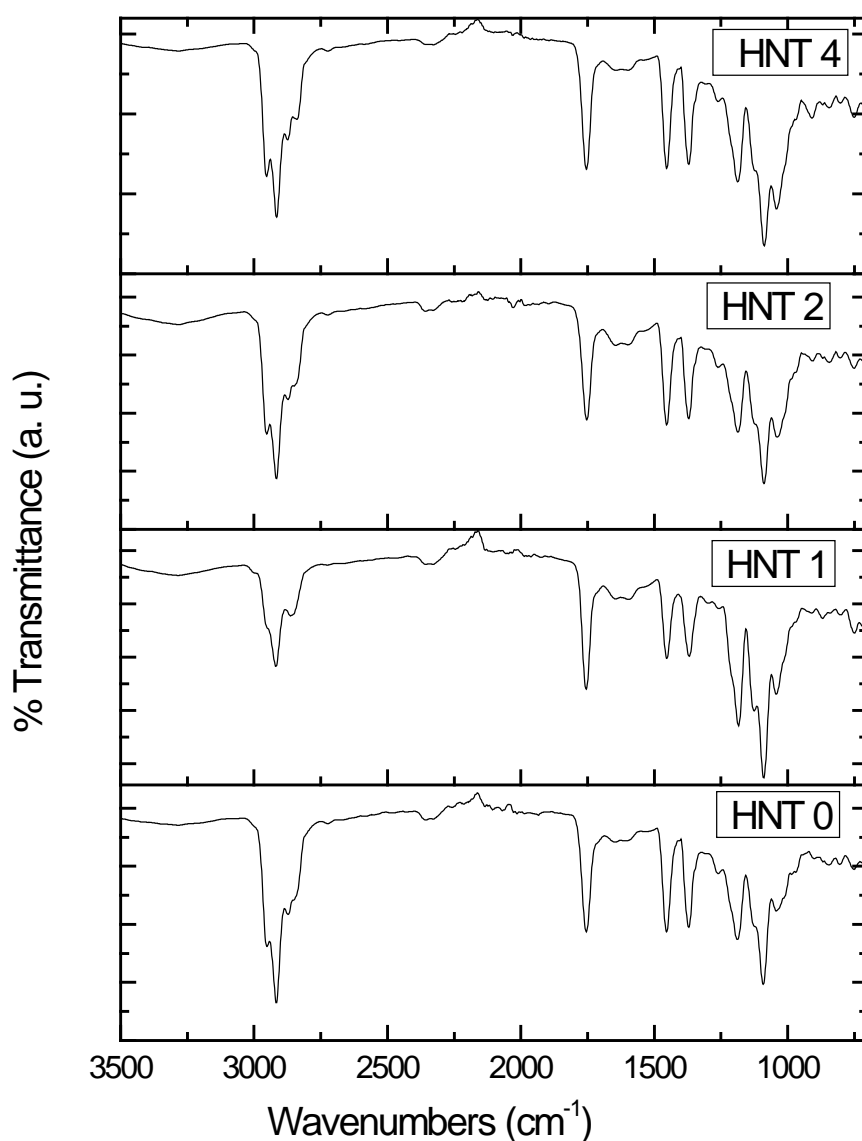
Figure 6.4FTIR spectra of nanocomposites up to 4 wt% of HNT

From the analysis of the spectra shown in figure 6.4, it is clear that the incorporation of HNT to the base matrix slowly resulted in a change in the peaks in the region 900 to 1100 cm^{-1}. This may be due to the interaction of the nanofiller with the PLA present in the matrix through hydrogen bonding. Similar observations can be seen in the study conducted by Liu et al. (Liu, Zhang et al. 2013). The change became clearer with further increase in the HNT loading to the base matrix (HNT 6 to HNT 10) as shown in figure 6.5
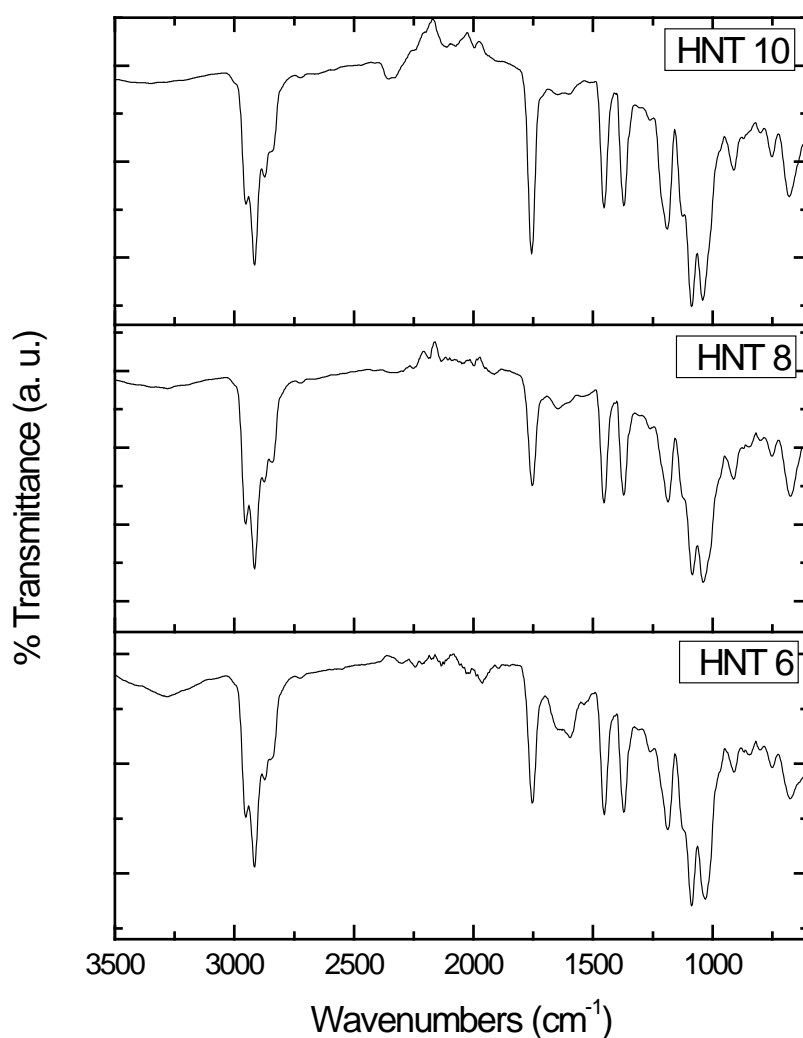
Figure 6.5FTIR spectra of nanocomposites from 6 to 10 wt% of HNT

6.4   Conclusion

The FTIR spectroscopic studies of the blends showed that the compatibilizer interacted with the PLA component of the blend and their interactions became optimum at a compatibilizer level of 3 wt%. The FTIR study of the nanocomposites based on this compatibilized blend also revealed interactions between the nanofiller and PLA.

CHAPTER-7

RHEOLOGY OF THE BLENDS AND NANOCOMPOSITES

7.1   Introduction

Melt rheological investigations are valuable tools to understand the effect of various parameters on the processability of polymers. The rheological behaviour of polymer blends and composites is very complex owing to the factors such as miscibility of the blend components, composition and microstructure of the blend, interfacial adhesion, compatibilizer content, interfacial activity of the compatibilizer, to name a few(Entezam, Khonakdar et al. 2012). Rheological data obtained from capillary rheometer has great importance in terms of processability because this technique provides insight on the effect of shear rate on viscosity over a wide range of shear rates that are commonly encountered in conventional plastics processing techniques.

7.2   Experimental procedure

Capillary rheometry was used to understand the high shear viscosity and anextensional viscosity of the prepared blends. Rosand Advanced Rheometer System (RH 2200, Malvern Instruments, UK) with twin-bore capability was used for this purpose. Experiments were carried out using a 20 mm long die (L/D – 20 mm) in the left bore and orifice die (zero length die) of the same diameter (1 mm)in the right bore. The shear rates were varied from 10 to 5000 s^{-1} at 220ºC. Bagley and Rabinowitsch corrections (Cogswell 1981) were performed automatically in order to account for the pressure drop at the capillary entry and the shear rate at the wall of the barrel respectively. The shear viscosity of the nanocomposites was also measured.

7.3   Results and discussion

The effect of corrected shear rates on the viscosities of PP and its blends with PLA with various compatibilizer contents (from 0 to 5 wt%) measured at 220ºC are shown in figure 7.1. With theincrease in shear rate, the melt shear viscosities of all the

samples decreased following a non-Newtonian and shear thinning behaviour. In the lower shear rate region, the shear viscosity of PP was lower than the 80:20 blend of PP and PLA, but with anincrease in shear rate, it showed higher values as compared with those of the blends, still maintained the shear thinning effect. In order to understand the rheological behaviour at higher shear rates, the viscosity values of PP and the blends at shear rates greater than 100 s^{-1} are plotted in figure 7.2. From figure 7.2, it is very clear that the viscosity of un- compatibilized blend is the lowest compared to PP and other compatibilized blends. This may be due to the low viscosity of PLA.
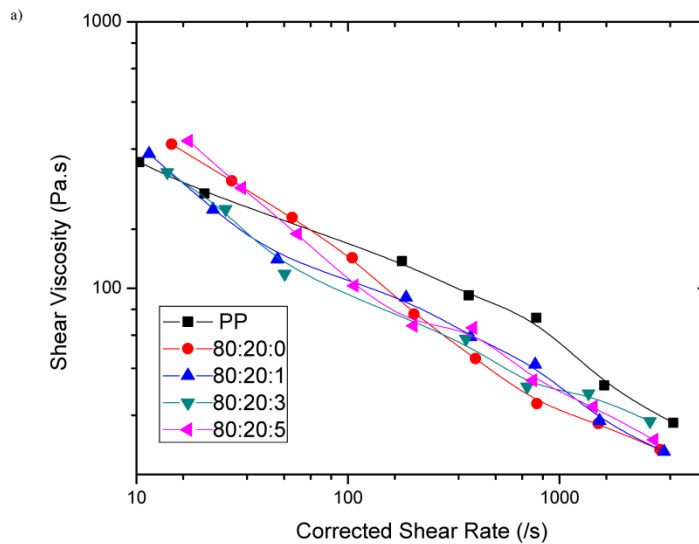
Figure 7.1Shear viscosity Vs corrected shear rate for PP and blends
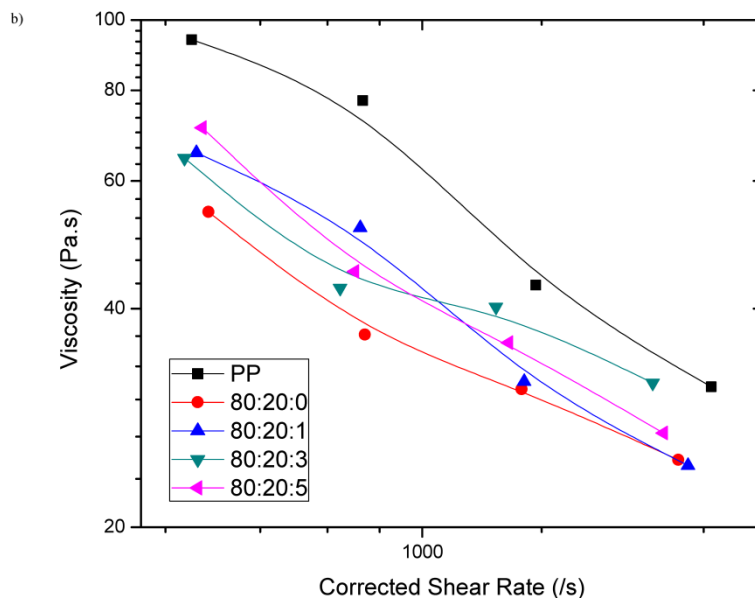
Figure 7.2Shear viscosity Vs corrected shear rate for PP and blends at higher shear rates

When compatibilizer is introduced into the blend (1 wt%), the shear viscosity increased considerably in the beginning but decreased and almost reached to the level of the un-compatibilized blends at higher shear rates. As the compatibilizer increased to 3 wt%, the viscosity was higher than the un-compatibilized blend, and it continued to increase at higher shear rates and showed the highest viscosity among all the blends. The increase in shear viscosity due to theincorporation of compatibilizer in immiscible polymer blends is a well-established phenomenon. A detailed compilation of similar attributes can be found in the literature(Utracki and Kanial 1982; Utracki 1983; Utracki and Wilkie 2002;Velankar, Van Puyvelde et al. 2004). When the compatibilizer content increased to 5 wt%, the viscosity was higher in the lower shear rate region but followed a downward trend in the higher shear rates. The reduction in viscosity at higher shear rates when the compatibilizer content reached 5 wt% suggests that the optimum level of thecompatibilizer is 3 wt% for effective compatibilization of PP and PLA in the ratio 80:20.

The increase in viscosity is attributed to the improved interfacial adhesion between the blend components and resulting chain entanglements due to the presence of compatibilizer at the interface. The mechanism of interaction of MA-g-PP with PLA and PP is described by Choudhary et al. in a polyblend system of PLA and PP in the ratio 90:10 (Choudhary, Mohanty et al. 2011).

Another important information obtained from the rheological data is the power law index n. It is an indication of the extent of thenon-Newtonianbehaviour of the polymer melt. For a shear thinning non-Newtonian fluid, the power law index n is less than 1. A decrease in n values indicates an exponential increase in flow (Sharma and Maiti 2015). The $n$values corresponding to PP and the blends are given in table 7.1. The value of$n$ for virgin PP is 0.61. For the 80:20 blend (without compatibilizer), the $n$value decreased to 0.48 and this is observed as a viscosity reduction in the shear viscosity versus shear rate curves shown in figure 1. When 1 wt% of thecompatibilizer is introduced to the blend, the n values increased to 0.56 and with further increase in compatibilizer addition (3 wt%), the value increased to 0.61. With further increase in the compatibilizer to 5 wt%, the n value decreased to 0.5, which is observed as a viscosity decrease in the corresponding curve in figure 7.1.

Table 7-1Non-Newtonian index, $n,$ values

Sample	n value
PP	0.61
80:20:0	0.48
80:20:1	0.56
80:20:3	0.61
80:20:5	0.50
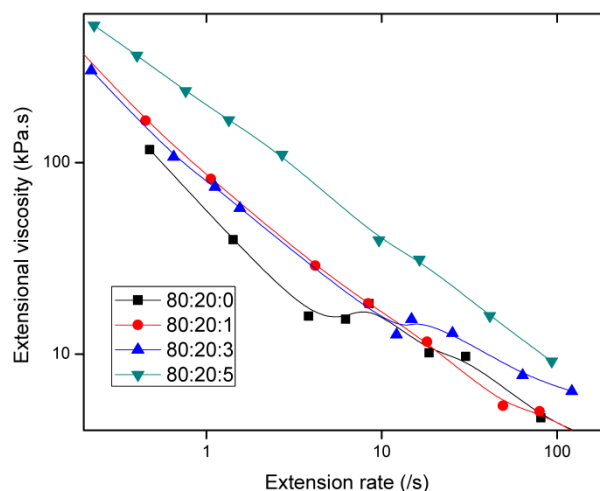
Figure 7.3 Extensional viscosity Vs extension rate for the blends

Extensional (elongational) viscosity is the resistance of a fluid to anextension.Several polymer processes involve extensionssuch as film blowing, melt spinning, blow moulding, thermoforming and sheet or film drawing and in all these processing operations, stretching and drawing is applied at various stages (Singh, Vimal et al. 2016). Hence determination of extensional viscosity provides a deep insight into the behaviour of polymer melts with extension rates. The extensional viscosities versus extension rate curves for the blends are shown in figure 7.3. From the curves, it can be seen that the extensional viscosity decreases with extension rate following a shear thinning behaviour and the un-compatibilized blend has the lowest extensional viscosity. The extensional viscosity increases with theaddition of compatibilizer to the blend and the increase are directly proportional to the compatibilizer content. It is interesting to note that with 3 wt% compatibilizer addition, the curve was almost similar to that having 1 wt% of the compatibilizer, but at higher extension rates, the viscosity increased appreciably.

The shear viscosity Vs corrected shear rate plot for the nanocomposites is shown in figure 7.4. All the samples showed the similar shear thinning behaviour. As the nano filter (HNT) is introduced to the base matrix, the shear viscosity started decreasing at

all shear rates as evident from the plot. But when the HNT content reached 6 wt% (HNT 6), the viscosity showed an increase and it is the highest compared with all other samples.
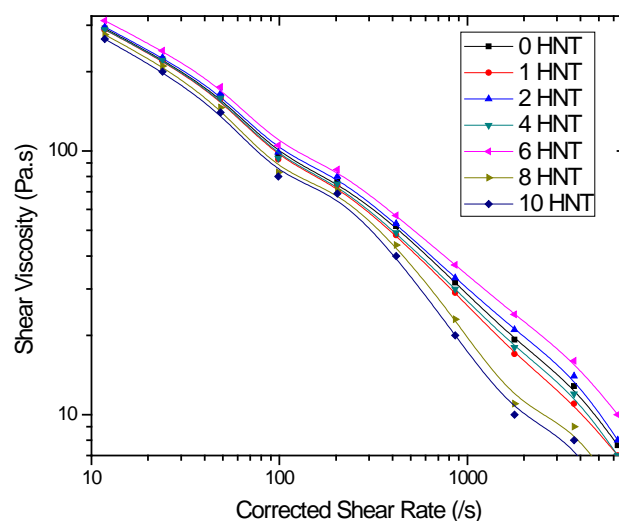
Figure 7.4Shear viscosity Vs corrected shear rate for the nanocomposites

This indicates that at 6 wt% of HNT, the matrix shows some interactions with the nanofiller and hence resulted in more entanglements of the chain and thereby ends up with more resistance to flow through the orifice and showed the highest viscosity. The improvement of static dynamic properties of the composites at 6 wt% of HNT addition can be correlated to this improvement in shear viscosity.

7.4   Conclusion

PP and PLA were blended in the ratio 80:20. The blend is compatibilized by adding MA-G-PP in ratios ranging from 0 to 5 wt%. Rheological measurements suggested that 3 wt% of the compatibilizer effectively compatibilized the selected blend. The shear viscosity of the nanocomposites became optimum with an HNT content of 6 wt%.

CHAPTER-8

WIDE ANGLE X-RAY DIFFRACTION STUDIES OF BLENDS AND NANOCOMPOSITES

8.1   Introduction

X-rays are considered as a component of electromagnetic radiations. When it interacts with a chemical substance, scattering occurs through the electrons of the atoms in the material. The combination of elastic scattering and destructive interference contribute to the phenomenon called X-ray diffraction. This can be determined by Bragg's law;

$$2d\sin\theta = n\lambda \qquad\qquad\qquad (8.1)$$

where, d is the spacing between the diffracting planes, θ is the incident angle, n is any integer (usually 1) and λ, the wavelength of the incident radiation. Crystalline materials give narrow and sharp peaks corresponding to specific crystal lattices present in them whereas, amorphous materials gives abroad and diffused peaks. Polymers being semi-crystalline in nature provide both sharp and broad peaks depending on the percentage of crystalline and amorphous portions present in them.

8.2   Experimental procedure

Wide-angle X-ray scattering (WAXS) patterns of the virgin materials, the prepared blends and nanocomposites were collected using Cu Ka radiation (λ = 1.54 nm) generated by a benchtop X-ray diffractometer (RigakuMiniFlex 600) operated at 30 kV and 10 mA.The scanning speed and diffraction angle (2θ)were kept at 5°/min and 3–90° respectively. From XRD data, crystallitesize (L) was measured according to the Schererequation(Klug and Alexander 1954);

$$L = \frac{k\lambda}{\beta\,cos\theta} \qquad\qquad\qquad (8.2)$$

where, β is full-width half maximum of the crystalline peak (in radian), $\lambda$is the wavelength of the X-ray radiation (1.54 Å), and k isthe Scherer constant having a value of 0.9 to 1.

8.3   Results and discussion

The XRD patterns for virgin PP and PLA is shown in figure 8.1. Virgin PP is characterised by 2θ peaks at 14.5°, 17.2° and 18.8° corresponding to α (110), α (040) and α (130) reflections(Liu, Guo et al. 2009; Wang and Huang 2013). Their corresponding crystallite sizes (L) according to Scherer equation are 71.5, 60 and 61 A° respectively. Virgin PLA is characterised by a peak at 2θ = 16.8°corresponding to (110), which is similar to the observation reported by other research groups(Ying-Chen, Hong-Yan et al. 2010; Dong, Marshall et al. 2015).
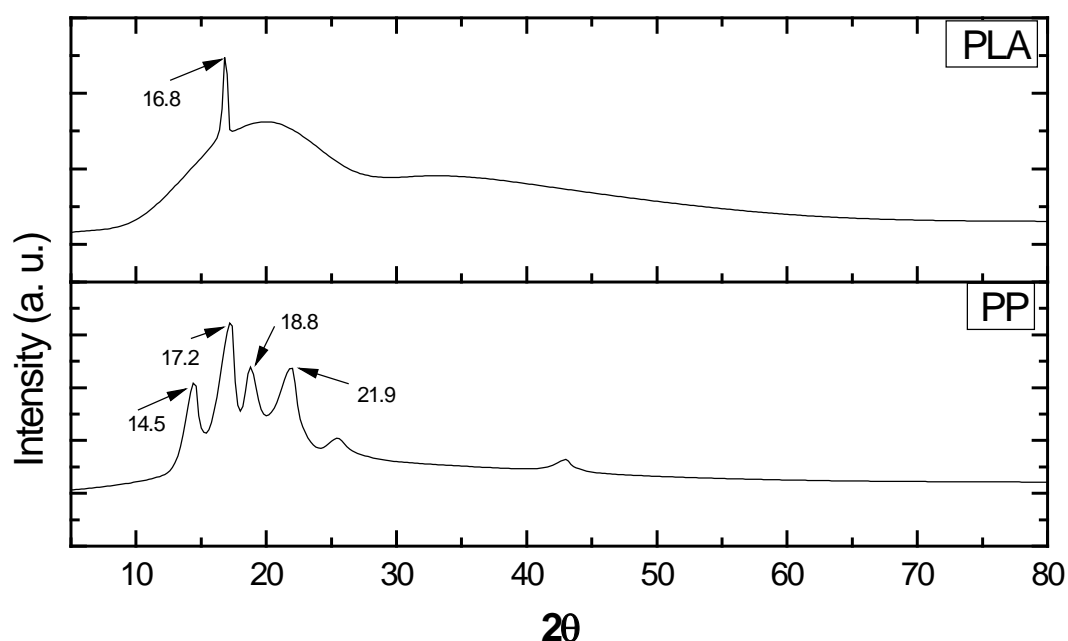
Figure 8.1XRD patterns for PP and PLA

The XRD patterns for the blends are shown in figure 8.2. The incorporation of 20 percentage of PLA into PP changed the crystal structure of PP as evident from the XRD pattern of 80:20:0 in figure 8.2. The 2θ peaks at 14.5°, 17.2° and 18.8° of virgin PP shifted to 13.8°, 16.3° and 18.3° respectively. This change in 2θ peaks can be attributed to the presence of completely immiscible PLA chains present in the material and the resulting uncompatible structure of the blend. With the addition of 1 wt% of compatibilizer to the blend, the 2θ peaks in the area of interest shifted to 14°, 16.7° and 18.3° respectively. With further increase in compatibilizer to 3 wt%, the 2θ peaks appeared at 14.5°, 17.3° and 18.8°, which are almost similar to that observed

with virgin PP, which indicates the effectiveness of compatibilizer to preserve the crystal structure of PP present in the blend. A similar observation can be seen in the investigation reported by Jain et al. (Jain, Madhu et al. 2015), where the 2θ peaks of the compatibilized blend matched almost similar to those of the virgin PP used in the blend. As the compatibilizer content in the blend increased further (to 5 wt%), the 2θ peaks appeared at 13.8°, 16.6° and 18.1° respectively, which are similar to those of the uncompatibilized blend.
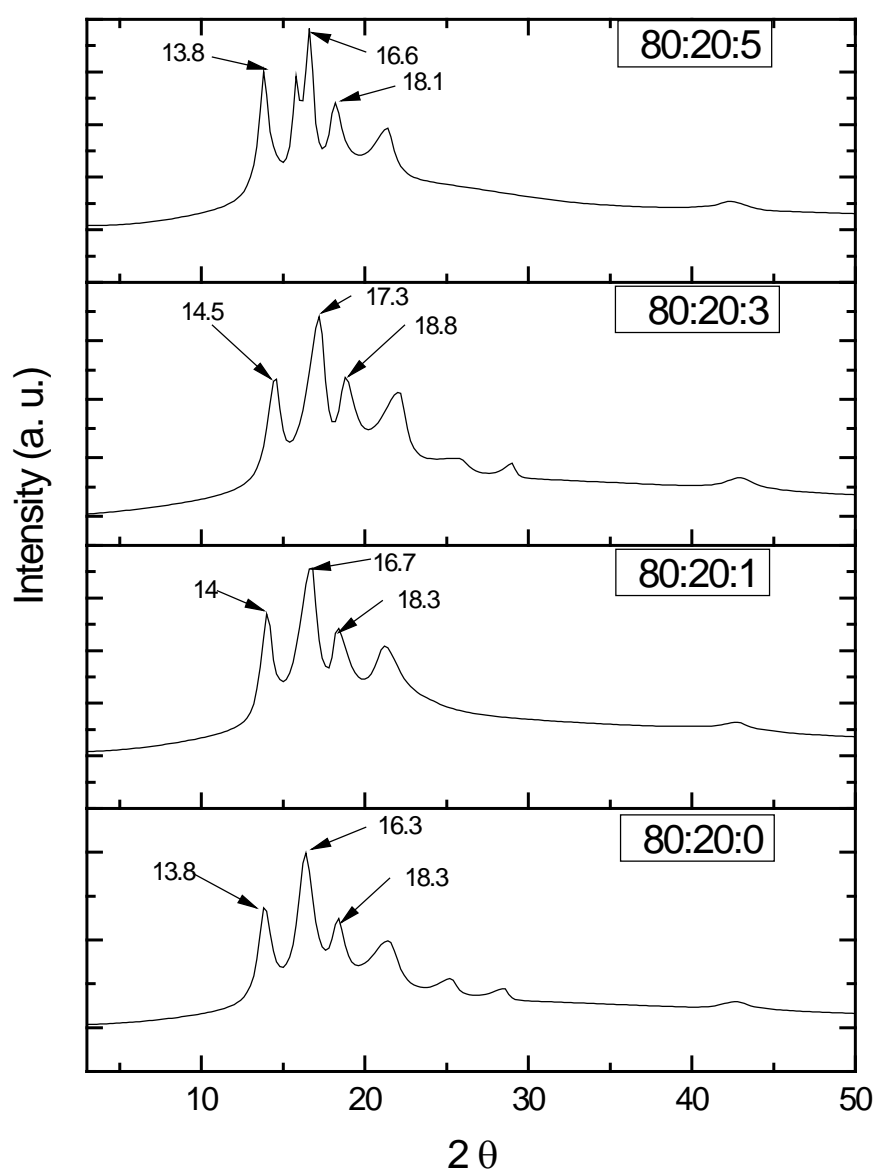
Figure 8.2XRD patterns for the blends

The XRD patterns of the raw materials used for the preparation of nanocomposites are shown in figure 8.3. HNT is characterised by 2θ peaks at 12.2°, 20° and 24.6°

corresponding to (001), (020), (110) and (002) with d-spacing values of 7.2, 4.4 and 3.6 A° respectively. This is in good agreement with values reported in the literature (Dong, Chaudhary et al. 2011; Liu, Zhang et al. 2013;Dong, Marshall et al. 2015). The hydration state of HNT is normally characterized by the presence of 2θ peaks at 8.76° (Levis and Deasy 2002). As the XRD pattern of HNT does not show any peak corresponding to this 2θ range, it can be considered as fully dehydrated HNT.
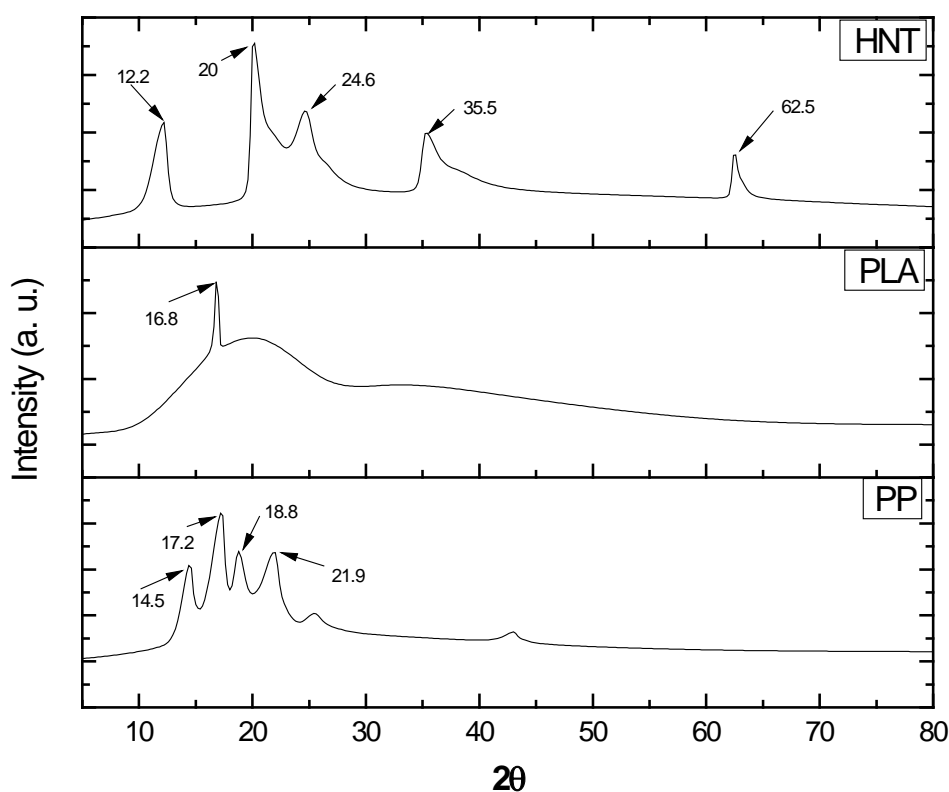
Figure 8.3XRD patterns for PP, PLA and HNT

The XRD patterns of the nanocomposites with HNT wt% varying from 0 to 10 are shown in figure 8.4. HNT 0 corresponds to the compatibilized blend of PP and PLA with 3 wt% of acompatibilizer, the spectra of which is described before. With the incorporation of 1 wt% of HNT, there is not much change for the resulting spectra of the nanocomposites (HNT 1) as compared with that of the base matrix (HNT 0). The characteristic 2θ peak at 12.2° of HNT was not visible in the spectra of HNT 0 and

also in HNT 1. This indicates that either at 1 and 2 wt% of addition, the XRD technique is not capable of detecting the typical crystal structures of HNT or the nanotubes are wide apart due to the homogenous blending of the available nanotubes in the polymer matrix. When the HNT loading reached 4 wt%, a small curvature appeared at the typical 2θ value of pure HNT (12.2), which shows the increase in nanotubes dispersed in the polymer matrix. With further increase in HNT wt% to 6, 8 and 10, the peak at 2θ value around 12.2 became more pronounced. Another major observation is the disappearance of 2θ peak of HNT at 20° from all the nanocomposites. This shows the interactions of HNT with the PLA component of the blend. Preferential orientation of nanotubes as reported by Liu et al. ((Liu, Zhang et al. 2013) can be the reason for this and also this indicates a 2D homogenization of the nanotubes in the base matrix.
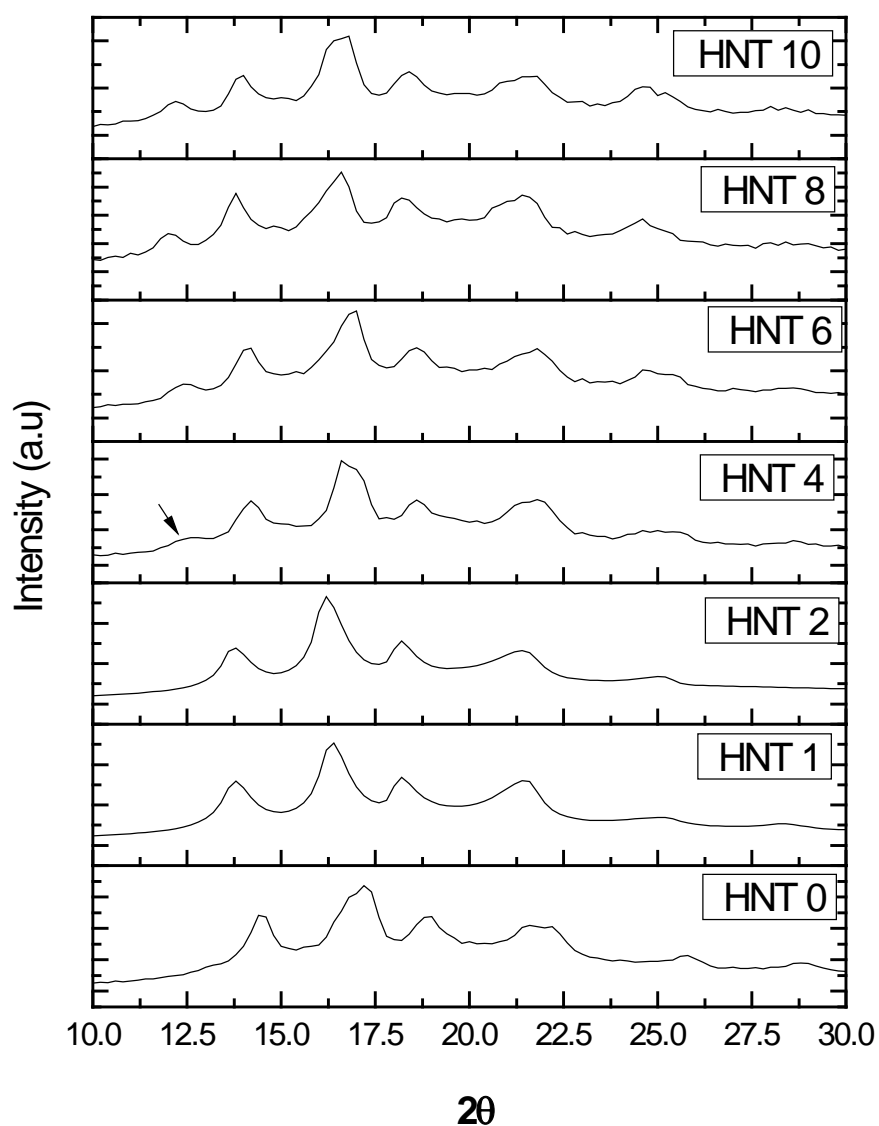
Figure 8.4XRD patterns of nanocomposites

8.4   Conclusion

The XRD analysis of the blends of PP and PLA with various % of compatibilizer showed that the crystal structure of PP in the blend changed with theincorporation of PLA whereas, incorporation of 3 wt% of compatibilizer could preserve it similar to virgin PP, which shows the effectiveness of the compatibilizer. In the analysis of nanocomposites, the characteristic peak of HNT appeared only when it reached 4 wt% in the composite. The analysis also revealed the interactions between PLA and HNT.

CHAPTER-9

DSC AND TGA OF NANOCOMPOSITES

9.1   Introduction

Differential scanning calorimetry (DSC) of the nanocomposites was performed to obtain information about the changes in melting and crystallisationbehaviour of the matrix material with the incorporation of varying amounts of HNT. Thermogravimetric analysis (TGA) provided valuable insights about the thermal decomposition characteristics of the nanocomposites.

9.2   Experimental procedure

The melting and the crystallisation behaviour of the nanocomposites were analysed using a Differential scanning calorimeter (DSC) [TA instruments DSC-Q 1000]from 25 to 200 °C, held at 200 °C for 2 minutes and then cooled to 25 °C and again heated to 200 °C.Thermogravimetric analysis (TGA) of the nanocomposites was carried out using TA instrument TA-SDT 2960 at a heating rate of 10°C /min and sample weight loss were continuously recorded against the sample temperature.

9.3   Results and discussion

9.3.1   DSC of nanocomposites

The representative second heating curve obtained from the DSC instrument for the nanocomposites is shown in figure 9.1. From the figure, two melting transitions are clearly visible, the one at the lower temperature corresponds to that of PP and the other one at a higher temperature corresponds to PLA in the base matrix.
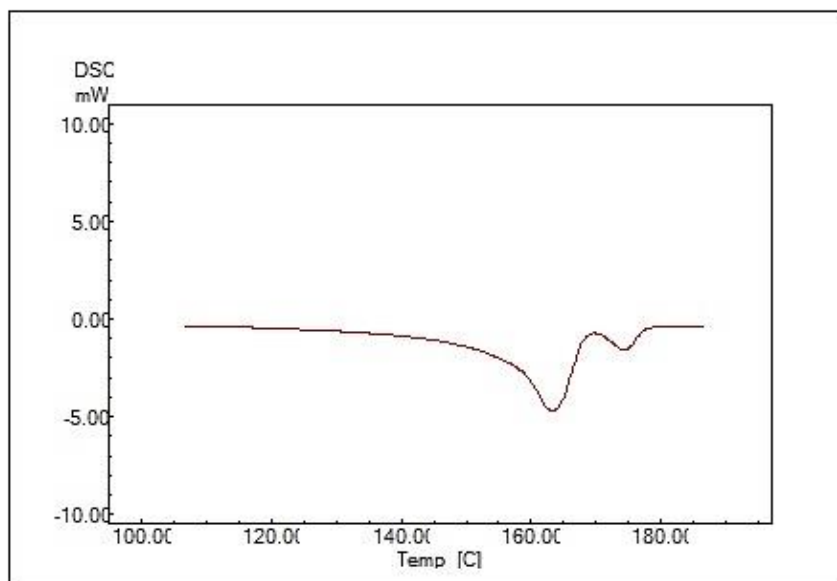
Figure 9.1Representative second heating curve of nanocomposites

The change in melting temperature (T_m) of these two blend components in the matrix with the incorporation of HNT in various loading is given in table 9.1.

Table 9-1DSC melting peaks of blend components present in nanocomposites

	DSC Melting Peaks corresponding to;	
Sample	**PP (^{o}C)**	**PLA (^{o}C)**
PP	162	
PLA		177
HNT 0	163	174
HNT 1	163	174
HNT 2	163	174
HNT 4	163	173
HNT 6	162	172
HNT 8	161	173
HNT 10	162	171

From table 9.1, it is clear that the melting peak corresponding to PP in the base matrix remained same (162°C) throughout the entire composition range, which again showed that the incorporation of HNT does not have any significant effect on the melting behaviour of PP. Virgin PLA has a melting peak at 177°C. It decreased to 174°C in the base matrix. This may be due to the compatibilization effect of MA-g-PP with the major component of the matrix (PP). With the incorporation of HNT to the base matrix, the T_m corresponding to PLA gradually decreased and reached a value of 172°C with an HNT content of 6 wt%. Further increase in HNT loading does not have any significant effect on the melting behaviour of PLA as evident from the values for HNT 8 and HNT 10. The reduction in melting temperature of PLA in the base matrix can be correlated to the interactions that HNT is capable of making with it as discussed in the analysis of FTIR spectra of the nanocomposites.

The representative DSC cooling curve corresponding to crystallisation peaks in the nanocomposites is shown in figure 9.2.
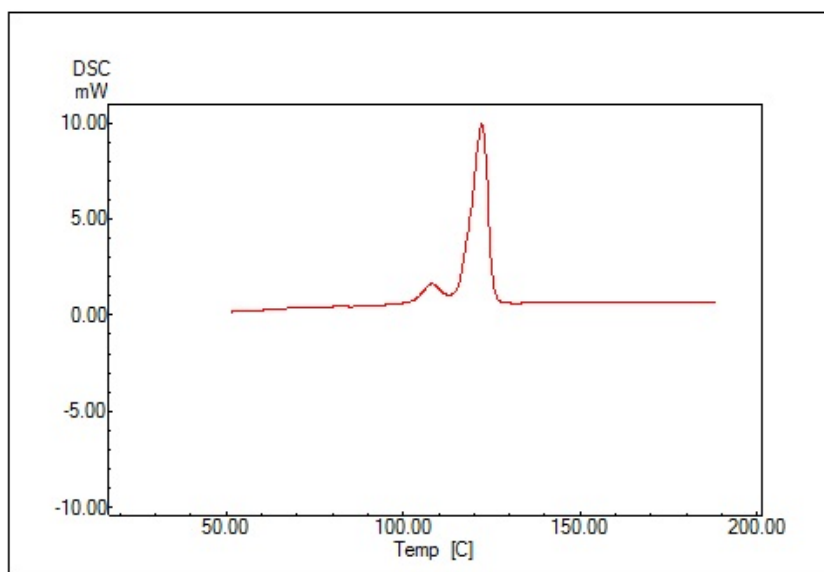
Figure 9.2Representative first cooling curve of nanocomposites

When the molten composite is cooled from a higher temperature to room temperature, the component polymers present in the matrix crystallise and give rise to two crystallisation peaks, one corresponds to PP (at a higher temperature) and the other one corresponds to PLA (at alower temperature). The percentage crystallinity, *Xc*, of PP in the nanocomposites was calculated by applying the relation, $Xc = \Delta H^*/\Delta H^\circ_{PP}$, where, ΔH^* is the enthalpy of fusion in Joules per gram of PP present in the nanocomposites, and ΔH°_{PP} is the heat of fusion of 100% crystalline PP (209J/g) (Kato, Usuki et al. 1997; Svoboda, Zeng et al. 2002) The percentage crystallinity, crystallisation peak temperatures for the individual blend components and their changes with respect to increasing in HNT content in the nanocomposites are given in table 9.2. Virgin PP and PLA crystallise at 116 and 101°C respectively. The crystallisation temperature of both the blend components increased in the base matrix (HNT 0) to 121 and 107°C respectively corresponding to PP and PLA components. This shows that the blending PP with PLA has improved the crystallisationbehaviour of the resulting compatibilized blend. With the incorporation of HNT to the base matrix, the crystallisation temperature of PP in the matrix remained almost similar to that of the base matrix (HNT 0), whereas, the crystallisation temperature of PLA showed a gradual increase and increased to 110°C with an HNT content of 6 wt%.

This indicates that the incorporation of HNT has a favourable effect on the crystallisation behaviour of PLA present in the matrix. This can also be attributed to the interactions that HNT can make with the PLA as evidenced from the FTIR analysis.

Table 9-2DSC crystallisation peaks of blend components in nanocomposites

Sample	DSC crystallisationpeak temperature for;		crystallinity (Xc) of PP (%)
	PP (^{o}C)	PLA (^{o}C)	
PP	116	--	43
PLA	---	101	---
HNT 0	121	107	28
HNT 1	123	104	30
HNT 2	123	108	34
HNT 4	122	108	34
HNT 6	121	110	48
HNT 8	121	110	40
HNT 10	122	110	36

The percentage crystallinity of virgin PP used in the present investigation is 43%. For the base matrix it reduced to 28% owing to the presence of 20% of amorphous PLA. The major contribution for the crystallization of the blend is due to the PP phase which is only 80% and hence showed a reduction in the percentage crystallinity value. With the incorporation of 1 wt% ofHNT to the base matrix, the crystallinity of the PP phase in the matrix improved to 30%, which indicates that HNT can act as nucleating agents for the PP to initiate the growth of crystallites within the blend matrix. The percentage crystallinity showed an increasing trend with the increase in HNT wt%

and reached a maximum of 48% at an HNT loading of 6 wt%. The *Xc*valuescorresponding to HNT 8 and HNT 10 showed a decreasing trend. This may be due to the agglomeration of nanotubes at certain areas within the blend. The improved tensile strength and modulus values of HNT 6 reported during the mechanical property evaluation can be directly correlated to the increased value of *Xc* in this investigation.

9.3.2   TGA of nanocomposites

The TGA thermograms for HNT powder and the nanocomposites are shown in figure 9.3. The HNT powder has only 4% weight loss in the experimental temperature range. The weight loss profile of the base blend and nanocomposites are almost similar as evident from figure 9.3. As the HNT content increased from 1 to 10 wt%, the residue remaining at 600°C also increase gradually. From the curves, the temperature at which 50% of the weight loss happened (t_{50}) was obtained for all the compositions and is given in table 9.3. There is no significant change in the t_{50}values for nanocomposites, which indicates that there is no major improvement in the thermal degradation profile of the nanocomposites with anincrease in HNT addition.
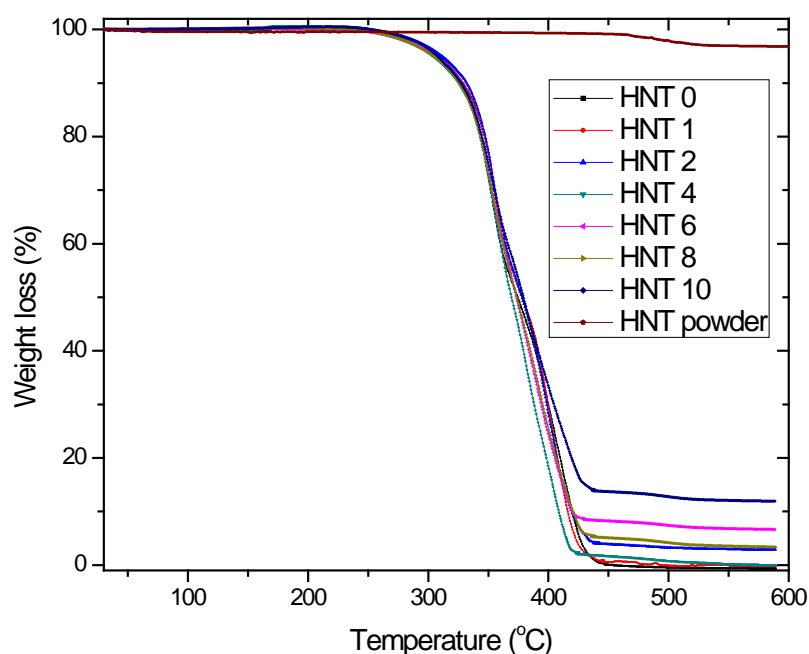
Figure 9.3TGA thermograms for HNT and nanocomposites
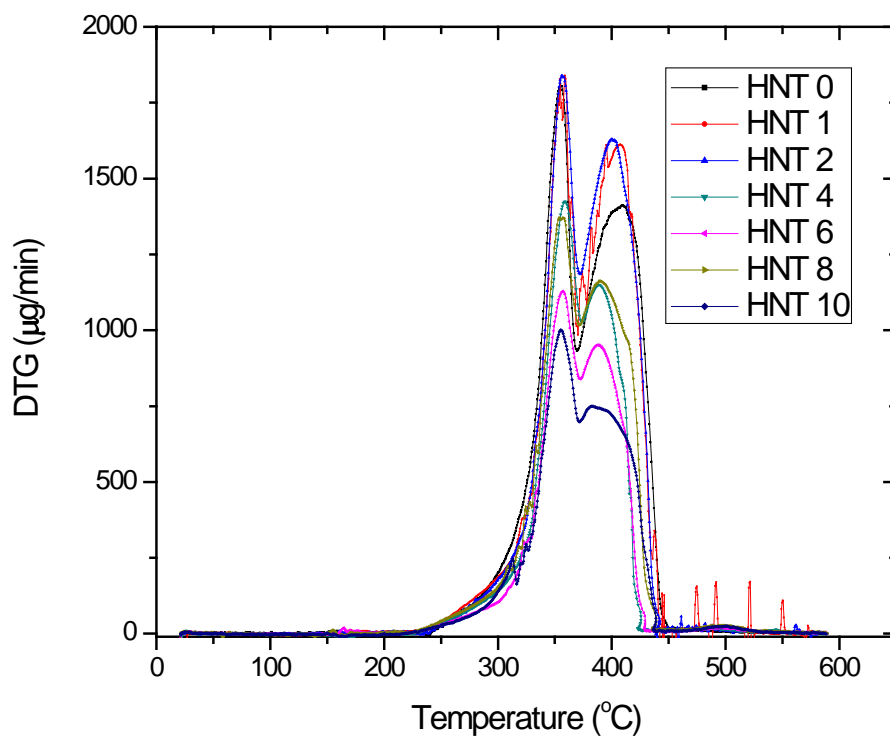
Figure 9.4DTG curves for nanocomposites

The derivative thermogram (DTG) of the nanocomposites showed two peak temperatures, one corresponding to PP and the other one for PLA in the base matrix. The DTG in curves for nanocomposites is shown in figure 9.4 and the corresponding peak temperatures are listed in table 9.3

Table 9-3Thermal degradation parameters obtained from TGA/DTG curves

Sample	t_{50} (^{o}C)	T_{max} for PP(^{o}C)	T_{max} for PLA(^{o}C)
HNT 0	375	356	409
HNT 1	378	356	407
HNT 2	378	358	402
HNT 4	369	360	390
HNT 6	374	358	389
HNT 8	373	356	392
HNT 10	379	356	390

The same trend is observed for the maximum degradation temperature values from the DTG peaks. The research work by Chen et al. (Chen, Geever et al. 2015) and Liu et al. (Liu, Zhang et al. 2013) for PLA/HNT nanocomposites also reported similar trends and this was attributed to the presence of voids existing between the filler and the matrix. Limited thermal stability improvement was also reported for other systems such as PLA/silica and PLA/graphite nanocomposites (Kim and Jeong 2010; Kontou, Niaounakis et al. 2011)

9.4   Conclusion

The DSC analysis revealed that the incorporation of HNT does not have any significant effect on the melting behaviour of PP whereas, the melting temperature (T_m) of PLA gradually decreased and reached a value of 172°C with an HNT content of 6 wt%. Further increase in HNT loading does not have any significant effect on the melting behaviour of PLA. The percentage crystallinity of PP in the base matrix showed an increase with increase in HNT addition and the value reached maximum at HNT 6. TG/DTA showed that incorporation of HNT did not alter the thermal degradation profile of the nanocomposites.

CHAPTER-10

DIELECTRIC ANALYSIS OF NANOCOMPSITES

10.1   Introduction

Various characterization techniques such as infrared (IR) and Raman spectroscopy, differential scanning calorimetry (DSC), thermogravimetric analysis (TGA), dynamic mechanical analysis (DMA), mechanical properties, rheological properties, X-ray diffraction analysis, scanning electron microscopy (SEM), transmission electron microscopy (TEM), atomic force microscopy (AFM) are utilized for exploring the properties of nanofiller-polymer interactions in polymer nanocomposites(Koo 2006). However, there is very few reported literature on the characterization of nanocomposites by dielectric analysis (DEA)(Cerezo, Preston et al. 2007; Xu and Wong 2007; Yang, Benitez et al. 2007; Yang and Kofinas 2007; Li, Tjong et al. 2010; Helal, Demarquette et al. 2015). DEA provides valuable insights about dielectric properties of materials such as ion conductivity, loss factor, permittivity and tanδ as a function of time,temperature and frequency.Here, a material is subjected to an oscillating electrical field and information regarding capacitive and conductive properties is elucidated from the response of the material. The dielectric permittivity, also known as dielectric constant refers to the ability of the material to store electrical charge. It indicates the easiness of aligning dipoles present in the material under the applied electric field(Sepe 1997; Kremer and Schönhals 2012). Loss factor indicates the energy required to align the dipoles and move the ions present in the material when the material is in the glassy state (below T_g)(Sepe 1997). Above T_g, theloss factor of the material is related to the ionic conductivity of the applied frequency. Ionic conductivity is related to the viscosity of the material and particularly important in monitoring the curing behaviour of thermosets. The dissipation factor, tanδ, is the ratio of loss factor to permittivity and is analogous to mechanical tanδ obtained from dynamic mechanical analysis (DMA)(Sepe 1997). Dielectric properties arise due to the response of dipoles present in the materials towards the applied electromagnetic field(Shepard and Twombly 1996). These properties can be correlated to the chemical structure, polarity, conformation, packing and interaction of molecules within the material on a molecular level(Campbell, Goodwin et al. 2001). As a result of this, the

rheological properties and molecular relaxations happening in polymer blends and composites can easily be explored(Maxwell, Monnerie et al. 1998; Campbell, Goodwin et al. 2001). Also, these studies provide valuable information about the processing aspects and morphological development in polymer nanocomposites(Shepard and Twombly 1996). Exploring the dielectric properties of materials is also important in the research and development activities related to themanufacture of electrodes for batteries, fuel cells, sensors, supercapacitors, microelectronic packaging materials for high-frequency devices etc(Raja, Sharma et al. 2004). The dielectric analysis of the nanocomposites was carried out to find the effect on permittivity, loss factor and tanδ as a function of temperature and frequency.

10.2   Experimental procedure

Dielectric analysis of the composite samples was performed using DEA 288 Epsilon (Netzsch-GMBH) dielectric analyser equipped with a DEA furnace. The sensor used was interdigitated comb type electrode sensor (IDEX). Rectangular sample of dimension 25mmX12.5mmX3mm was placed on the sensor surface and kept inside the furnace. The sample was tightly kept on the sensor surface using Kapton adhesive tape. This step ensured excellent contact of the sample with the sensor surface. The test was carried out from 1 Hz to 1 kHz over a temperature range from 30°C to 120°C.

10.3   Results and discussions

10.3.1 Permittivity analysis

Permittivity curves of the compatibilized blend without HNT (HNT 0) as a function of temperature and frequency are shown in figure 10.1.At a frequency of 1Hz and at a temperature of 30°C, the permittivity of the blend matrix was almost 1. As the temperature increased, the permittivity slowly increased and reached almost 3 at a temperature of 120°C.This shows that blending non-polar PP with polar PLA imparts some polarity to the resulting blend system. For non-polar polymers, the permittivity remains almost unchanged with temperature, but for polar polymers, permittivity

increase with an increase in temperature.(Yang, Benitez et al. 2007) Similar observations were also reported by Wong et al.(Wong, Wouterson et al. 2006)in acrylate composites reinforced by graphite. As the frequency increased from 1Hz to 1 kHz, the permittivity values decreased in the lower temperature range and all the curves followed the same trend as that of 1Hz at higher temperatures. Figures 10.2-10.4 presents the permittivity curves for the nanocomposites with 1 to 10 wt% of HNT respectively. For all the composites, the effect of temperature and frequency on the permittivity followed the same trend as that of the base matrix (HNT 0). As the frequency increased from 1Hz to 1kHz, permittivity values decreased sharply at all temperature range. This can be attributed to the fact that the dipoles present in the material are unable to follow the field variations at high frequencies. As the frequency increased, the intermittent reversal of the electric field happens very rapidly and the excess ion diffusion in the direction of the field becomes nil. As a result, the polarisation due to charge accumulation becomes very low and the permittivity values tend to the lower side(Raja, Sharma et al. 2004). Similar observations were made by Yang et al. in polyethene composites reinforced with vapourgrew carbon nanofibers(Yang, Benitez et al. 2007). Figure 10.5 shows the effect of increasing HNT content in the composites on permittivity values measured at 40°C and 1Hz frequency. It can be seen that the permittivity value slightly decreased as the HNT content is increased from 0 to 2 wt%, but it increased at 4 wt% of HNT and again slightly decreased at 6 wt% of HNT, and with further increase in HNT (HNT 8 and HNT 10) showed an increasing trend. Polymers with very low permittivity are especially useful in microelectronic packaging applications to minimise capacitive coupling effects and to reduce the signal delay (Todd and Shi 2002).
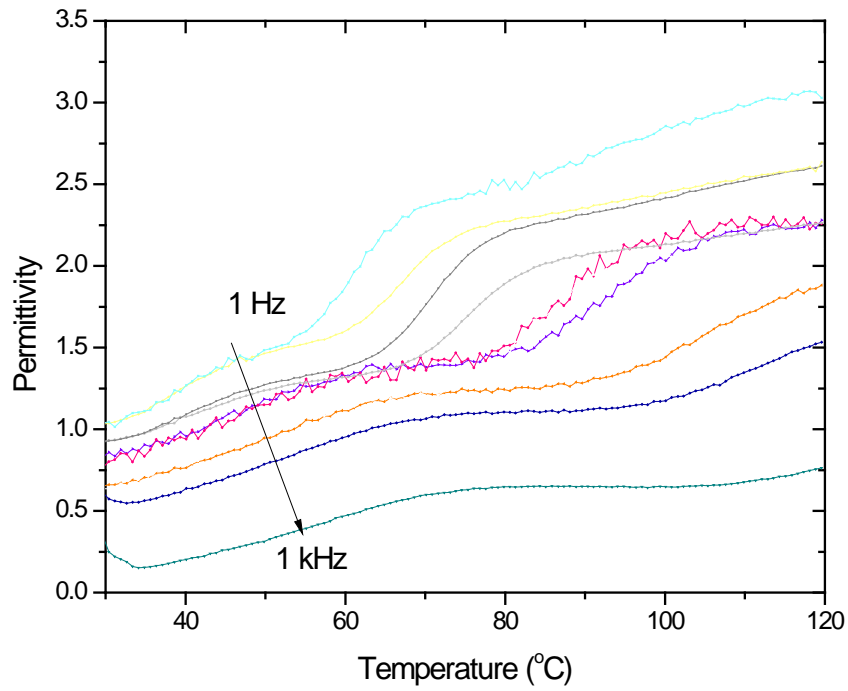
Figure 10.1Permittivity Vs temperature and frequency for HNT0

a.

b.
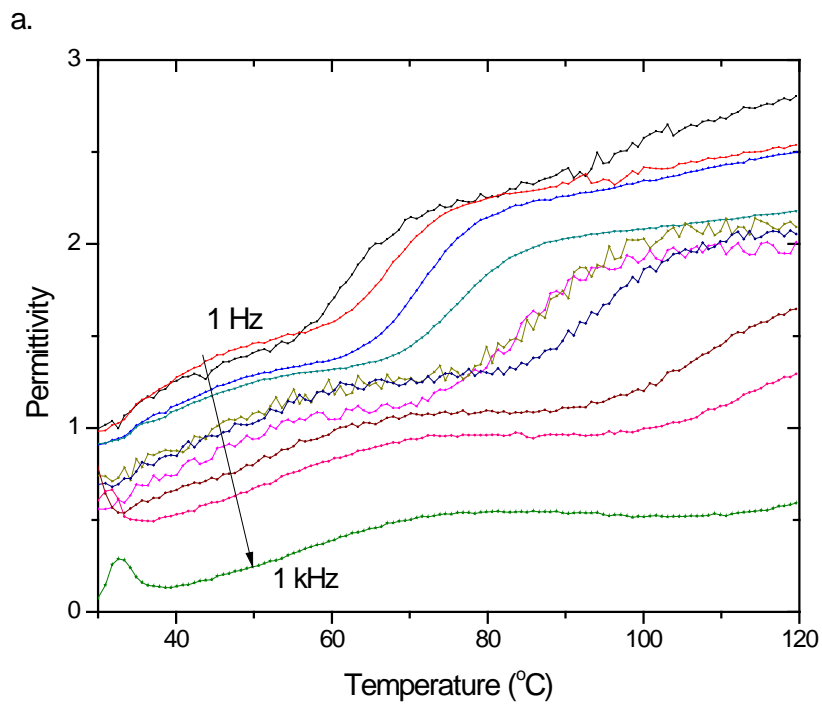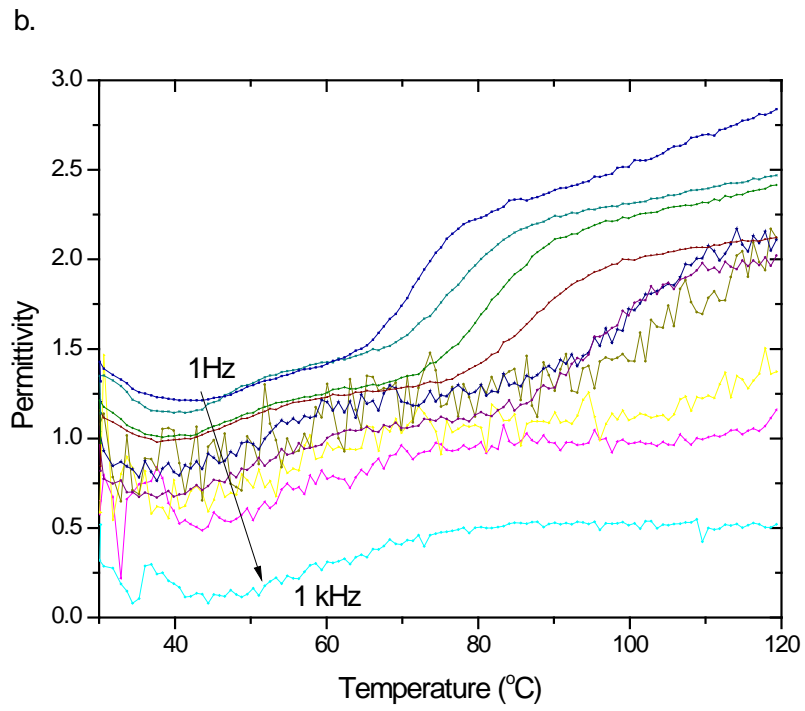
Figure 10.2Permittivity Vs temperature and frequency for a. HNT 1 b. HNT 2

a.

b.
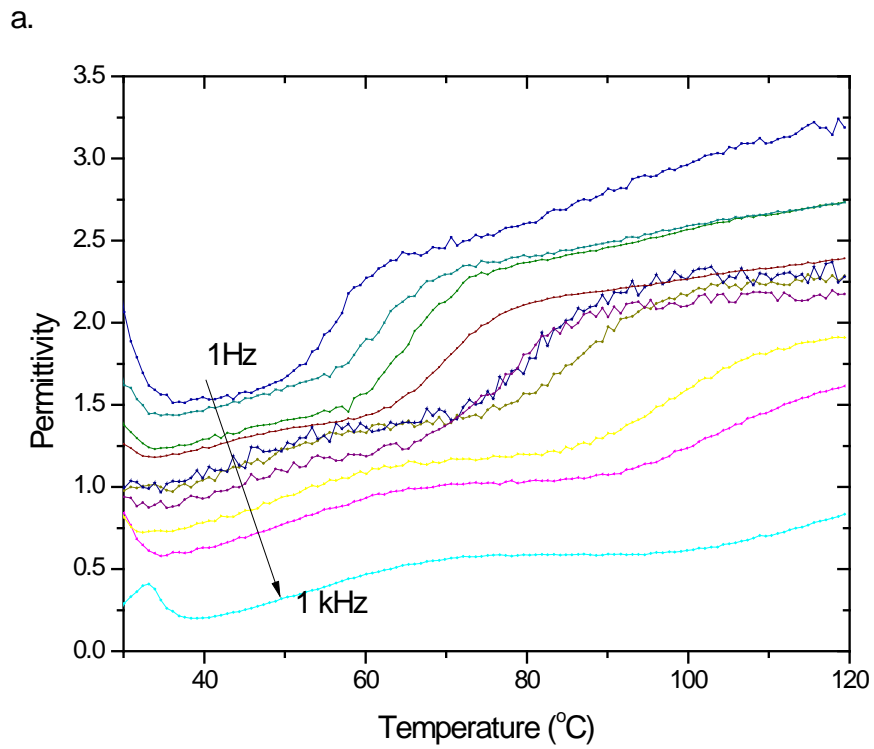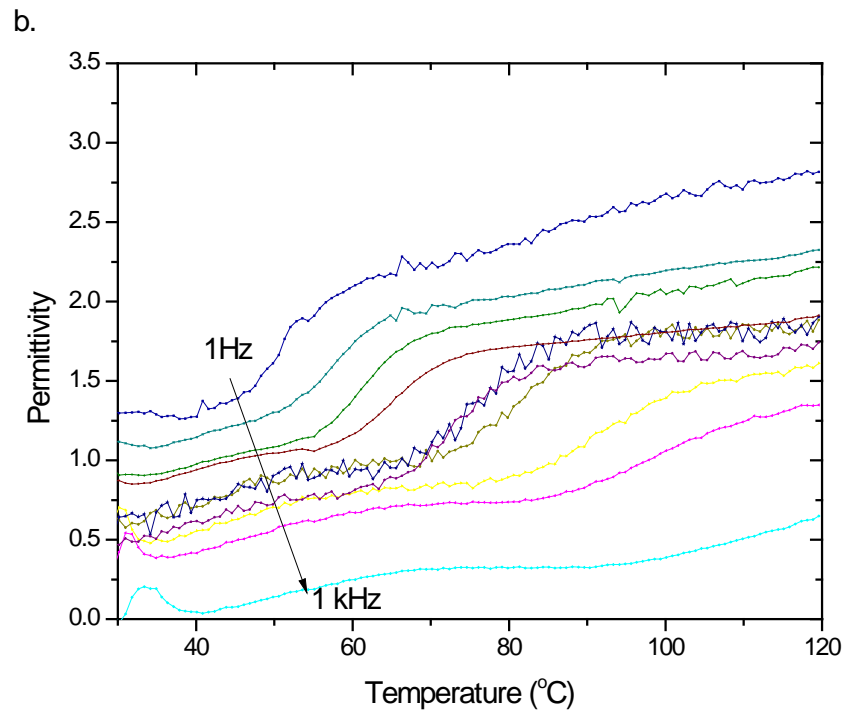
Figure 10.3Permittivity Vs temperature and frequency for a. HNT 4, b. HNT 6

a.

b.
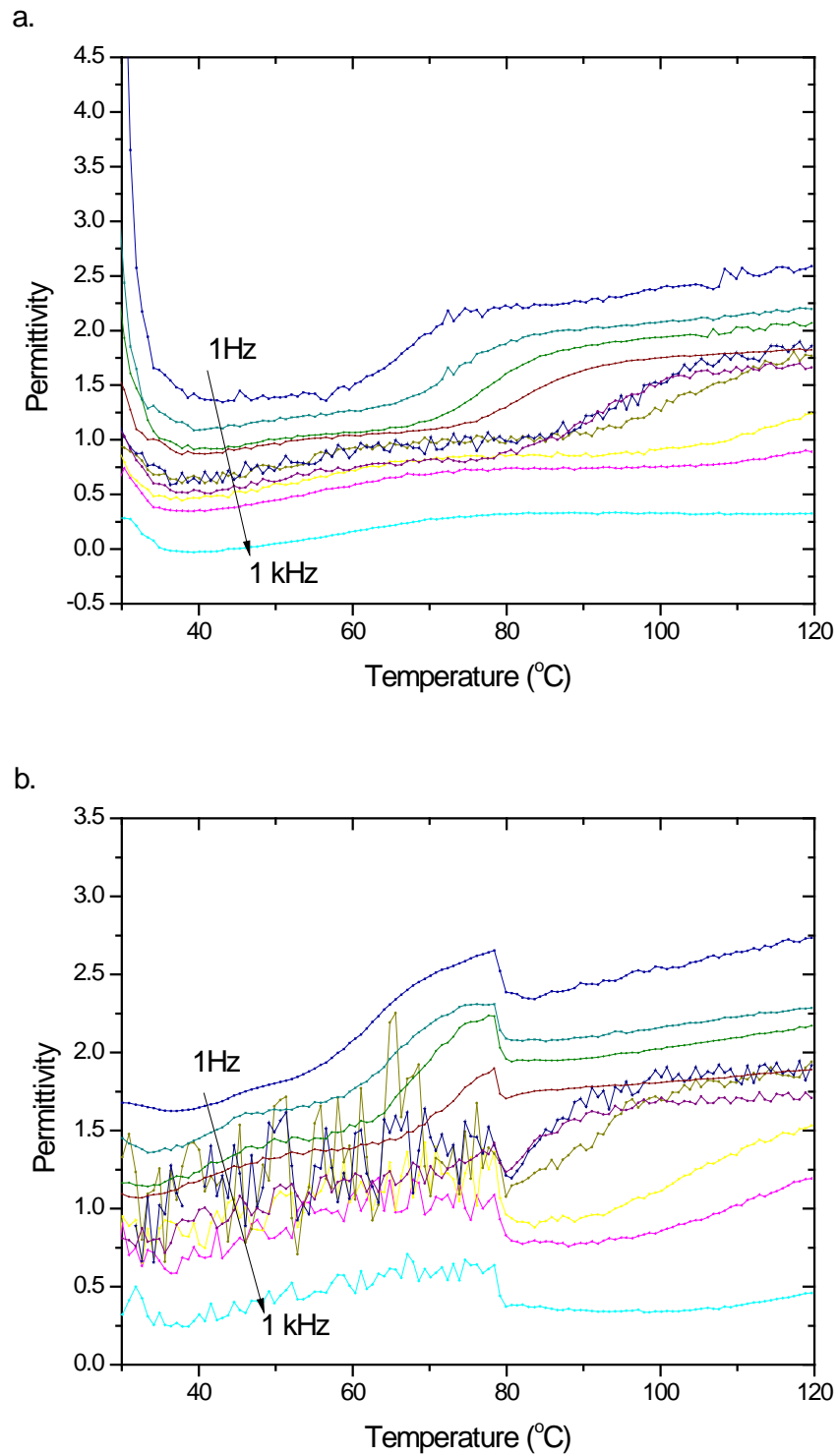
Figure 10.4Permittivity Vs temperature and frequency for a. HNT 8, b. HNT 10
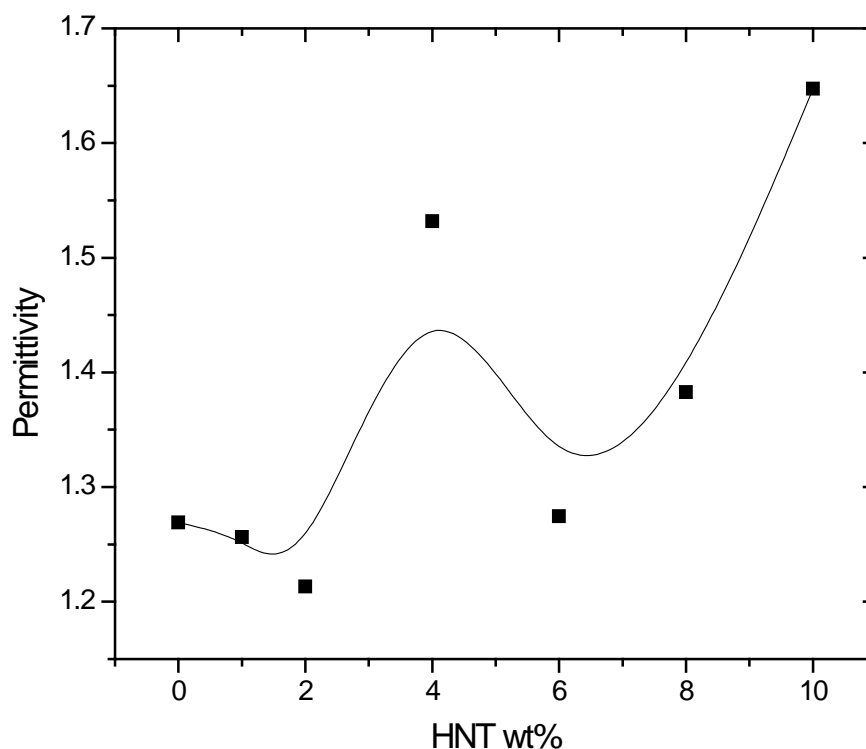
Figure 10.5Permittivity at 40°C and 1Hz for the composites

10.3.2 Loss factor analysis

Loss factor curves for the compatibilized blend without HNT (HNT 0) as a function of temperature and frequency are shown in figure 10.6. The loss factor values lie in between 0 and 2.6. For frequencies of 1Hz to 10Hz, there exist peak values for loss factor in between 60°C and 80°C, which may be correlated to the molecular relaxation process occurring in the PLA phase in the compatibilized blend. During relaxation process, the change in the dipole moment becomes more noticeable, which leads to peaks in loss factor and tanδ in both dynamic mechanical analysis (DMA) and DEA.(Shepard and Twombly 1996) Loss factor Vs temperature and frequency for the composites (HNT1 to HNT 10) are shown in figures 10.7 to 10.9. The curves showed a similar trend as that of base matrix except for HNT 8. For HNT 8, the loss factor in the lower temperature region (below 40°C), showed very high values. The variation of loss factor with HNT content in the nanocomposites at a temperature of 40°C and at a

frequency of 1 Hz is shown graphically in figure 10.10. As the HNT content in the composites increased from 0 to 4 wt%, the loss factor decreased slightly, but with further increase of HNT, the loss factor showed a sharp increase.
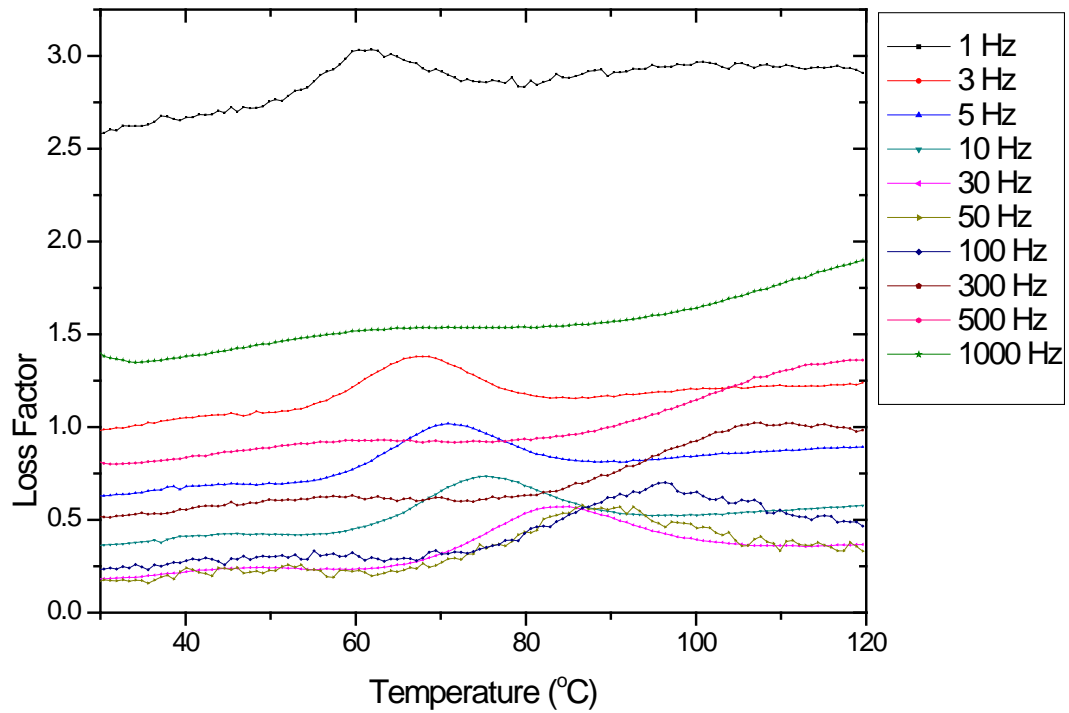
Figure 10.6Loss factor Vs temperature and frequency for HNT
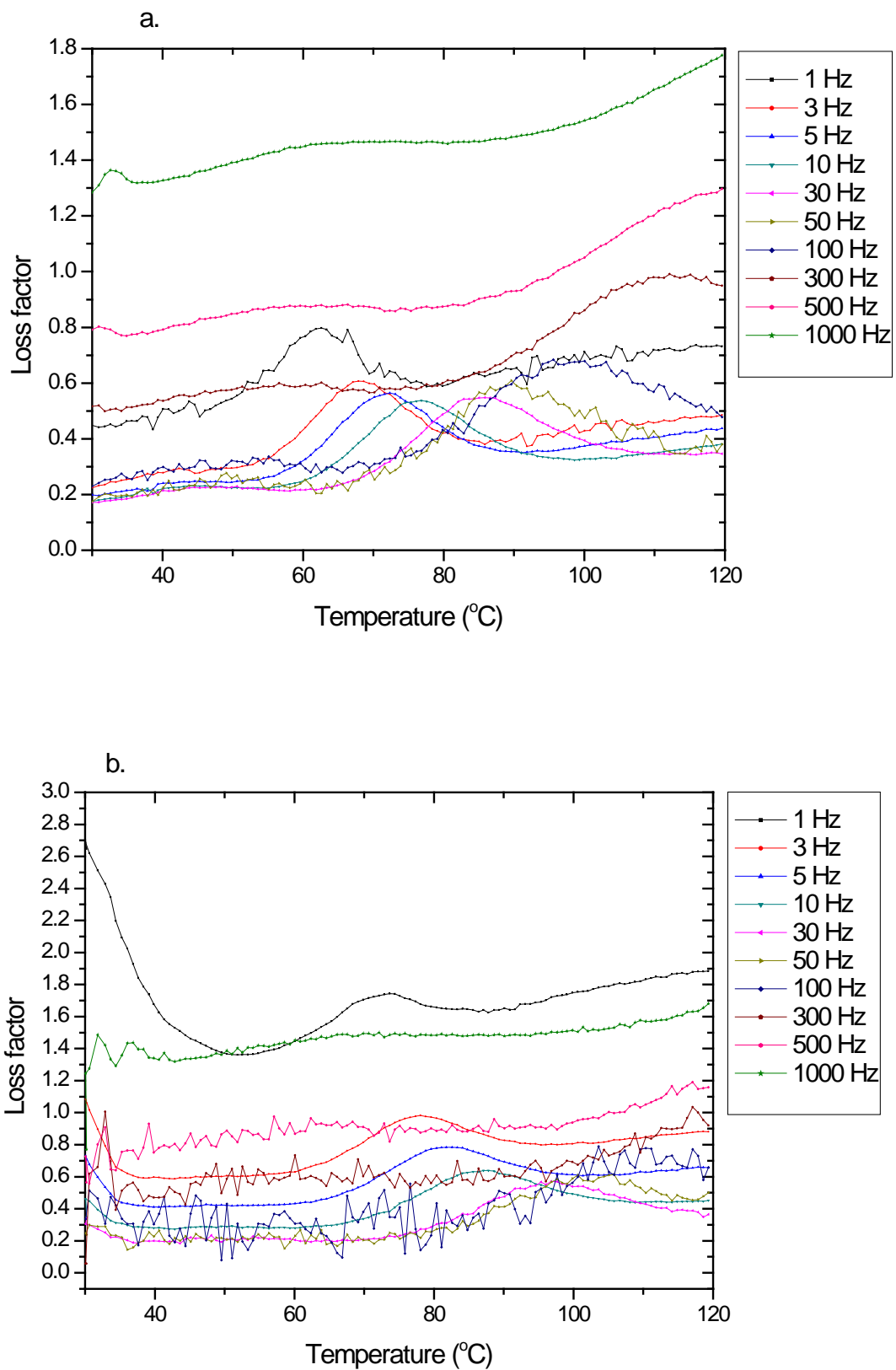
Figure 10.7Loss factor Vs temperature and frequency for a. HNT 1 and b. HNT 2
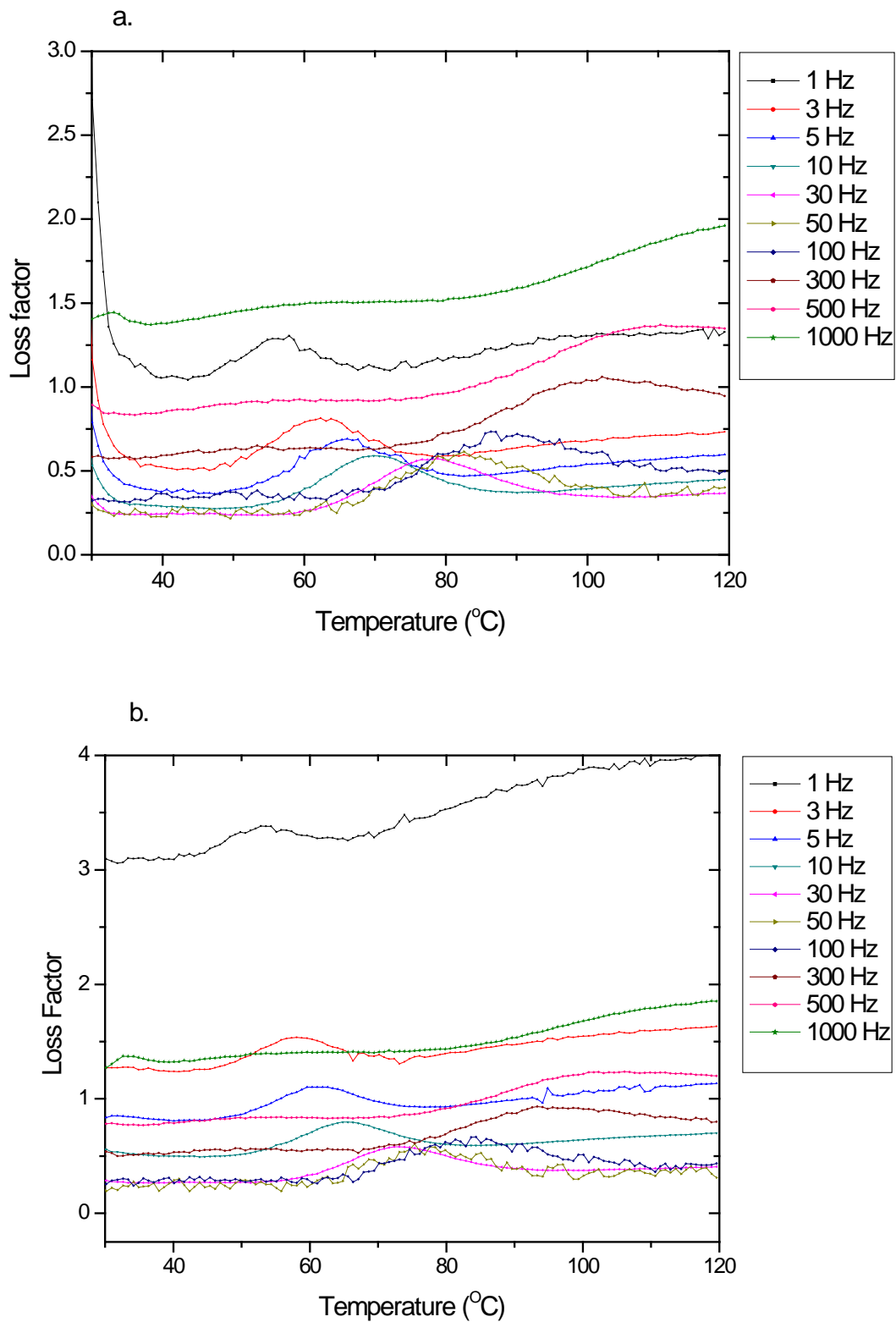
Figure 10.8Loss factor Vs temperature and frequency for a. HNT 4 and b. HNT 6
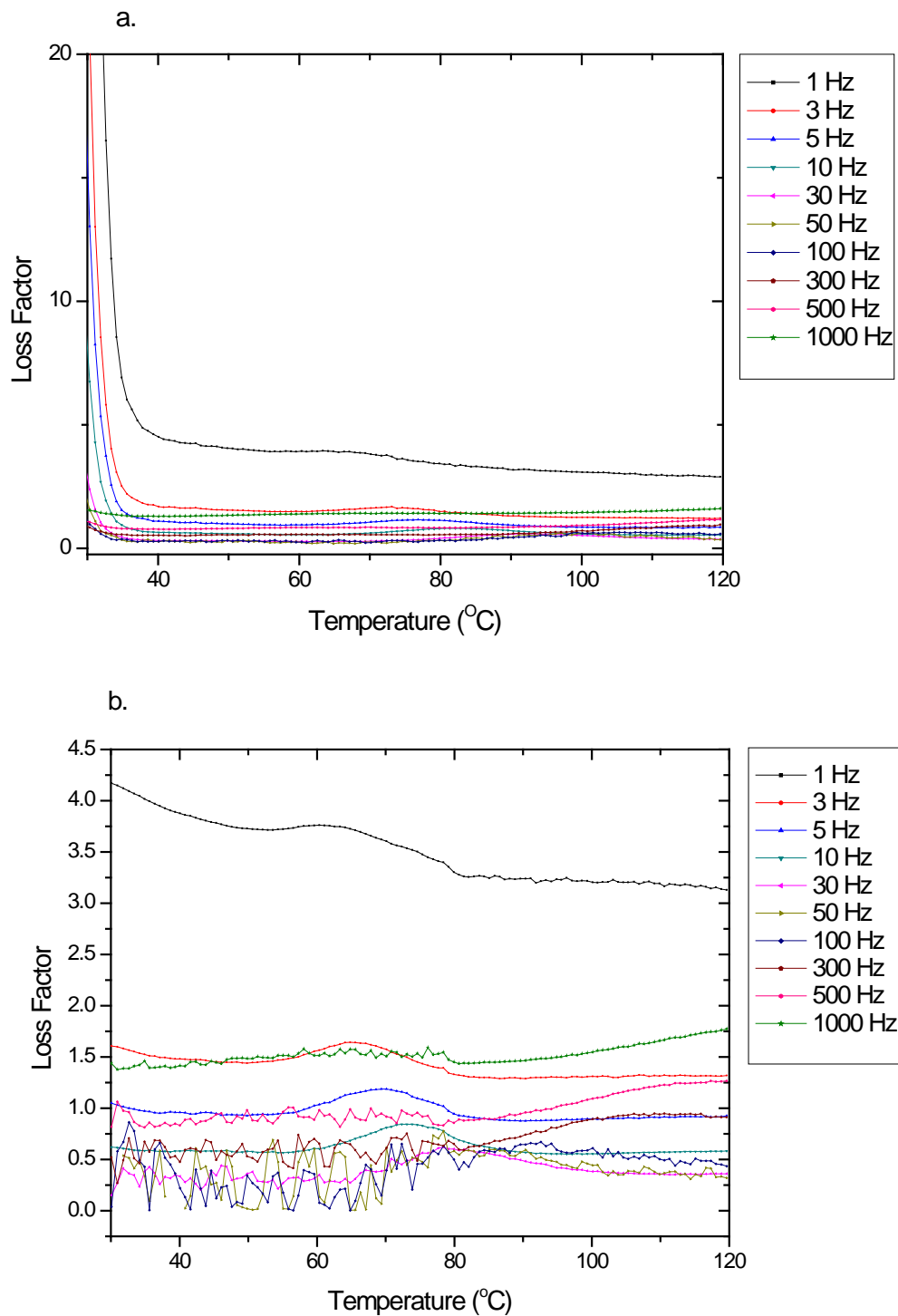
Figure 10.9Loss factor Vs temperature and frequency for a. HNT 8 and b. HNT 10
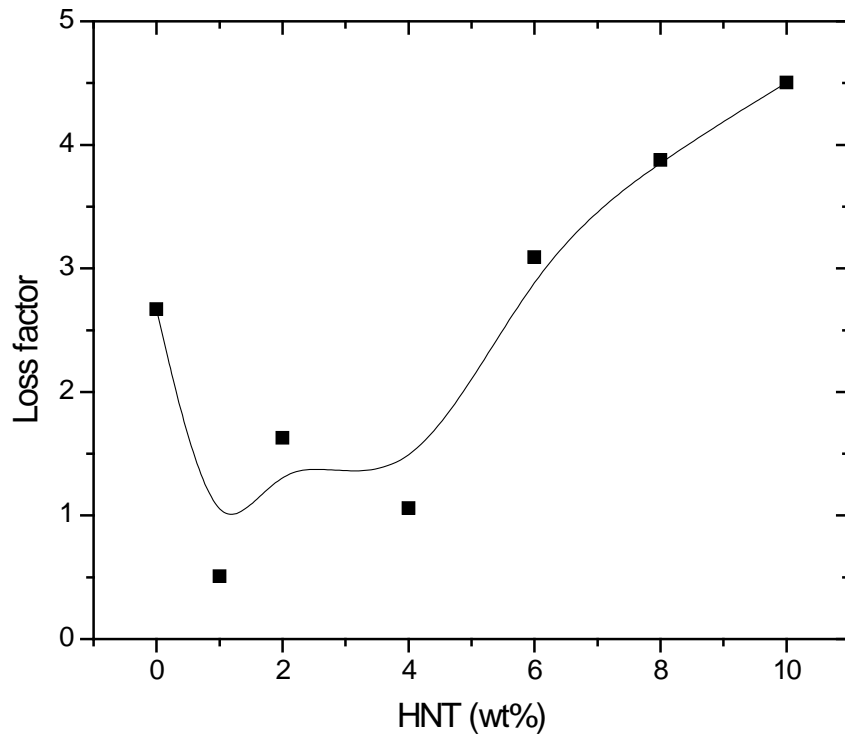
Figure 10.10Loss factor at 40°C and 1Hz for the composites

10.3.3 Analysis of loss tangent (tanδ) or dissipation factor

Loss tangent (tanδ) is calculated by dividing loss factor with the relative permittivity. It is a measurement of the ratio of dielectric energy loss to energy storage in an intermittent field(Yang, Benitez et al. 2007). Loss tangent measurements are extremely important for materials intended for microelectronic packaging applications, where low values of loss tangent reduce signal attenuation(Todd and Shi 2002). The variation of loss tangent (tanδ) with the temperature at a frequency of 10 Hz for all the composites (HNT 0 to HNT 10) is shown in figure 10.11. The loss tangent values are well below 1 and it can be seen that there exist a peak in between 60°C and 80°C for all the curves which can be attributed to the glass transition temperature of PLA in the matrix. The variation of tanδ with HNT content at frequencies of 1 Hz and 10 Hz is shown in figure 10.12. The common observation is

144

that the tanδ values decreased up to HNT 4 and then increased up to HNT 8 and then decreased slightly (for HNT 10).
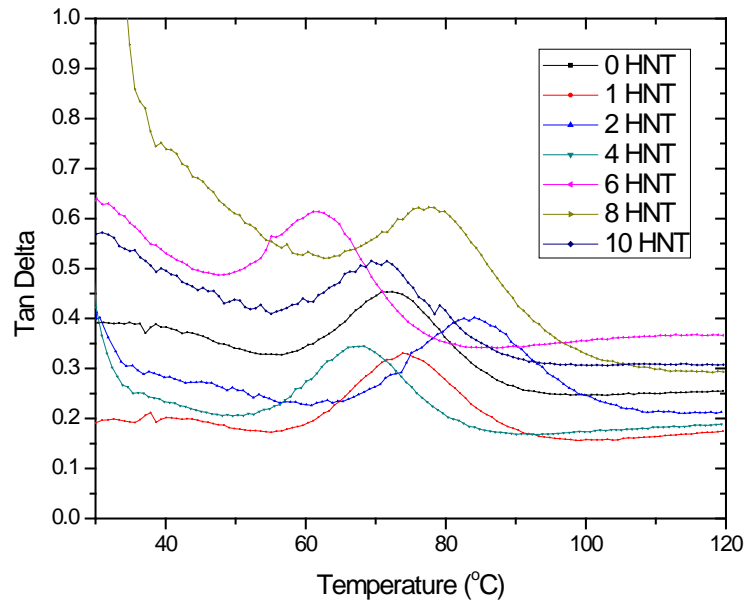
Figure 10.11 Variation of tan δ with temperature at 10 Hz for nanocomposites
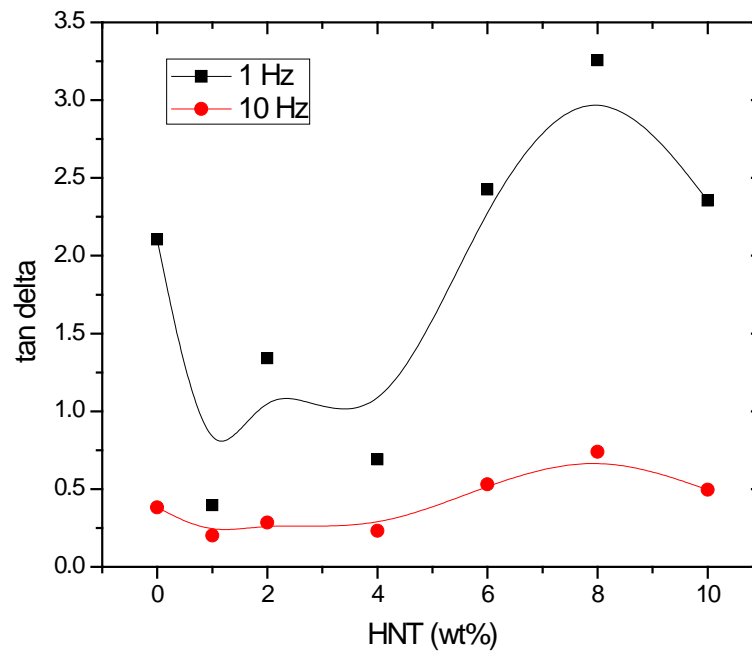
Figure 10.12 Variation of tanδ with HNT content in the composite

10.4   Conclusion

Nanocomposites of a compatibilized blend of PP and PLA with HNT were prepared by melt mixing technique. The dielectric properties of the composites were measured at temperatures from 30 to 120°C at various frequencies ranging from 1 Hz to 1 kHz. Permittivity values slightly decreased as the HNT content is increased from 0 to 2 wt%, but it increased at 4 wt% of HNT and again slightly decreased at 6 wt% of HNT, and with further increase in HNT (HNT 8 and HNT 10) started increasing to higher values. Loss factor values decreased slightly as the HNT content in the composites increased from 0 to 4 wt%, but with further increase of HNT, the loss factor showed a sharp increase. Loss tangent (tanδ) values decreased up to 4 wt% of HNT (HNT 4) and then increased up to 8 wt% (HNT 8) of HNT and then decreased slightly (for HNT 10). The analysis showed that the composites are ideal candidates for use in microelectronic devices or in microelectronic packaging applications.

CHAPTER-11

MICROSCOPIC STUDIES OF NANCOMPOSITES

11.1   Introduction

The microscopic studies are used as complimentary techniques to confirm the changes in crystal morphology, microstructure or filler dispersion and their orientation in the matrix so that these attributes can be used to explain the properties of the blends or composites.

11.2   Experimental procedure

The morphologies and growth of spherulites in the composites were observed and recorded using Zeiss AxioCamMRc 5 polarised optical microscope (POM) equipped with Linkam hot stage. Samples in the form of the thin film were placed between two glass slides, melted to 210 ^{o}C and held for 2 minutes to erase the thermal history of the samples. The samples then cooled to their respective crystallisation peak temperature (obtained from DSC cooling curves) at a cooling rate of 1 ^{o}C min^{-1} to record their final crystallite morphology.

The morphology of the nanocomposites and the dispersion of HNT in the matrix were observed using a transmission electron microscope (TEM, JEOL JEM-2100). Ultra-thin sections of the nanocomposites were prepared by using an ultramicrotome (Leica EM UC6) and the thin sections of approximately 80 nm thicknesses were supported on a copper grid.The accelerating voltage was 200 kV.

11.3   Results and discussion

Polarised optical microscope (POM) provides a visualisation of the morphology of crystals. In the present investigation, PP is the major component in the composite matrix and PP is also a crystallizable polymer compared with the amorphous PLA. Hence the crystalline morphology observed through the POM predominantly corresponds to the crystal growth of PP in the matrix. In optical micrographs, β spherulites appear brighter compared with α spherulites (Varga 1992).
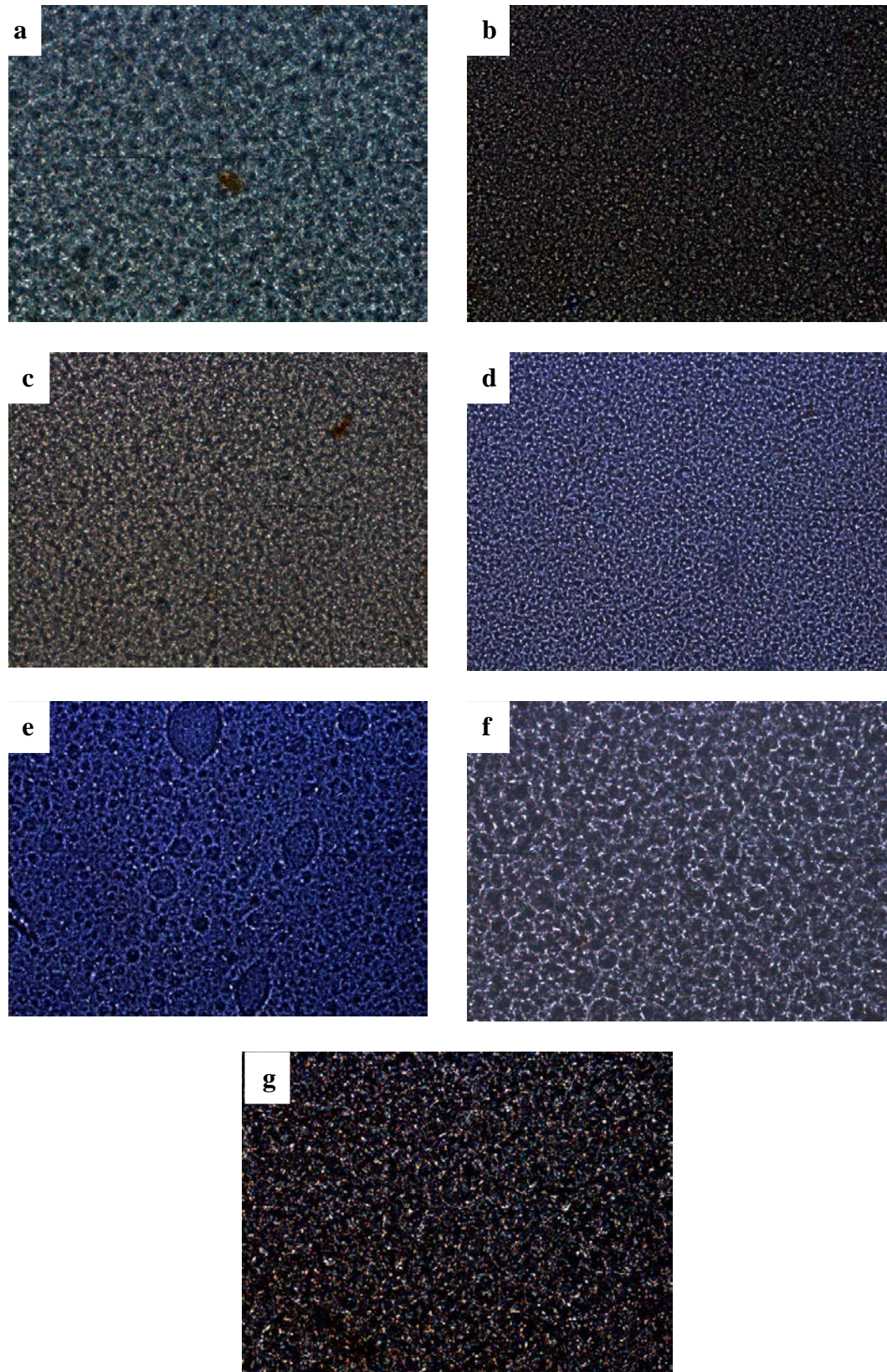
Figure 11.1POM images of nanocomposites
a) HNT 0 b) HNT 1 c) HNT 2 d) HNT 4 e) HNT 6 f) HNT 8 and g) HNT 10

Figure 11.1 shows the POM morphology of the nanocomposites with increasing amount of HNT (HNT 0 to HNT 10) with the same magnification of 100 μm.A large number of spherulites with weak boundary in between are clearly visible in the POM image of base matrix (figure 11.1 a.). With the introduction of 1 wt% of HNT, a large number of tiny spherulites with uniform distribution is visible in figure 11.1 b. This shows that HNT can act as a nucleating agent for the base matrix. The appearance of spherulites remained same for HNT 2 (figure 11.1 c). But with HNT 4, the size of the spherulites reduced but their number became more as evident from figure 11.1 d. The major observation is with figure 11.1 e, which corresponds to 6 wt% of HNT (HNT 6), where large spherulites with clear boundaries started appearing. This shows that with the introduction of 6 wt% of HNT, the nanocomposites crystal structure behaved in an entirely different manner and the growth of a large number of crystallites can be directly co-related to the improved mechanical properties and shear viscosity of the corresponding nanocomposites. With further increase in HNT wt% (figure 11.1 f), the number spherulites were still higher but their size reduced and with 10 wt% of HNT (figure 11.1 g), the growth of spherulites resembled more or less to that of the base matrix (figure 11.1 a).

Transmission electron micrographs (TEM) of the nanocomposites with different weight percentage of HNT are shown in figure 11.2. The TEM images provide information about the dispersion of nanofiller in the base matrix and their morphology. All the images are of the same resolution of 100 nm. In the images, the bright contrast corresponds to the PP and dark contrast corresponds to PLA present in the base blend. One common observation is that the dark contrast always attached to the surface of halloysite nanotubes, which shows the affinity of nanotubes with polar PLA. In figure 11.2 a, which corresponds to HNT 1, the cylindrical morphology of the halloysite nanotubes is clearly seen, which indicates that the morphology of the HNT is preserved even with high shear melt mixing. This is good in terms of processing aspect, where high shear rates are involved in polymer processing operations such as extrusion and injection moulding.
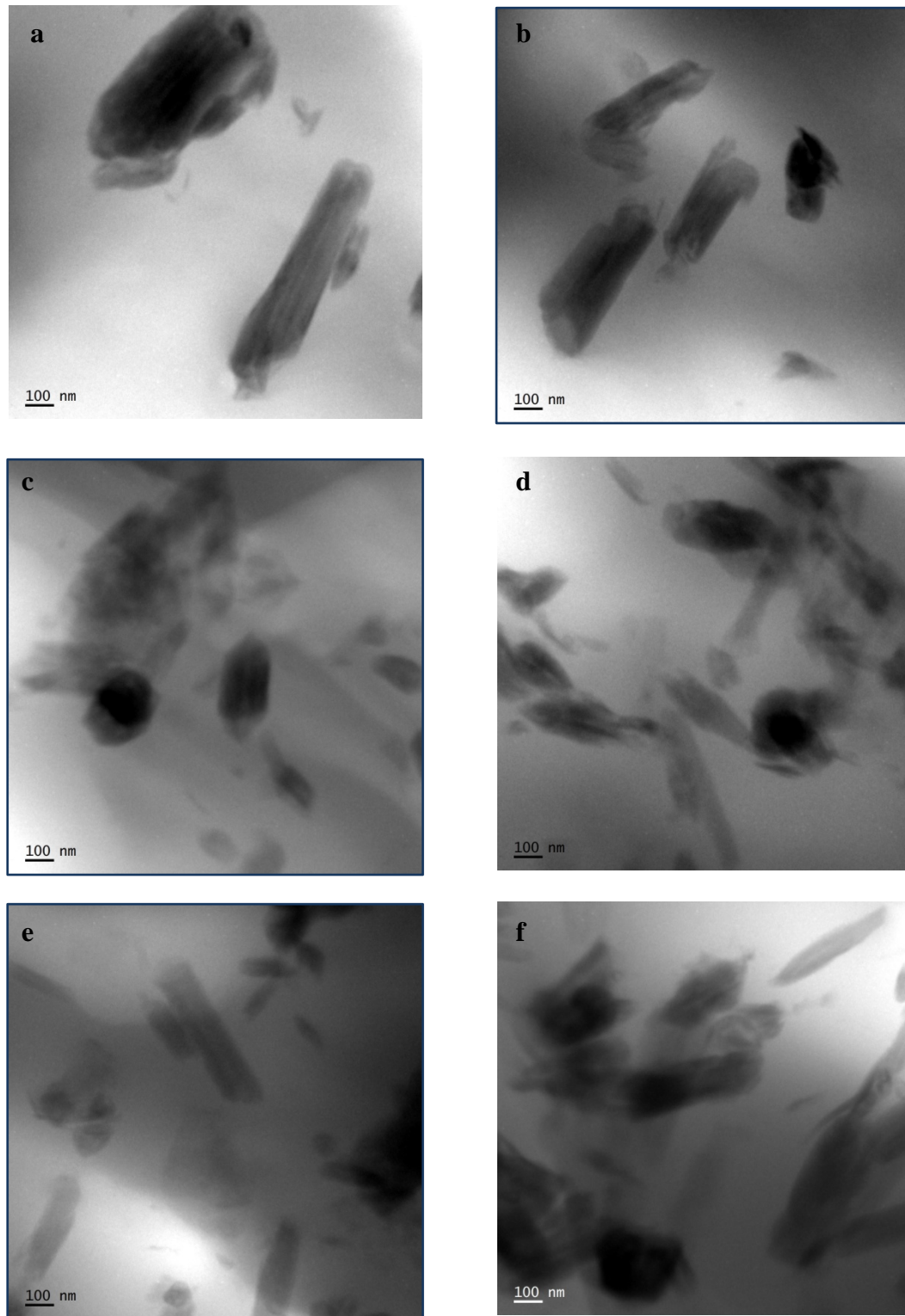
Figure 11.2TEM images of nanocomposites

a) HNT 1 b) HNT 2 c) HNT 4 d) HNT 6 e) HNT 8 and f) HNT 10

With theincrease in HNT loading, the number of nanotubes visible in the images is also more. Also, the nanotubes are uniformly distributed throughout the matrix without any aggregation or agglomeration. More uniform distribution and orientation of the nanotubes are seen in figure 11.2 d which corresponds to HNT 6. This shows that the nanotubes are more homogeneously distributed in the matrix when its dosage reached 6 wt%.

The limited intertubular contact area and favourable rod-like geometry can be the reasons for the homogenous distribution of the HNT without agglomeration (Murariu, Dechief et al. 2012) This may be the reason for the improved mechanical properties and shear viscosity at an HNT loading of 6 wt%. The number of nanotubes increased further with HNT 8 and HNT 10 as seen from figure 11.2 e and f.

11.4   Conclusion

The optical microscopy and transmission electron microscopy provided information about the growth of spherulites and the dispersion of nanofiller respectively. At 6 wt% of HNT, the nanocomposites exhibited improved spherulitic growth as well as uniform distribution of the nanofiller in the matrix.These results corroborate the results obtained from mechanical, thermal and rheological properties of the nanocomposites.

CHAPTER-12

CONCLUSIONS AND FUTURE PROSPECTS

12.1   Conclusions

Polymers have been an integral part of mankind since its great discovery due to their ubiquitous properties.Research on enhancing their properties to suit specific applications is done by numerous research groups all over the world. Blends (compounding two or more polymers together), alloys and composites (compounding polymers with heterogeneous materials) are the general categories to do this. All these methods may affect the properties synergistically or reversely depending on the inherent properties of the components and their interactions. The research work depicted in this thesis involved both blends and composites to improve the characteristic properties of polypropylene (PP), one of the most commonly used commodity plastics.

Polyblends of PP and polylactic acid (PLA) with PP as major component were prepared by adopting melt blending technique. 80:20 blend of PP and PLA were selected for further investigations based on their favorable set of mechanical properties and processing easiness compared with other blend systems. The chosen blend was compatibilized with the incorporation of maleic anhydride grafted PP (MA-g-PP) as a reactive compatibilizer. The mechanical, thermal, rheological and structural analysis proved that 3wt% of compatibilizer resulted in an effective compatibilization of the blend components. The key property improvements are:

➢ Tensile strength of the blend improved by 15% over the uncompatibilized blend and by 20% compared with virgin PP.

➢ Tensile modulus improved by 10% over the uncompatibilized blend and by 47% compared with virgin PP.

➢ Dynamic mechanical analysis (DMA) of the blend showed 10^oC improvement in the tan δ peak corresponding to glass transition temperature (T_g) of PLA which is attributed to the interaction between MA-g-PP and PLA phase which was further confirmed by FTIR and XRD analysis.

➢ Non isothermal degradation studies showed a first order kinetics with random nucleation model.

➢ The inclusion of compatibilizer enhanced crystallization process as evident from the reduction in crystallization activation energy values.

➢ The non-isothermal crystallization studies showed a two-dimensional crystal growth mechanism and the addition of the compatibilizer accelerated the crystallization of the blend.

➢ The rheological behaviour of the blend showed improvement in shear viscosity at a compatibilizer level of 3 wt%

Development of polymeric nanocomposites by the incorporation of nanofillers leads to new class of materials with excellent set of properties. Nanocomposites find applications in biomedical, aerospace, construction, automobiles, packaging, communication and information technology fields. The attractive feature of nanocomposites is the achievement of unique properties with addition of very low dosage of nanomaterials. There are various types of nanofillers available for the fabrication of nanocomposites. Among them, kaolinite type of halloysite nanotubes (HNT) are gaining attraction in recent years because of their inherent nanotubular structure and ease of processing.

The compatibilized blend containing 3 wt% of MA-g-PP (80:20:3) was chosen as the matrix for reinforcement with HNT. The nanocomposites were prepared with HNT varying from 0 to 10 wt%. The prepared nanocomposites were thoroughly characterized by mechanical and dynamic mechanical, thermal, rheological, structural, morphological and dielectric analysis. The key findings from these investigations are:

➢ The mechanical properties of the base blend showed a minor improvement of 10% with the addition of 6 wt% of HNT.

➢ HNT interacted with the PLA fraction of the blend as evident from the IR spectra and XRD analysis.

➢ The rheological analysis showed an increase in shear viscosity at 6 wt% of HNT which is also the reason behind the improvement of mechanical properties.

➢ The DSC results showed that the T_m of PP remain unaltered at 162°C, whereas T_m of PLA reached 172°C (a 4°C decrease from virgin PLA) which is an advantage in a processing point of view.

➤ The crystallization temperature of PP phase shifted to higher temperature (by 6°C), which favours crystal growth during cooling from molten state and thereby contribute to improvement in mechanical properties.

➤ The morphological analysis revealed tubular morphology of HNT which is homogeneously distributed in the base matrix. This shows that the HNT can withstand higher shear rates encountered in most of the polymer processing operations.

➤ Dielectric analysis (DEA) showed that the prepared nanocomposites are ideal candidates for fabrication of microelectronic devices or microelectronic packaging applications which needs low signal attenuation.

12.2   Future prospects

Any research opens the door for further advancements and investigations for fine tuning the material for the fabrication of commercially viable products. The HNT reinforced blends of PP and PLA could be investigated further for finding its suitability in various fields of applications. Some specific recommendations for further investigations are:

➤ Surface treatment of HNT and its effect on the properties of the resulting nanocomposites.

➤ Thermal degradation and crystallization kinetics of the composites in order to thoroughly understand the thermal stability and processability.

➤ Permeability studies of the nanocomposites to understand the barrier properties.

➤ Biodegradation studies of the nanocomposites.

REFERENCES

Abdel-Rahman, M. A., Y. Tashiro and K. Sonomoto (2013), Recent advances in lactic acid production by microbial fermentation processes, Biotechnology Advances**31**(6): 877-902.

Abdelwahab, M. A., A. Flynn, B.-S. Chiou, S. Imam, W. Orts and E. Chiellini (2012), Thermal, mechanical and morphological characterization of plasticized PLA–PHB blends, Polymer Degradation and Stability **97**(9): 1822-1828.

Aboulkas, A., K. El harfi and A. El Bouadili (2010), Thermal degradation behaviors of polyethylene and polypropylene. Part I: Pyrolysis kinetics and mechanisms, Energy Conversion and Management **51**(7): 1363-1369.

Acioli-Moura, R. and X. S. Sun (2008), Thermal degradation and physical aging of poly(lactic acid) and its blends with starch, Polymer Engineering & Science **48**(4): 829-836.

Akahira, T. and T. Sunose (1971), Method of determining activation deterioration constant of electrical insulating materials, Res. Rep. Chiba Inst. Technol.(Sci. Technol.) **16**: 22-31.

Akos, N. I., M. U. Wahit, R. Mohamed and A. A. Yussuf (2013), Comparative studies of mechanical properties of poly(ε-caprolactone) and poly(lactic acid) blends reinforced with natural fibers, Composite Interfaces.

Akos, N. I., M. U. Wahit, R. Mohamed and A. A. Yussuf (2013), Preparation, characterization, and mechanical properties of poly(ε-caprolactone)/polylactic acid blend composites, Polymer Composites **34**(5): 763-768.

Alimuzzaman, S., R. H. Gong and M. Akonda (2013), Nonwoven polylactic acid and flax biocomposites, Polymer Composites**34**(10): 1611-1619.

Allahvaisi, S. (2012). Polypropylene in the Industry of Food Packaging, INTECH Open Access Publisher.

An Tran, N. H., H. Brünig, C. Hinüber and G. Heinrich (2013), Melt Spinning of Biodegradable Nanofibrillary Structures from Poly(lactic acid) and Poly(vinyl alcohol) Blends, Macromolecular Materials and Engineering**299**(2): 219-227

Anderson, K. S., S. H. Lim and M. A. Hillmyer (2003), Toughening of polylactide by melt blending with linear low-density polyethylene, Journal of Applied Polymer Science **89**(14): 3757-3768.

Aoyagi, Y., K. Yamashita and Y. Doi (2002), Thermal degradation of poly[(R)-3-hydroxybutyrate], poly[ε-caprolactone], and poly[(S)-lactide], Polymer Degradation and Stability **76**(1): 53-59.

Arroyo, O. H., M. A. Huneault, B. D. Favis and M. N. Bureau (2010), Processing and Properties of PLA/Thermoplastic Starch/Montmorillonite Nanocomposites, Polymer Composites **31**(1): 114-127.

Auras, R. A., L.-T. Lim, S. E. Selke and H. Tsuji (2011). Poly (lactic acid): synthesis, structures, properties, processing, and applications, Wiley.

Avrami, M. (1939), Kinetics of phase change. I General theory, The Journal of Chemical Physics 7(12): 1103-1112.

Avrami, M. (1940), Kinetics of phase change. II transformation-time relations for random distribution of nuclei, The Journal of Chemical Physics **8**(2): 212-224.

Avrami, M. (1941), Granulation, phase change, and microstructure kinetics of phase change. III, The Journal of Chemical Physics **9**(2): 177-184.

Azarmgin, S., B. Kaffashi and S. Davachi (2015), Investigating Thermal Stability and Flame Retardant Properties of Synthesized Halloysite Nanotubes (HNT)/Ethylene Propylene Diene Monomer (EPDM) Nanocomposites, International Polymer Processing **30**(1): 29-37.

Babanalbandi, A., D. J. T. Hill, D. S. Hunter and L. Kettle (1999), Thermal stability of poly(lactic acid) before and after γ-radiolysis, Polymer International **48**(10): 980-984.

Bai, Z.-f. and Q. Dou (2016), Non-isothermal crystallization kinetics of polypropylene/poly (lactic acid)/maleic anhydride-grafted polypropylene blends, Journal of Thermal Analysis and Calorimetry: 1-10.

BAI, Z.-F. and Q. DOU (2015), Melting and Crystallization Behaviors of Poly (lactic acid)/Polypropylene Blends.

Bartczak, Z., A. Galeski, M. Kowalczuk, M. Sobota and R. Malinowski (2013), Tough Blends of Poly(lactide) and Amorphous poly([R,S]-3-hydroxy

butyrate) – Morphology and Properties, European Polymer Journal **49**(11): 3630-3641..

Benninga, H. (1990). A history of lactic acid making: a chapter in the history of biotechnology, Springer.

Bijarimi, M., M. Piah, A. Sahrim and R. Rozaidi (2012), Mechanical, thermal and morphological properties of PLA/PP melt blends.

Blümm, E. and A. J. Owen (1995), Miscibility, crystallization and melting of poly(3-hydroxybutyrate)/ poly(l-lactide) blends, Polymer **36**(21): 4077-4081.

Boissard, C. I., P.-E. Bourban, C. J. G. Plummer, R. C. Neagu and J.-A. E. Månson (2012), Cellular biocomposites from polylactide and microfibrillated cellulose, Journal of Cellular Plastics **48**(5): 445-458.

Burnham, A. K. and L. Dinh (2007), A comparison of isoconversional and model-fitting approaches to kinetic parameter estimation and application predictions, Journal of Thermal Analysis and Calorimetry **89**(2): 479-490.

Cai, J., M. Liu, L. Wang, K. Yao, S. Li and H. Xiong (2011), Isothermal crystallization kinetics of thermoplastic starch/poly(lactic acid) composites, Carbohydrate Polymers **86**(2): 941-947.

Cai, N., Q. Dai, Z. Wang, X. Luo, Y. Xue and F. Yu (2015), Toughening of electrospun poly (l-lactic acid) nanofiber scaffolds with unidirectionally aligned halloysite nanotubes, Journal of Materials Science **50**(3): 1435-1445.

Campbell, J., A. Goodwin and G. Simon (2001), Dielectric relaxation studies of miscible polycarbonate/polyester blends, Polymer **42**(10): 4731-4741.

Cerezo, F., C. Preston and R. Shanks (2007), Structural, mechanical and dielectric properties of poly (ethylene-co-methyl acrylate-co-acrylic acid) graphite oxide nanocomposites, Composites Science and Technology **67**(1): 79-91.

Chabrat, E., H. Abdillahi, A. Rouilly and L. Rigal (2012), Influence of citric acid and water on thermoplastic wheat flour/poly(lactic acid) blends. I: Thermal, mechanical and morphological properties, Industrial Crops and Products **37**(1): 238-246.

Chavalitpanya, K. and S. Phattanarudee (2013), Poly(Lactic Acid)/Polycaprolactone Blends Compatibilized with Block Copolymer, Energy Procedia **34**(0): 542-548.

Chen, X., L. Wang, J. Shi, H. Shi and Y. Liu (2011), Environmental Degradation of Starch/Poly(Lactic Acid) Composite in Seawater, Polymers & Polymer Composites **19**(7): 559-565.

Chen, Y., L. M. Geever, J. A. Killion, J. G. Lyons, C. L. Higginbotham and D. M. Devine (2015), Halloysite nanotube reinforced polylactic acid composite, Polymer Composites.

Choudhary, P., S. Mohanty, S. K. Nayak and L. Unnikrishnan (2011), Poly(L-lactide)/Polypropylene Blends: Evaluation of Mechanical, Thermal, and Morphological Characteristics, Journal of Applied Polymer Science **121**(6): 3223-3237.

Chrissafis, K., K. Paraskevopoulos and D. Bikiaris (2005), Thermal degradation mechanism of poly (ethylene succinate) and poly (butylene succinate): comparative study, Thermochimica Acta **435**(2): 142-150.

Coats, A. and J. Redfern (1964), Kinetic parameters from thermogravimetric data.

Cogswell, F. (1972), Converging flow of polymer melts in extrusion dies, Polymer Engineering & Science **12**(1): 64-73.

Cogswell, F. N. (1972), Measuring the Extensional Rheology of Polymer Melts, Transactions of The Society of Rheology **16**(3): 383-403.

Cogswell, F. N. (1981). Polymer melt rheology: a guide for industrial practice, Elsevier.

Cohn, D. and A. Hotovely Salomon (2005), Designing biodegradable multiblock PCL/PLA thermoplastic elastomers, Biomaterials **26**(15): 2297-2305.

Costa, L. I., F. Tancini, S. Hofmann, F. Codari and U. Trommsdorff (2016) From Laboratory to Industrial Continuous Production of Polylactic Acid with Low Residual Monomer. Macromolecular Symposia, Wiley Online Library.

Dai, L., L.-Y. Wang, T.-Q. Yuan and J. He (2014), Study on thermal degradation kinetics of cellulose-graft-poly(l-lactic acid) by thermogravimetric analysis, Polymer Degradation and Stability **99**(0): 233-239.

Davoodi, S., E. Oliaei, S. M. Davachi, I. Hejazi, J. Seyfi, B. S. Heidari and H. Ebrahimi (2016), Preparation and characterization of interface-modified PLA/starch/PCL ternary blends using PLLA/triclosan antibacterial nanoparticles for medical applications, RSC Advances **6**(46): 39870-39882.

de Groot, J. H., F. M. Zijlstra, H. W. Kuipers, A. J. Pennings, J. Klompmaker, R. P. H. Veth and H. W. B. Jansen (1997), Meniscal tissue regeneration in porous 5050 copoly(l-lactide/ϵ-caprolactone) implants, Biomaterials **18**(8): 613-622.

Deng, X., Z. Zhu, C. Xiong and L. Zhang (1997), Synthesis and characterization of biodegradable block copolymers of ϵ-caprolactone and D,L-lactide initiated by potassium poly(ethylene glycol)ate, Journal of Polymer Science Part A: Polymer Chemistry **35**(4): 703-708.

Dhanvijay, P. U. and V. V. Shertukde (2011), Review: Crystallization of biodegradable polymers, Polymer-Plastics Technology and Engineering **50**(13): 1289-1304.

Dong, Y., D. Chaudhary, H. Haroosh and T. Bickford (2011), Development and characterisation of novel electrospun polylactic acid/tubular clay nanocomposites, Journal of materials science **46**(18): 6148-6153.

Dong, Y., J. Marshall, H. J. Haroosh, S. Mohammadzadehmoghadam, D. Liu, X. Qi and K.-T. Lau (2015), Polylactic acid (PLA)/halloysite nanotube (HNT) composite mats: Influence of HNT content and modification, Composites Part A: Applied Science and Manufacturing **76**: 28-36.

Donnelly, Z. (2010). POLYOLEFIN/POLYLACTIC ACID BLENDS, U.S. Patent Application 13/264,433.

Doyle, C. (1962), Estimating isothermal life from thermogravimetric data, Journal of Applied Polymer Science **6**(24): 639-642.

Doyle, C. D. (1965), Series approximations to the equation of thermogravimetric data.

Drumright, R. E., P. R. Gruber and D. E. Henton (2000), Polylactic acid technology, Advanced materials **12**(23): 1841-1846.

Du, M., B. Guo and D. Jia (2006), Thermal stability and flame retardant effects of halloysite nanotubes on poly (propylene), European Polymer Journal **42**(6): 1362-1369.

Du, M., B. Guo and D. Jia (2010), Newly emerging applications of halloysite nanotubes: a review, Polymer International **59**(5): 574-582.

Du, M., B. Guo, M. Liu and D. Jia (2007), Thermal decomposition and oxidation ageing behaviour of polypropylene/halloysite nanotube nanocomposites, Polymers & polymer composites **15**(4): 321.

Du, M., B. Guo, J. Wan, Q. Zou and D. Jia (2010), Effects of halloysite nanotubes on kinetics and activation energy of non-isothermal crystallization of polypropylene, Journal of polymer research **17**(1): 109-118.

Dunnen, W. F. A., J. M. Schakenraad, G. J. Zondervan, A. J. Pennings, B. Lei and P. H. Robinson (1993), A new PLLA/PCL copolymer for nerve regeneration, Journal of Materials Science: Materials in Medicine **4**(5): 521-525.

El-Hadi, A. M. (2011), Effect of processing conditions on the development of morphological features of banded or nonbanded spherulites of poly(3-hydroxybutyrate) (PHB) and polylactic acid (PLLA) blends, Polymer Engineering & Science **51**(11): 2191-2202.

Entezam, M., H. A. Khonakdar, A. A. Yousefi, S. H. Jafari, U. Wagenknecht, G. Heinrich and B. Kretzschmar (2012), Influence of interfacial activity and micelle formation on rheological behavior and microstructure of reactively compatibilized PP/PET blends, Macromolecular Materials and Engineering **297**(4): 312-328.

Essawy, H. A., F. M. Helaly and M. A. Shabana (2007), Synthesis of Poly(lactide) Blends by Melt/Solid Polycondensation, Journal of Elastomers and Plastics **39**(4): 303-316.

Fan, Q., F. Duan, H. Guo and T. Wu (2015), Non-isothermal crystallization kinetics of polypropylene and hyperbranched polyester blends, Chinese Journal of Chemical Engineering **23**(2): 441-445.

Fan, Y., H. Nishida, S. Hoshihara, Y. Shirai, Y. Tokiwa and T. Endo (2003), Pyrolysis kinetics of poly(l-lactide) with carboxyl and calcium salt end structures, Polymer Degradation and Stability **79**(3): 547-562.

Faruk, O., A. K. Bledzki, H.-P. Fink and M. Sain (2012), Biocomposites reinforced with natural fibers: 2000–2010, Progress in Polymer Science **37**(11): 1552-1596.

Favaro Ferrarezi, M. M., M. d. O. Taipina, L. C. Escobar da Silva and M. d. C. Goncalves (2013), Poly(Ethylene Glycol) as a Compatibilizer for Poly(Lactic Acid)/Thermoplastic Starch Blends, Journal of Polymers and the Environment **21**(1): 151-159.

Ferreira, B. M. P., C. A. C. Zavaglia and E. A. R. Duek (2002), Films of PLLA/PHBV: Thermal, morphological, and mechanical characterization, Journal of Applied Polymer Science **86**(11): 2898-2906.

Fischer, H., E. Werwein and N. Graupner (2012), Nettle fibre (Urtica dioica L.) reinforced poly (lactic acid): A first approach, Journal of Composite Materials: 0021998311435676.

Flynn, J. (1983), The isoconversional method for determination of energy of activation at constant heating rates, Journal of Thermal Analysis and Calorimetry **27**(1): 95-102.

Flynn, J. and L. Wall (1966), Thermal analysis of polymer by thermogravemetric analysis, J. Res. Natl. Bur. Stand. Sect. A **70**: 487.

Flynn, J. H. and L. A. Wall (1966), A quick, direct method for the determination of activation energy from thermogravimetric data, Journal of Polymer Science Part B: Polymer Letters **4**(5): 323-328.

Focarete, M. L., M. Scandola, P. Dobrzynski and M. Kowalczuk (2002), Miscibility and Mechanical Properties of Blends of (l)-Lactide Copolymers with Atactic Poly(3-hydroxybutyrate), Macromolecules **35**(22): 8472-8477.

Folkes, M. and P. Hope (1993). Polymer blends and alloys, Springer.

Foruzanmehr, M., P. Y. Vuillaume, S. Elkoun and M. Robert (2016), Physical and mechanical properties of PLA composites reinforced by TiO2 grafted flax fibers, Materials & Design **106**: 295-304.

Friedman, H. L. (1964) Kinetics of thermal degradation of char-forming plastics from thermogravimetry. Application to a phenolic plastic. Journal of Polymer Science Part C: Polymer Symposia, Wiley Online Library.

Gabbott, P. (2008). Principles and applications of thermal analysis, John Wiley & Sons.

Gallego, R., S. López-Quintana, F. Basurto, K. Núñez, N. Villarreal and J. Merino (2013), Synthesis of new compatibilizers to poly(lactic acid) blends, Polymer Engineering and Science**54**(3): 522-530.

Gao, H., S. Hu, F. Su, J. Zhang and G. Tang (2011), Mechanical, thermal, and biodegradability properties of PLA/modified starch blends, Polymer Composites **32**(12): 2093-2100.

Garcia, N. L., M. Lamanna, N. D'Accorso, A. Dufresne, M. Aranguren and S. Goyanes (2012), Biodegradable materials from grafting of modified PLA onto starch nanocrystals, Polymer Degradation and Stability **97**(10): 2021-2026.

Garlotta, D. (2001), A literature review of poly (lactic acid), Journal of Polymers and the Environment **9**(2): 63-84.

Gerard, T. and T. Budtova (2012), Morphology and molten-state rheology of polylactide and polyhydroxyalkanoate blends, European Polymer Journal **48**(6): 1110-1117.

Gloria, A., P. J. Bártolo and T. Patrício (2013), PCL and PCL/PLA scaffolds for bone tissue regeneration, Advanced Materials Research **683**: 168-171.

Goriparthi, B. K., K. Suman and N. M. Rao (2012), Effect of fiber surface treatments on mechanical and abrasive wear performance of polylactide/jute composites, Composites Part A: Applied Science and Manufacturing **43**(10): 1800-1808.

Graupner, N., A. S. Herrmann and J. Müssig (2009), Natural and man-made cellulose fibre-reinforced poly(lactic acid) (PLA) composites: An overview about mechanical characteristics and application areas, Composites Part A: Applied Science and Manufacturing **40**(6–7): 810-821.

Grijpma, D. W., G. J. Zondervan and A. J. Pennings (1991), High molecular weight copolymers of l-lactide and ε-caprolactone as biodegradable elastomeric implant materials, Polymer Bulletin **25**(3): 327-333.

Guo, J., J. Qiao and X. Zhang (2016), Effect of an alkalized-modified halloysite on PLA crystallization, morphology, mechanical, and thermal properties of PLA/halloysite nanocomposites, Journal of Applied Polymer Science.

Hamad, K., M. Kaseem and F. Deri (2011), Rheological and mechanical characterization of poly(lactic acid)/polypropylene polymer blends, Journal of Polymer Research **18**(6): 1799-1806.

Handge, U. A., K. Hedicke-Höchstötter and V. Altstädt (2010), Composites of polyamide 6 and silicate nanotubes of the mineral halloysite: influence of molecular weight on thermal, mechanical and rheological properties, Polymer **51**(12): 2690-2699.

Harada, M., K. Iida, K. Okamoto, H. Hayashi and K. Hirano (2008), Reactive compatibilization of biodegradable poly(lactic acid)/poly(ε-caprolactone)

blends with reactive processing agents, Polymer Engineering & Science **48**(7): 1359-1368.

Helal, E., N. Demarquette, L. Amurin, E. David, D. Carastan and M. Fréchette (2015), Styrenic block copolymer-based nanocomposites: Implications of nanostructuration and nanofiller tailored dispersion on the dielectric properties, Polymer **64**: 139-152.

Henton, D. E., P. Gruber, J. Lunt and J. Randall (2005), Polylactic acid technology, Natural Fibers, Biopolymers, and Biocomposites, Taylor & Francis, Boca Raton, FL: 527-577.

Hiljanen-Vainio, M., P. Varpomaa, J. Seppälä and P. Törmälä (1996), Modification of poly(L-lactides) by blending: mechanical and hydrolytic behavior, Macromolecular Chemistry and Physics **197**(4): 1503-1523.

Hollaway, L. C. (2001). Advanced polymer composites and polymers in the civil infrastructure, Elsevier.

Hong, C. H. (2012). Eco-friendly polypropylene-polylactic acid composite composition, US Patent 8211966 B2.

Hongwei Ma and Chang Whan Joo (2011), Structure and mechanical properties of jute—polylactic acid biodegradable composites, Journal of Composite Materials **45**(14): 1451-1460.

Horowitz, H. H. and G. Metzger (1963), A New Analysis of Thermogravimetric Traces, Analytical Chemistry **35**(10): 1464-1468.

Hu, R. and J.-K. Lim (2007), Fabrication and Mechanical Properties of Completely Biodegradable Hemp Fiber Reinforced Polylactic Acid Composites, Journal of Composite Materials **41**(13): 1655-1669.

Hu, Y., Q. Wang and M. Tang (2013), Preparation and properties of Starch-g-PLA/poly(vinyl alcohol) composite film, Carbohydrate Polymers **96**(2): 384-388.

Huang, M.-H., S. Li and M. Vert (2004), Synthesis and degradation of PLA–PCL–PLA triblock copolymer prepared by successive polymerization of ε-caprolactone and dl-lactide, Polymer **45**(26): 8675-8681.

Ismail, H., P. Pasbakhsh, M. A. Fauzi and A. A. Bakar (2008), Morphological, thermal and tensile properties of halloysite nanotubes filled ethylene

propylene diene monomer (EPDM) nanocomposites, Polymer Testing **27**(7): 841-850.

Ismail, H., S. Salleh and Z. Ahmad (2013), Fatigue and hysteresis behavior of halloysite nanotubes-filled natural rubber (SMR L and ENR 50) nanocomposites, Journal of Applied Polymer Science **127**(4): 3047-3052.

Ismail, H., S. Salleh and Z. Ahmad (2013), Properties of halloysite nanotubes-filled natural rubber prepared using different mixing methods, Materials & Design **50**: 790-797.

Jain, K., G. Madhu, H. Bhunia, P. K. Bajpai, G. B. Nando and M. S. Reddy (2015), Physico-mechanical characterization and biodegradability behavior of polypropylene/poly (L-lactide) polymer blends, Journal of Polymer Engineering **35**(5): 407-415.

Jamshidian, M., E. A. Tehrany, M. Imran, M. Jacquot and S. Desobry (2010), Poly-Lactic Acid: Production, Applications, Nanocomposites, and Release Studies, Comprehensive Reviews in Food Science and Food Safety **9**(5): 552-571.

Jandas, P. J., S. Mohanty, S. K. Nayak and H. Srivastava (2011), Effect of surface treatments of banana fiber on mechanical, thermal, and biodegradability properties of PLA/banana fiber biocomposites, Polymer Composites **32**(11): 1689-1700.

Jawalkar, S. S. and T. M. Aminabhavi (2006), Molecular modeling simulations and thermodynamic approaches to investigate compatibility/incompatibility of poly(l-lactide) and poly(vinyl alcohol) blends, Polymer **47**(23): 8061-8071.

Jia, Z., Y. Luo, B. Guo, B. Yang, M. Du and D. Jia (2009), Reinforcing and flame-retardant effects of halloysite nanotubes on LLDPE, Polymer-Plastics Technology and Engineering **48**(6): 607-613.

Jia, Z., T. Xu, S. Yang, Y. Luo and D. Jia (2016), Interfacial mechano-chemical grafting in styrene-butadiene rubber/halloysite nanotubes composites, Polymer Testing **54**: 29-39.

Jiang, A., J. Xi and H. Wu (2012), Effect of surface treatment on the morphology of sisal fibers in sisal/polylactic acid composites, Journal of Reinforced Plastics and Composites **31**(9): 621-630.

Jiao, M., K. Yang, J. Cao, H. Liu, W. Pan and P. Gao (2013), Designing and Characterization of Poly(L-Lactide)/Poly(ϵ-Caprolactone) Multiblock Copolymers, Journal of Macromolecular Science, Part B.

Johnson, W. A. and R. F. Mehl (1939), Reaction kinetics in processes of nucleation and growth, Trans. Aime **135**(8): 396-415.

Joraid, A. and I. Alhosuini (2014), Effect of heating rate on the kinetics and mechanism of crystallization in amorphous Se 85 Te 10 Pb 5 glasses, Thermochimica Acta **595**: 28-34.

JORAID, A., M. EL-OYOUN and N. AFIFY (2016), PHASE SEPARATION AND CRYSTALLIZATION KINETICS STUDIES OF AMORPHOUS Si 10 Te 90, Chalcogenide Letters **13**(2): 79-89.

Ju, D., L. Han, F. Li, S. Chen and L. Dong (2013), Crystallization, mechanical properties, and enzymatic degradation of biodegradable poly(ε-caprolactone) composites with poly(lactic acid) fibers, Polymer Composites**34**(10):1745-1752.

Kaneko, H., J. Saito, N. Kawahara, S. Matsuo, T. Matsugi and N. Kashiwa (2009). Polypropylene-graft-Poly(methyl methacrylate) Graft Copolymers: Synthesis and Compatibilization of Polypropylene/Polylactide. Controlled/Living Radical Polymerization: Progress in Atrp. K. Matyjasewski. **1023:** 357-371.

Kang, H., X. Lu and Y. Xu (2015), Properties of immiscible and ethylene-butyl acrylate-glycidyl methacrylate terpolymer compatibilized poly (lactic acid) and polypropylene blends, Polymer Testing **43**: 173-181.

Karian, H. (2003). Handbook of polypropylene and polypropylene composites, revised and expanded, CRC press.

Kato, M., A. Usuki and A. Okada (1997), Synthesis of polypropylene oligomer—clay intercalation compounds, Journal of Applied Polymer Science **66**(9): 1781-1785.

Kawashima, N., S. Ogawa, S. Obuchi, M. Matsuo and T. Yagi (2002), Polylactic acid "LACEA", Biopolymers Online: 251-274.

Ke, T. and X. Sun (2003), Starch, Poly(lactic acid), and Poly(vinyl alcohol) Blends, Journal of Polymers and the Environment **11**(1): 7-14.

Kelnar, I., J. Kratochvíl, I. Fortelný, L. Kaprálková, A. Zhigunov, V. Khunová and M. Nevoralová (2016), Effect of halloysite on structure and properties of melt-drawn PCL/PLA microfibrillar composites, Express Polymer Letters **10**(5): 381-393.

Khunová, V., I. Kelnar, J. Kristóf, J. Dybal, J. Kratochvíl and L. Kaprálková (2015), The effect of urea and urea-modified halloysite on performance of PCL, Journal of Thermal Analysis and Calorimetry **120**(2): 1283-1291.

Khunova, V., J. Kristof, I. Kelnar and J. Dybal (2013), The effect of halloysite modification combined with in situ matrix modifications on the structure and properties of polypropylene/halloysite nanocomposites, eXPRESS Polymer Letters 7(5): 471-479.

Kim, H. S. and H. J. Kim (2013), Miscibility and performance evaluation of natural-flour-filled PP/PBS and PP/PLA bio-composites, Fibers and Polymers **14**(5): 793-803.

Kim, I. H. and Y. G. Jeong (2010), Polylactide/exfoliated graphite nanocomposites with enhanced thermal stability, mechanical modulus, and electrical conductivity, Journal of Polymer Science Part B: Polymer Physics **48**(8): 850-858.

Kim, Y., C. Choi, Y. Kim, K. Lee and M. Lee (2004), Compatibilization of immiscible poly(l-lactide) and low density polyethylene blends, Fibers and Polymers **5**(4): 270-274.

Kissinger, H. E. (1956), Variation of peak temperature with heating rate in differential thermal analysis, Journal of Research of the National Bureau of Standards **57**(4): 217-221.

Kissinger, H. E. (1957), Reaction Kinetics in Differential Thermal Analysis, Analytical Chemistry **29**(11): 1702-1706.

Klug, H. P. and L. E. Alexander (1954). X-ray diffraction procedures, Wiley New York.

Koenig, J. L. (2001). Infrared and Raman Spectroscopy of Polymers, Rapra Technology.

Koning, C., M. Van Duin, C. Pagnoulle and R. Jerome (1998), Strategies for compatibilization of polymer blends, Progress in Polymer Science **23**(4): 707-757.

Kontou, E., M. Niaounakis and P. Georgiopoulos (2011), Comparative study of PLA nanocomposites reinforced with clay and silica nanofillers and their mixtures, Journal of Applied Polymer Science **122**(3): 1519-1529.

Koo, J. H. (2006). Polymer nanocomposites, McGraw-Hill Professional Pub.

Kopinke, F. D., M. Remmler, K. Mackenzie, M. Möder and O. Wachsen (1996), Thermal decomposition of biodegradable polyesters—II. Poly(lactic acid), Polymer Degradation and Stability **53**(3): 329-342.

Koyama, N. and Y. Doi (1995), Morphology and biodegradability of a binary blend of poly((R)-3-hydroxybutyric acid) and poly((R,S)-lactic acid), Canadian Journal of Microbiology **41**(13): 316-322.

Koyama, N. and Y. Doi (1997), Miscibility of binary blends of poly[(R)-3-hydroxybutyric acid] and poly[(S)-lactic acid], Polymer **38**(7): 1589-1593.

Kremer, F. and A. Schönhals (2012). 2 Broadband Dielectric Measurement Techniques (10–6 Hz to 1012 Hz), Springer.

Lahcini, M., S. Elhakioui, D. Szopinski, B. Neuer, A. El Kadib, F. Scheliga, M. Raihane, F. B. Calleja and G. Luinstra (2016), Harnessing synergies in tin-clay catalyst for the preparation of poly (ε-caprolactone)/halloysite nanocomposites, European Polymer Journal **81**: 1-11.

Lasprilla, A. J., G. A. Martinez, B. H. Lunelli and A. L. Jardini (2012), Poly-lactic acid synthesis for application in biomedical devices—A review, Biotechnology Advances **30**(1): 321-328.

Lecouvet, B., M. Sclavons, S. Bourbigot and C. Bailly (2013), Thermal and flammability properties of polyethersulfone/halloysite nanocomposites prepared by melt compounding, Polymer Degradation and Stability **98**(10): 1993-2004.

Lee, H. S. and J. D. Kim (2012), Effect of a hybrid compatibilizer on the mechanical properties and interfacial tension of a ternary blend with polypropylene, poly(lactic acid), and a toughening modifier, Polymer Composites **33**(7): 1154-1161.

Lee, K. S. and Y. W. Chang (2013), Thermal, mechanical, and rheological properties of poly (ε-caprolactone)/halloysite nanotube nanocomposites, Journal of Applied Polymer Science **128**(5): 2807-2816.

Lee, S.-H., S. Hyun Kim, Y.-K. Han and Y. H. Kim (2001), Synthesis and degradation of end-group-functionalized polylactide, Journal of Polymer Science Part A: Polymer Chemistry **39**(7): 973-985.

Lee, S. Y. and M. A. Hanna (2009), Tapioca Starch-Poly(lactic acid)-Cloisite 30B Nanocomposite Foams, Polymer Composites **30**(5): 665-672.

Levis, S. and P. Deasy (2002), Characterisation of halloysite for use as a microtubular drug delivery system, International Journal of Pharmaceutics **243**(1): 125-134.

Li, G., P. Sarazin, W. J. Orts, S. H. Imam and B. D. Favis (2011), Biodegradation of Thermoplastic Starch and its Blends with Poly(lactic acid) and Polyethylene: Influence of Morphology, Macromolecular Chemistry and Physics **212**(11): 1147-1154.

Li, H. and M. A. Huneault (2008), Crystallization of PLA/Thermoplastic Starch Blends, International Polymer Processing **23**(5): 412-418.

Li, J., W. Zheng, L. Li, Y. Zheng and X. Lou (2009), Thermal degradation kinetics of g-HA/PLA composite, Thermochimica Acta **493**(1–2): 90-95.

Li, S., Z. Xiong, P. Fei, J. Cai, H. Xiong, J. Tan and Y. Yu (2013), Parameters characterizing the kinetics of the nonisothermal crystallization of thermoplastic starch/poly(lactic acid) composites as determined by differential scanning calorimetry, Journal of Applied Polymer Science **129**(6): 3566-3573.

Li, Y., S. C. Tjong and R. Li (2010), Electrical conductivity and dielectric response of poly (vinylidene fluoride)–graphite nanoplatelet composites, Synthetic Metals **160**(17): 1912-1919.

Liu, C., Y. Luo, Z. Jia, S. Li, D. Huang and D. Jia (2014), Particle configuration and properties of poly (vinyl chloride)/halloysite nanotubes nanocomposites via in situ suspension polymerization, Polymer Composites **35**(5): 856-863.

Liu, J., H. Jiang and L. Chen (2012), Grafting of Glycidyl Methacrylate onto Poly(lactide) and Properties of PLA/Starch Blends Compatibilized by the Grafted Copolymer, Journal of Polymers and the Environment **20**(3): 810-816.

Liu, M., B. Guo, M. Du, F. Chen and D. Jia (2009), Halloysite nanotubes as a novel β-nucleating agent for isotactic polypropylene, Polymer **50**(13): 3022-3030.

Liu, M., Z. Jia, D. Jia and C. Zhou (2014), Recent advance in research on halloysite nanotubes-polymer nanocomposite, Progress in Polymer Science **39**(8): 1498-1525.

Liu, M., Z. Jia, F. Liu, D. Jia and B. Guo (2010), Tailoring the wettability of polypropylene surfaces with halloysite nanotubes, Journal of Colloid and Interface Science **350**(1): 186-193.

Liu, M., Y. Zhang and C. Zhou (2013), Nanocomposites of halloysite and polylactide, Applied Clay Science **75**: 52-59.

Lopes, M. S., A. L. Jardini and R. M. Filho (2012), Poly (Lactic Acid) Production for Tissue Engineering Applications, Procedia Engineering **42**(0): 1402-1413.

López-Rodríguez, N., A. López-Arraiza, E. Meaurio and J. R. Sarasua (2006), Crystallization, morphology, and mechanical behavior of polylactide/poly(ε-caprolactone) blends, Polymer Engineering & Science **46**(9): 1299-1308.

Lvov, Y., A. Aerov and R. Fakhrullin (2014), Clay nanotube encapsulation for functional biocomposites, Advances in Colloid and Interface Science **207**: 189-198.

Márquez, Y., L. Franco and J. Puiggalí (2012), Thermal degradation studies of poly(trimethylene carbonate) blends with either polylactide or polycaprolactone, Thermochimica Acta **550**(0): 65-75.

Maxwell, A., L. Monnerie and I. Ward (1998), Secondary relaxation processes in polyethylene terephthalate–additive blends: 2. Dynamic mechanical and dielectric investigations, Polymer **39**(26): 6851-6859.

Mehta, R., V. Kumar, H. Bhunia and S. N. Upadhyay (2005), Synthesis of Poly(Lactic Acid): A Review, Journal of Macromolecular Science, Part C **45**(4): 325-349.

Menard, K. P. (2008). Dynamic mechanical analysis: a practical introduction, CRC press.

Murariu, M., A.-L. Dechief, Y. Paint, S. Peeterbroeck, L. Bonnaud and P. Dubois (2012), Polylactide (PLA)—halloysite nanocomposites: production,

morphology and key-properties, Journal of Polymers and the Environment **20**(4): 932-943.

Murray, P. and J. White (1955), Kinetics of the thermal dehydration of clays. Part IV. Interpretation of the differential thermal analysis of the clay minerals, Trans Br Ceram Soc **54**: 204-238.

Ning, N.-y., Q.-j. Yin, F. Luo, Q. Zhang, R. Du and Q. Fu (2007), Crystallization behavior and mechanical properties of polypropylene/halloysite composites, Polymer **48**(25): 7374-7384.

Nor Azowa Ibrahim, W. M. Z. W. Yunus, M. Othman and K. Abdan (2011), Effect of chemical surface treatment on the mechanical properties of reinforced plasticized poly(lactic acid) biodegradable composites, Journal of Reinforced Plastics and Composites **30**(5): 381-388.

Nunez, K., C. Rosales, R. Perera, N. Villarreal and J. M. Pastor (2011), Nanocomposites of PLA/PP blends based on sepiolite, Polymer Bulletin **67**(9): 1991-2016.

Ohkoshi, I., H. Abe and Y. Doi (2000), Miscibility and solid-state structures for blends of poly[(S)-lactide] with atactic poly[(R,S)-3-hydroxybutyrate], Polymer **41**(15): 5985-5992.

Oksman, K., M. Skrifvars and J.-F. Selin (2003), Natural fibres as reinforcement in polylactic acid (PLA) composites, Composites Science and Technology **63**(9): 1317-1324.

Omura, M., T. Tsukegi, Y. Shira and H. Nsuda (2007), Selective depolymerization of poly-L-lactic acid into L, L-lactide from blends with polystyrene, Kobunshi Ronbunshu **64**(11): 745-750.

Omura, M., T. Tsukegi, Y. Shirai, H. Nishida and T. Endo (2006), Thermal degradation behavior of poly (lactic acid) in a blend with polyethylene, Industrial & engineering chemistry research **45**(9): 2949-2953.

Omura, M., T. Tsukegi, Y. Shirai and H. Nishuda (2007), Selective depolymerization of poly-L-lactic acid into L, L-lactide from blends with polybutylene succinate-related copolymers, Kobunshi Ronbunshu **64**(11): 751-757.

Ouyang, C., Y. Wang, N. Zhao, X. Liu, S. Li and Z. Zhang (2012), Preparation of poly(lactic acid) and modified starch composites, Polymer Bulletin **68**(7): 2009-2019.

Ozawa, T. (1965), A new method of analyzing thermogravimetric data, Bulletin of the Chemical Society of Japan **38**(11): 1881-1886.

Ozawa, T. (1970), Kinetic analysis of derivative curves in thermal analysis, Journal of Thermal Analysis and Calorimetry **2**(3): 301-324.

Paglicawan, M. A., B. A. Basilia, M. T. V. Navarro and C. S. Emolaga (2013), Influence of Nanoclay on the Properties of Thermoplastic Starch/Poly(lactic acid) Blends, Journal of Biobased Materials and Bioenergy **7**(1): 102-107.

Park, J. W., Y. Doi and T. Iwata (2004), Uniaxial Drawing and Mechanical Properties of Poly[(R)-3-hydroxybutyrate]/Poly(l-lactic acid) Blends, Biomacromolecules **5**(4): 1557-1566.

Park, S. J., M. K. Kim and S. Y. Lee (2012), One-Step fermentative production of polylactic acid, Chemical Engineering Progress **108**(5): 51-55.

Pasbakhsh, P., H. Ismail, M. A. Fauzi and A. A. Bakar (2010), EPDM/modified halloysite nanocomposites, Applied Clay Science **48**(3): 405-413.

Pedrazzoli, D., A. Pegoretti, R. Thomann, J. Kristof and J. Karger-Kocsis (2015), Toughening linear low-density polyethylene with halloysite nanotubes, Polymer Composites **36**(5): 869-883.

Phetwarotai, W., P. Potiyaraj and D. Aht-Ong (2012), Characteristics of biodegradable polylactide/gelatinized starch films: Effects of starch, plasticizer, and compatibilizer, Journal of Applied Polymer Science **126**: E162-E172.

Prashantha, K., M. Lacrampe and P. Krawczak (2011), Processing and characterization of halloysite nanotubes filled polypropylene nanocomposites based on a masterbatch route: effect of halloysites treatment on structural and mechanical properties, Express Polymer Letters **5**(4): 295-307.

Prashantha, K., B. Lecouvet, M. Sclavons, M. F. Lacrampe and P. Krawczak (2013), Poly (lactic acid)/halloysite nanotubes nanocomposites: structure, thermal, and mechanical properties as a function of halloysite treatment, Journal of Applied Polymer Science **128**(3): 1895-1903.

Prescott, S. C. and C. G. Dunn (1949), Industrial microbiology, Industrial microbiology.

Raja, V., A. Sharma and V. N. Rao (2004), Impedance spectroscopic and dielectric analysis of PMMA-CO-P4VPNO polymer films, Materials Letters **58**(26): 3242-3247.

Rajan, K. P., A. Al-Ghamdi, R. Parameswar and G. Nando (2013), Blends of thermoplastic polyurethane and polydimethylsiloxane rubber: assessment of biocompatibility and suture holding strength of membranes, International journal of biomaterials **2013**.

Rajan, K. P., A. Al-Ghamdi, P. Ramesh and G. B. Nando (2012), Blends of thermoplastic polyurethane (TPU) and polydimethyl siloxane rubber (PDMS), part-I: assessment of compatibility from torque rheometry and mechanical properties, Journal of Polymer Research **19**(5): 1-13.

Rasal, R. M., A. V. Janorkar and D. E. Hirt (2010), Poly(lactic acid) modifications, Progress in Polymer Science **35**(3): 338-356.

Rawtani, D. and Y. Agrawal (2012), Multifarious applications of halloysite nanotubes: a review, Rev. Adv. Mater. Sci **30**: 282-295.

Ray, S. S. and M. Okamoto (2003), Polymer/layered silicate nanocomposites: a review from preparation to processing, Progress in Polymer Science **28**(11): 1539-1641.

Reddy, G., M. Altaf, B. J. Naveena, M. Venkateshwar and E. V. Kumar (2008), Amylolytic bacterial lactic acid fermentation — A review, Biotechnology Advances **26**(1): 22-34.

Reddy, J. P., M. Misra and A. Mohanty (2013), Injection moulded biocomposites from oat hull and polypropylene/polylactide blend: Fabrication and performance evaluation, Advances in Mechanical Engineering **2013**.

Reddy, N., D. Nama and Y. Yang (2008), Polylactic acid/polypropylene polyblend fibers for better resistance to degradation, Polymer Degradation and Stability **93**(1): 233-241.

Ren, J., T. Yu, H. Li, T. Ren and S. Yang (2008), Studies on morphologies and thermal properties of poly(lactic acid)/polycaprolactone/organic-modified montmorillonite nanocomposites, Polymer Composites **29**(10): 1145-1151.

Reyes-Alva, L., A. Gonzalez-Montiel and M. Aguilar-Vega (2014), Diffusion of organic volatile molecules in LDPE/Halloysite nanocomposites, Polymer Composites**37**(4): 1267-1273.

Rizvi, R., B. Cochrane, H. Naguib and P. C. Lee (2011), Fabrication and characterization of melt-blended polylactide-chitin composites and their foams, Journal of Cellular Plastics **47**(3): 283-300.

Roduit, B., L. Xia, P. Folly, B. Berger, J. Mathieu, A. Sarbach, H. Andres, M. Ramin, B. Vogelsanger and D. Spitzer (2008), The simulation of the thermal behavior of energetic materials based on DSC and HFC signals, Journal of Thermal Analysis and Calorimetry **93**(1): 143-152.

Rooj, S., A. Das, V. Thakur, R. Mahaling, A. K. Bhowmick and G. Heinrich (2010), Preparation and properties of natural nanocomposites based on natural rubber and naturally occurring halloysite nanotubes, Materials & Design **31**(4): 2151-2156.

Rybiński, P. and G. Janowska (2013), Influence synergetic effect of halloysite nanotubes and halogen-free flame-retardants on properties nitrile rubber composites, Thermochimica Acta **557**: 24-30.

Rybinski, P., G. Janowska, M. Jozwiak and A. Pajak (2012), Thermal properties and flammability of nanocomposites based on diene rubbers and naturally occurring and activated halloysite nanotubes, Journal of Thermal Analysis and Calorimetry **107**(3): 1243-1249.

Sahoo, R. K., S. Mohanty and S. K. Nayak (2015), Effect of nanoclay on the nucleation, crystallization and melting behaviour of polypropylene A study on non-isothermal crystallization kinetics, Journal of Thermoplastic Composite Materials: 0892705715569825.

Salehiyan, R. and K. Hyun (2013), Effect of organoclay on non-linear rheological properties of poly(lactic acid)/poly(caprolactone) blends, Korean Journal of Chemical Engineering **30**(5): 1013-1022.

Salehiyan, R., A. A. Yussuf, N. F. Hanani, A. Hassan and A. Akbari (2013), Polylactic acid/polycaprolactone nanocomposite: Influence of montmorillonite and impact modifier on mechanical, thermal, and morphological properties, Journal of Elastomers and Plastics**47**(1): 69-87.

Sarazin, P., G. Li, W. J. Orts and B. D. Favis (2008), Binary and ternary blends of polylactide, polycaprolactone and thermoplastic starch, Polymer **49**(2): 599-609.

Schwach, E., J.-L. Six and L. Averous (2008), Biodegradable Blends Based on Starch and Poly(Lactic Acid): Comparison of Different Strategies and Estimate of Compatibilization, Journal of Polymers and the Environment **16**(4): 286-297.

Semba, T., K. Kitagawa, U. S. Ishiaku and H. Hamada (2006), The effect of crosslinking on the mechanical properties of polylactic acid/polycaprolactone blends, Journal of Applied Polymer Science **101**(3): 1816-1825.

Sencadas, V., C. M. Costa, J. G. Ribelles and S. Lanceros-Méndez (2010), Isothermal crystallization kinetics of poly (vinylidene fluoride) in the α-phase in the scope of the Avrami equation, Journal of materials science **45**(5): 1328-1335.

Sepe, M. P. (1997). Thermal analysis of polymers, iSmithers Rapra Publishing.

Sharma, R. and S. N. Maiti (2015), Melt rheological properties of PBT/SEBS and reactively compatibilized PBT/SEBS/SEBS-g-MA polymer blends, Journal of Applied Polymer Science **132**(5).

Shemesh, R., M. Krepker, M. Natan, Y. Danin-Poleg, E. Banin, Y. Kashi, N. Nitzan, A. Vaxman and E. Segal (2015), Novel LDPE/halloysite nanotube films with sustained carvacrol release for broad-spectrum antimicrobial activity, RSC Advances **5**(106): 87108-87117.

Shepard, D. D. and B. Twombly (1996), Simultaneous dynamic mechanical analysis and dielectric analysis of polymers, Thermochimica Acta **272**: 125-129.

Shi, Q., C. Chen, L. Gao, L. Jiao, H. Xu and W. Guo (2011), Physical and degradation properties of binary or ternary blends composed of poly (lactic acid), thermoplastic starch and GMA grafted POE, Polymer Degradation and Stability **96**(1): 175-182.

Shin, B. Y., S. H. Jang and B. S. Kim (2011), Thermal, Morphological, and Mechanical Properties of Biobased and Biodegradable Blends of Poly(lactic acid) and Chemically Modified Thermoplastic Starch, Polymer Engineering and Science **51**(5): 826-834.

Shirai, M. A., M. V. E. Grossmann, S. Mali, F. Yamashita, P. S. Garcia and C. M. O. Mueller (2013), Development of biodegradable flexible films of starch and

poly(lactic acid) plasticized with adipate or citrate esters, Carbohydrate Polymers **92**(1): 19-22.

Shirai, M. A., J. B. Olivato, I. M. Demiate, C. M. O. Müller, M. V. E. Grossmann and F. Yamashita (2016), Poly (lactic acid)/thermoplastic starch sheets: effect of adipate esters on the morphological, mechanical and barrier properties, Polímeros(AHEAD)

Shogren, R. L., W. M. Doane, D. Garlotta, J. W. Lawton and J. L. Willett (2003), Biodegradation of starch/polylactic acid/poly(hydroxyester-ether) composite bars in soil, Polymer Degradation and Stability **79**(3): 405-411.

Shogren, R. L., G. Selling and J. L. Willett (2011), Effect of Orientation on the Morphology and Mechanical Properties of PLA/Starch Composite Filaments, Journal of Polymers and the Environment **19**(2): 329-334.

Shuai, X., Y. He, N. Asakawa and Y. Inoue (2001), Miscibility and phase structure of binary blends of poly(L-lactide) and poly(vinyl alcohol), Journal of Applied Polymer Science **81**(3): 762-772.

Siengchin, S., T. Pohl, L. Medina and P. Mitschang (2013), Structure and properties of flax/polylactide/alumina nanocomposites, Journal of Reinforced Plastics and Composites **32**(1): 23-33.

Silva, K. M. D., K. Tarverdi, R. Withnall and J. Silver (2011), Incorporation of wheat starch and coupling agents into poly(lactic acid) to develop biodegradable composite, Plastics Rubber and Composites **40**(1): 17-24.

Singh, V. P., K. Vimal, G. Kapur, S. Sharma and V. Choudhary (2016), High-density polyethylene/halloysite nanocomposites: morphology and rheological behaviour under extensional and shear flow, Journal of Polymer Research **23**(3): 1-17.

Smitthipong, W., R. Tantatherdtam and R. Chollakup (2013), Effect of pineapple leaf fiber-reinforced thermoplastic starch/poly(lactic acid) green composite: Mechanical, viscosity, and water resistance properties, Journal of Thermoplastic Composite Materials**28**(5): 717-729.

Soares, F. C., F. Yamashita, C. M. O. Mueller and A. T. N. Pires (2013), Thermoplastic starch/poly(lactic acid) sheets coated with cross-linked chitosan, Polymer Testing **32**(1): 94-98.

Socrates, G. (2004). Infrared and Raman characteristic group frequencies: tables and charts, John Wiley & Sons.

Sperling, L. H. (2005). Introduction to physical polymer science, John Wiley & Sons.

Svoboda, P., C. Zeng, H. Wang, L. J. Lee and D. L. Tomasko (2002), Morphology and mechanical properties of polypropylene/organoclay nanocomposites, Journal of Applied Polymer Science **85**(7): 1562-1570.

Swierz-Motysia, B., R. Jeziorska, A. Szadkowska and M. Piotrowska (2011), SYNTHESIS AND PROPERTIES OF BIODEGRADABLE POLYLACTIDE AND THERMOPLASTIC STARCH BLENDS, Polimery **56**(4): 271-280.

Szczygielska, A. and J. Kijeński (2011). Studies of properties of polypropylene/halloysite composites. Polish Journal of Chemical Technology. **13:** 61.

Takayama, T., M. Todo, K. Arakawa and H. Tsuji (2006), Effect of additive on fracture properties of PLA/PCL polymer blend, Nippon Kikai Gakkai Ronbunshu A Hen(Transactions of the Japan Society of Mechanical Engineers Part A)(Japan) **18**(2): 173-178.

Takayama, T., M. Todo and H. Tsuji (2011), Effect of annealing on the mechanical properties of PLA/PCL and PLA/PCL/LTI polymer blends, Journal of the Mechanical Behavior of Biomedical Materials **4**(3): 255-260.

Todd, M. G. and F. G. Shi (2002), Validation of a novel dielectric constant simulation model and the determination of its physical parameters, Microelectronics Journal **33**(8): 627-632.

Tri, P. N., S. Domenek, A. Guinault and C. Sollogoub (2013), Crystallization behavior of poly(lactide)/poly(β-hydroxybutyrate)/talc composites, Journal of Applied Polymer Science **129**(6): 3355-3365.

Tsuji, H. and H. Muramatsu (2001), Blends of aliphatic polyesters. IV. Morphology, swelling behavior, and surface and bulk properties of blends from hydrophobic poly(L-lactide) and hydrophilic poly(vinyl alcohol), Journal of Applied Polymer Science **81**(9): 2151-2160.

Tsuji, H. and H. Muramatsu (2001), Blends of aliphatic polyesters: V non-enzymatic and enzymatic hydrolysis of blends from hydrophobic poly(l-lactide) and

hydrophilic poly(vinyl alcohol), Polymer Degradation and Stability **71**(3): 403-413.

Utracki, L. (1983), Melt flow of polymer blends, Polymer Engineering & Science **23**(11): 602-609.

Utracki, L. (1995), History of commercial polymer alloys and blends (from a perspective of the patent literature), Polymer Engineering & Science **35**(1): 2-17.

Utracki, L. and M. Kanial (1982), Melt rheology of polymer blends, Polymer Engineering & Science **22**(2): 96-114.

Utracki, L. A. (2002), Compatibilization of polymer blends, The Canadian Journal of Chemical Engineering **80**(6): 1008-1016.

Utracki, L. A. and C. A. Wilkie (2002). Polymer blends handbook, Springer.

Varga, J. (1992), Supermolecular structure of isotactic polypropylene, Journal of Materials Science **27**(10): 2557-2579.

Velankar, S., P. Van Puyvelde, J. Mewis and P. Moldenaers (2004), Steady-shear rheological properties of model compatibilized blends, Journal of Rheology (1978-present) **48**(4): 725-744.

Vogel, C., G. G. Hoffmann and H. W. Siesler (2009), Rheo-optical FT-IR spectroscopy of poly(3-hydroxybutyrate)/poly(lactic acid) blend films, Vibrational Spectroscopy **49**(2): 284-287.

Vogel, C. and H. W. Siesler (2008), Thermal Degradation of Poly(ε-caprolactone), Poly(L-lactic acid) and their Blends with Poly(3-hydroxy-butyrate) Studied by TGA/FT-IR Spectroscopy, Macromolecular Symposia **265**(1): 183-194.

Vogel, C., E. Wessel and H. W. Siesler (2007), FT-IR Imaging Spectroscopy of Phase Separation in Blends of Poly(3-hydroxybutyrate) with Poly(l-lactic acid) and Poly(ε-caprolactone), Biomacromolecules **9**(2): 523-527.

Vyazovkin, S., A. K. Burnham, J. M. Criado, L. A. Pérez-Maqueda, C. Popescu and N. Sbirrazzuoli (2011), ICTAC Kinetics Committee recommendations for performing kinetic computations on thermal analysis data, Thermochimica Acta **520**(1): 1-19.

Vyazovkin, S. and N. Sbirrazzuoli (2006), Isoconversional kinetic analysis of thermally stimulated processes in polymers, Macromolecular Rapid Communications **27**(18): 1515-1532.

Wahit, M. U., N. I. Akos and W. A. Laftah (2012), Influence of natural fibers on the mechanical properties and biodegradation of poly(lactic acid) and poly(ε-caprolactone) composites: A review, Polymer Composites **33**(7): 1045-1053.

Wang, B. and H.-X. Huang (2013), Effects of halloysite nanotube orientation on crystallization and thermal stability of polypropylene nanocomposites, Polymer Degradation and Stability **98**(9): 1601-1608.

Wang, L., W. Ma, R. A. Gross and S. P. McCarthy (1998), Reactive compatibilization of biodegradable blends of poly(lactic acid) and poly(ε-caprolactone), Polymer Degradation and Stability **59**(1–3): 161-168.

Wang, L., Z. Tong, L. O. Ingram, Q. Cheng and S. Matthews (2013), Green Composites of Poly (Lactic Acid) and Sugarcane Bagasse Residues from Bio-refinery Processes, Journal of Polymers and the Environment**21**(3): 780-788.

Wang, N., J. Yu and X. Ma (2007), Preparation and characterization of thermoplastic starch/PLA blends by one-step reactive extrusion, Polymer International **56**(11): 1440-1447.

Wang, Y. and M. A. Hillmyer (2001), Polyethylene-poly(L-lactide) diblock copolymers: Synthesis and compatibilization of poly(L-lactide)/polyethylene blends, Journal of Polymer Science Part A: Polymer Chemistry **39**(16): 2755-2766.

Wong, S. C., E. M. Wouterson and E. M. Sutherland (2006), Dielectric properties of graphite nanocomposites, Journal of Vinyl and Additive Technology **12**(3): 127-130.

Woo Park, J., S. Cheon Oh, H. Pyeong Lee, H. Taik Kim and K. Ok Yoo (2000), A kinetic analysis of thermal degradation of polymers using a dynamic method, Polymer Degradation and Stability **67**(3): 535-540.

Wu, D., D. Lin, J. Zhang, W. Zhou, M. Zhang, Y. Zhang, D. Wang and B. Lin (2011), Selective Localization of Nanofillers: Effect on Morphology and Crystallization of PLA/PCL Blends, Macromolecular Chemistry and Physics **212**(6): 613-626.

Wu, J. H., M. C. Kuo, C. W. Chen, P. H. Kuan, Y. J. Wang and S. Y. Jhang (2013), Crystallization behavior of α-cellulose short-fiber reinforced poly(lactic acid) composites, Journal of Applied Polymer Science **129**(5): 3007-3018.

Wu, X. S. (2011), Effect of Glycerin and Starch Crosslinking on Molecular Compatibility of Biodegradable Poly(lactic acid)-Starch Composites, Journal of Polymers and the Environment **19**(4): 912-917.

Xiong, Z., C. Li, S. Ma, J. Feng, Y. Yang, R. Zhang and J. Zhu (2013), The properties of poly(lactic acid)/starch blends with a functionalized plant oil: Tung oil anhydride, Carbohydrate Polymers **95**(1): 77-84.

Xiong, Z., Y. Yang, J. Feng, X. Zhang, C. Zhang, Z. Tang and J. Zhu (2013), Preparation and characterization of poly(lactic acid)/starch composites toughened with epoxidized soybean oil, Carbohydrate Polymers **92**(1): 810-816.

Xiong, Z., L. Zhang, S. Ma, Y. Yang, C. Zhang, Z. Tang and J. Zhu (2013), Effect of castor oil enrichment layer produced by reaction on the properties of PLA/HDI-g-starch blends, Carbohydrate Polymers **94**(1): 235-243.

Xu, J. and C. Wong (2007), Characterization and properties of an organic–inorganic dielectric nanocomposite for embedded decoupling capacitor applications, Composites Part A: Applied Science and Manufacturing **38**(1): 13-19.

Xu, T., Y. Wang, Y. Xu, W. Cao, C. Liu and C. Shen (2014), Crystallization behavior and nucleation analysis of isotactic polypropylene with a multiamide nucleating agent, Polymer Testing **36**: 62-68.

Xu, W., G. Liang, H. Zhai, S. Tang, G. Hang and W.-P. Pan (2003), Preparation and crystallization behaviour of PP/PP-g-MAH/Org-MMT nanocomposite, European Polymer Journal **39**(7): 1467-1474.

Xu, Y., J. Loi, P. Delgado, V. Topolkaraev, R. J. McEneany, C. W. Macosko and M. A. Hillmyer (2015), Reactive compatibilization of polylactide/polypropylene blends, Industrial & engineering chemistry research **54**(23): 6108-6114.

Xue, P., K. Wang, M. Jia and M. Yang (2013), Biodegradation and mechanical property of polylactic acid/thermoplastic starch blends with poly (ethylene glycol), Journal of Wuhan University of Technology-Materials Science Edition **28**(1): 157-162.

Yang, S., R. Benitez, A. Fuentes and K. Lozano (2007), Dielectric analysis of VGCNF reinforced polyethylene composites, Composites Science and Technology **67**(6): 1159-1166.

Yang, T.-I. and P. Kofinas (2007), Dielectric properties of polymer nanoparticle composites, Polymer **48**(3): 791-798.

Yeh, J.-T., M.-C. Yang, C.-J. Wu, X. Wu and C.-S. Wu (2008), Study on the Crystallization Kinetic and Characterization of Poly(lactic acid) and Poly(vinyl alcohol) Blends, Polymer-Plastics Technology and Engineering **47**(12): 1289-1296.

Yew, G. H., A. M. Mohd Yusof, Z. A. Mohd Ishak and U. S. Ishiaku (2005), Water absorption and enzymatic degradation of poly(lactic acid)/rice starch composites, Polymer Degradation and Stability **90**(3): 488-500.

Ying-Chen, Z., W. Hong-Yan and Q. Yi-Ping (2010), Morphology and properties of hybrid composites based on polypropylene/polylactic acid blend and bamboo fiber, Bioresource Technology **101**(20): 7944-7950.

Yokesahachart, C. and R. Yoksan (2011), Effect of amphiphilic molecules on characteristics and tensile properties of thermoplastic starch and its blends with poly(lactic acid), Carbohydrate Polymers **83**(1): 22-31.

Yoo, T. W., H. G. Yoon, S. J. Choi, M. S. Kim, Y. H. Kim and W. N. Kim (2010), Effects of compatibilizers on the mechanical properties and interfacial tension of polypropylene and poly (lactic acid) blends, Macromolecular Research **18**(6): 583-588.

Zafar, M. T., S. N. Maiti and A. K. Ghosh (2016), Effect of surface treatment of jute fibers on the interfacial adhesion in poly(lactic acid)/jute fiber biocomposites, Fibers and Polymers **17**(2): 266-274.

Zembouai, I., M. Kaci, S. Bruzaud, L. Dumazert, A. Bourmaud, M. Mahlous, J. M. Lopez-Cuesta and Y. Grohens (2016), Gamma irradiation effects on morphology and properties of PHBV/PLA blends in presence of compatibilizer and Cloisite 30B, Polymer Testing **49**: 29-37.

Zembouai, I., M. Kaci, S. Bruzaud, I. Pillin, J.-L. Audic, S. Shayanfar and S. D. Pillai Electron beam radiation effects on properties and ecotoxicity of PHBV/PLA

blends in presence of organo-modified montmorillonite, Polymer Degradation and Stability.

Zeng, J.-B., K.-A. Li and A.-K. Du (2015), Compatibilization strategies in poly (lactic acid)-based blends, RSC Advances **5**(41): 32546-32565.

Zhang, H., Q. Zhang and C. Sun (2008), Nonisothermal crystallization kinetics of polypropylene/polyethersulfone blend, Polymer Bulletin **60**(2-3): 291-300.

Zhang, L., C. Xiong and X. Deng (1996), Miscibility, crystallization and morphology of poly(β-hydroxybutyrate)/poly(d,l-lactide) blends, Polymer **37**(2): 235-241.

Zhang, M. and N. L. Thomas (2011), Blending polylactic acid with polyhydroxybutyrate: The effect on thermal, mechanical, and biodegradation properties, Advances in Polymer Technology **30**(2): 67-79.

Zhang, S., X. Feng, S. Zhu, Q. Huan, K. Han, Y. Ma and M. Yu (2013), Novel toughening mechanism for polylactic acid (PLA)/starch blends with layer-like microstructure via pressure-induced flow (PIF) processing, Materials Letters **98**: 238-241.

Zhao, H., Z. Cui, X. Wang, L. S. Turng and X. Peng (2013), Processing and characterization of solid and microcellular poly(lactic acid)/polyhydroxybutyrate-valerate (PLA/PHBV) blends and PLA/PHBV/Clay nanocomposites, Composites Part B: Engineering **51**: 79-81.

Zhu, Y., C. Liang, Y. Bo and S. Xu (2015), Non-isothermal crystallization behavior of compatibilized polypropylene/recycled polyethylene terephthalate blends, Journal of Thermal Analysis and Calorimetry **119**(3): 2005-2013.

Zou, H., L. Wang, H. Gan and C. Yi (2012), Effect of fiber surface treatments on the properties of short sisal fiber/poly(lactic acid) biocomposites, Polymer Composites **33**(10): 1659-1666.

Zou, H., C. Yi, L. Wang, H. Liu and W. Xu (2009), Thermal degradation of poly(lactic acid) measured by thermogravimetry coupled to Fourier transform infrared spectroscopy, Journal of Thermal Analysis and Calorimetry **97**(3): 929-935.

APPENDIX

Krishna Prasad Rajan
rajank@rcyci.edu.sa

Experience Profile

❖ **Lecturer in Chemical Engineering**

Yanbu Industrial College, Yanbu Al-Sinaiah, KSA, from 19th September 2009 till date.

❖ **Senior Executive (Research&Development)**

Manali Petrochemical Ltd, Chennai from 7th May 2008 to 7th September 2009

❖ **Senior Lecturer**

Amrita School of Engineering, Dept of Chemical Engineering and Materials Science, Ettimadai, Coimbatore, India From 14th May 2002 to 5th May 2008.

❖ Engineer Trainee

M/s. Apollo Tyres Limited, Perambra Factory, Thrissur, Kerala. From July 2001 to May 2002.

❖ Faculty in Polymer Engineering

UniversityCollege of Engineering, Thodupuzha, Kerala, From December 2000 to March 2001

Educational Profile

o **M.Tech (Rubber Technology)** with CGPA 9.24/10 from Indian Institute of Technology (**IIT**), **Kharagpur, India** (2005).

o **B.Tech (Polymer Engineering)** with Distinction (79.6%) from **Mahatma Gandhi University**, Kottayam, Kerala, India (2000).

Areas of Interest

o Polymer compounding, Processing and Testing

o Development of Novel Polymer Blends and Composites

Achievements

o Received **Talents in Plastics Award-2011** of Gulf Petrochemicals and Chemicals Association (GPCA)

o Research and career biography included in Marquis Who's Who in the World – 2011 edition and 2000 outstanding intellectuals of the 21st century-2011 edition onwards.

o Received **First Prize** for the Charles Goodyear Memorial National Quiz Competition on Polymer Technology organized by Indian Institute of Technology, Kharagpur during November 2003

o **Coordinator** of various seminars, conferences and workshops organized by the Department of Polymer Engineering, Amrita School of Engineering, Coimbatore.

o **Delivered lectures** and Participated in various national and international seminars, conferences and workshops.

o **Convener** of "National Conference on Polymers in Medical Applications" organized by Department of Polymer Engineering on 20-21 November 2006.

o **Treasurer** of "National Conference on Advanced materials for aerospace and defence applications" organized by Department of Polymer Engineering on 7-8 January 2008.

o **Conducted** a series of **in-house training programs** for R&D technicians and officers at Manali Petrochemical Ltd, Chennai, India.

Membership in Professional Bodies

o Professional Member of Society for Plastics Engineers (SPE), USA

o Life Member of Society for Biomaterials and Artificial Organs (India) [SBAOI].

o Life Member of Indian Society for Technical Education (ISTE)

Publications in conferences

o "Double network of NR/BR blends" National Seminar on Rubber Technology for Special Applications, organized by Institution of Engineers (India) and AnnaUniversity, Chennai, June 2003.

o "Recycling of Scrap Tyres and Tyre Derived Fuel" at Emerging Trends in Polymer Engineering, organized by Mahatma Gandhi University Kottayam, Kerala, March 2004.

o "Energetic Polymers for Defence Applications" at Emerging Trends in Polymer Engineering, organized by Mahatma Gandhi University Kottayam, Kerala, March 2004.

o "Polymers for Tissue Engineering" at International Conference on Science and Technology for Sustainable Development organized by SB College, Changanacherry, Kerala. August 10-13, 2005.

o "Chitin and its Derivatives for Biomedical Applications" at International Conference on Science and Technology for Sustainable Development organized by SB College, Changanacherry, Kottayam, Kerala. August 10-13, 2005.

o "Optimization of Process Parameters for Thermoplastic Polyurethane   (TPU) and Poly Dimethylsiloxane Rubber (PDMS) Blends by using Taguchi Method" at 19th Rubber Conference organized by Indian Rubber Manufacturers Research Association (IRMRA) at Mumbai. December 19th and 20th, 2005.

o "*In vitro* Cytotoxicity and Cell Adhesion Studies on Compatibilized Polymer Blends" at National Conference on Polymers in Medical Applications organized by Dept. of Polymer Engineering, Amrita School of Engineering, Coimbatore. November 20-21, 2006.

o "Biocompatibility Evaluation of Compatibilized blends of Thermoplastic Polyurethane (TPU) and Polydimethyl Siloxane Rubber (PDMS)", ANTEC, Dubai – January, 2014.

o "Preparation of a compatibilized blend of Polypropylene (PP) and Polylactic Acid (PLA)". International Conference on New Dimension in Chemistry & Chemical Technologies - Applications in Pharma Industry (NDCT-2014), Jawaharlal Nehru Technological University Hyderabad, India. June, 2014.

o "Development of Novel Nanocomposites of Compatibilized Polypropylene (PP) Polylactic Acid (PLA) Blends Containing Halloysite Nanotubes", ANTEC, Dubai —January, 2016 (http://gpcaplastics.com/2016/index.php/agenda/).

Publications in International Journals

o Krishnaprasad R, Veena N, Maria H, Rajan R, Skrifvars M and Joseph K. Mechanical and Thermal Properties of Bamboo Microfibril Reinforced Polyhydroxybutyrate Biocomposites. *J Polym Environ.* 2009; 17: 109-114.

o Rajan KP, Veena NR, Singh P and Nando GB. Optimization of Processing Parameters for a Polymer Blend using Taguchi Method. *Yanbu Journal of Engineering and Science.* 2010; 1: 59-67.

o Rajan KP, Veena NR, Maria HJ, Rajan R, Skrifvars M and Joseph K. Extraction of bamboo microfibrils and development of biocomposites based on polyhydroxy butyrate and bamboo microfibrils. *J Compos Mater.* 2011; 45: 1325-1329.

o Rajan KP, Dhilipraj DB, Manikandan R and Veena N. Preparation of Molded Viscoelastic Polyurethane Foam for Pillow Applications. *Cell Polym.* 2011; 30: 13-21.

o Rajan KP, Al-Ghamdi A, Ramesh P and Nando GB. Blends of thermoplastic polyurethane (TPU) and polydimethyl siloxane rubber (PDMS), part-I: assessment of compatibility from torque rheometry and mechanical properties. *Journal of Polymer Research.* 2012; 19: 1-13.

o Rajan KP, Al-Ghamdi A, Parameswar R and Nando G. Blends of thermoplastic polyurethane and polydimethylsiloxane rubber: assessment of biocompatibility and suture holding strength of membranes. *International Journal of biomaterials.* 2013.

o Thomas SP, Rajan KP and Chavali M. Polymer Nanocomposites, a birds eye view. *International Journal of NanoScience and Technology.* 2013; 2: 19-31.

o Rajan KP, Alghamdi A, Thomas SP, Gopanna A and Chavali M. Polyblends and composites of poly (lactic acid) (PLA): a review on the state of the art, *Progress in Rubber, Plastics & Recycling Technology* (Accepted, 2017) Impact Factor 0.452, ISSN: 1478-2413.

o Rajan KP, Alghamdi A, Thomas SP, Gopanna A and Chavali M., Rheology, mechanical properties and thermal degradation kinetics of polypropylene (PP) and polylactic acid (PLA) blends, *Indian Journal of Chemical Technology* (Submitted, 2016) Impact Factor 0.491 ISSN: 0971-457X (Print).

o Krishna Prasad Rajan, Ahmed Al-Ghamdi, Selvin P. Thomas, Aravinthan Gopanna, Murthy Chavali, Dielectric analysis of polypropylene (PP) and polylactic acid (PLA)

blends reinforced with halloysite nanotubes, *Journal of Thermoplastic Composite Materials* (Submitted, 2016) Impact Factor 0.922 ISSN: 0892-7057.

o Krishna Prasad Rajan, Ahmed Al-Ghamdi, Selvin P. Thomas, Aravinthan Gopanna, Murthy Chavali, Non-isothermal crystallization kinetics of polypropylene (PP) and polylactic acid (PLA) blends, *Journal of Non-Crystalline Solids* (Submitted, 2016) Impact Factor 1.825 ISSN: 0022-3093.

Books/Book Chapters

o Rajan KP, Veena NR and Joseph K. Biocomposites from Poly Hydroxybutyrate and Bamboo Microfibrils: Green Composites from Bamboo Fiber and PHB. LAP Lambert Academic Publishing, 2011.

o Krishna Prasad Rajan, Selvin P Thomas, Aravinthan Gopanna, Murthy Chavali Yadav, Polyurethane nanostructures for drug delivery applications; Nanostructures In Therapeutic Medicine, Multi Volume SET (I-V), Edited by Dr. Alexandru Mihai Grumezescu, Elsevier Publishers / 2016 (Accepted).

Personal Profile

DOB : 27.05.1977

Present Address : P.O Box-30436, Chemical Engg. Technology Department,
Yanbu Industrial College, Yanbu Al-Sinaiah, 21477
Kingdom of Saudi Arabia, Ph: 00966 535456251

Permanent Address : Devi Nivas, CMC-12,
Cherthala (P.O.)
Alappuzha (Dist.)
Kerala – 688 524
India, Ph: 0478 2821428

Research publications originated from thesis related research

Journals

1. Thomas SP, Rajan KP and Chavali M. Polymer Nanocomposites, a birds eye view. **International Journal of NanoScience and Technology.** 2013; 2: 19-31.

2. Rajan KP, Alghamdi A, Thomas SP, Gopanna A and Chavali M. Polyblends and composites of poly (lactic acid) (PLA): a review on the state of the art, **Progress in Rubber, Plastics & Recycling Technolog**y **(Accepted, 2017) Impact Factor 0.452, ISSN: 1478-2413**

3. Rajan KP, Alghamdi A, Thomas SP, Gopanna A and Chavali M., **Rheology, mechanical properties and thermal degradation kinetics of polypropylene (PP) and polylactic acid (PLA) blends, Indian Journal of Chemical Technology (Submitted, 2016) Impact Factor 0.491 ISSN: 0971-457X (Print)**

4. Krishna Prasad Rajan, Ahmed Al-Ghamdi, Selvin P. Thomas, AravinthanGopanna, Murthy Chavali, Dielectric analysis of polypropylene (PP) and polylactic acid (PLA) blends reinforced with halloysite nanotubes, **Journal of Thermoplastic Composite Materials (Submitted, 2016) Impact Factor 0.922 ISSN: 0892-7057**

5. Krishna Prasad Rajan, Ahmed Al-Ghamdi, Selvin P. Thomas, Aravinthan Gopanna, Murthy Chavali, Non-isothermal crystallisation kinetics of polypropylene (PP) and polylactic acid (PLA) blends, **Journal of Non-Crystalline Solids (Submitted, 2016) Impact Factor 1.825 ISSN: 0022-3093**

Conferences/Posters

1. Rajan KP. Preparation and Biocompatibility Evaluation of Compatibilized blends of Thermoplastic Polyurethane (TPU) and Polydimethyl Siloxane Rubber (PDMS), ANTEC, Dubai - 2014.

2. Rajan KP, Chavali M. Preparation of a compatibilized blend of Polypropylene (PP) and Polylactic Acid (PLA). International Conference on New Dimension in Chemistry & Chemical Technologies -Applications in Pharma Industry (NDCT-2014), Jawaharlal Nehru Technological University Hyderabad, India. 2014.

3. Rajan KP, Chavali M. Development of Novel Nanocomposites of Compatibilized Polypropylene (PP) Polylactic Acid (PLA) Blends Containing Halloysite Nanotubes, ANTEC, Dubai-2016 (http://gpcaplastics.com/2016/index.php/agenda).

Books/Book Chapters

1. Krishna Prasad Rajan, Selvin P Thomas, Aravinthan Gopanna, Murthy Chavali Yadav, Polyurethane nanostructures for drug delivery applications; Nanostructures In Therapeutic Medicine, Multi-Volume SET (I-V), Edited by Dr Alexandru Mihai Grumezescu, Elsevier Publishers/2016(Accepted).

Research Flow Chart

NIU

Admission for Ph.D. Program at N I University 2012, August

⬇

Research Topic Approval and Course Work Approval

⬇

Pre PhD Course Work:
1. Research Methodology (B grade)
2. Introduction to Nanoscale Science and Technology (A grade)
3. Polymer nanotechnology (A grade)
4. Advanced Polymer Composites (B grade)   (Passed in 2013)

⬇

VFSTRU

Identification of Research Gap in the Proposed Research Area Selection of raw materials

⬇

1. Preparation of blend with various compatibilizer contents
2. Characterization of the blend (Mechanical and Thermal)

VFSTRU

Investigation of the thermal degradation kinetics of the blend
Investigation of the non-isothermal crystallization kinetics of the blend

⬇

Preparation of nanocomposites of PP/PLA blend with Halloysite nanotubes (HNT's) as reinforcement (HNT 0 to HNT 10)

⬇

Characterization of the nanocomposites;
1. Mechanical and dynamic mechanical
2. Thermogravimetric analysis
3. Differential scanning calorimetry
4. Wide angle X-ray diffraction
5. Capillary Rheometry
6. Dielectric Analysis
7. Polarized Light Microscopy
8. Transmission Electron Microscopy
9. Infra Red Spectroscopy (FTIR)

⬇

Applications:
1. Microelectronic packaging
2. Microelectronic devices with low signal attenuation